UNIVERSITY OF BELGRADE

MEDICAL FACULTY

Sanja Ćirović

EXPRESSION OF NEURAL ADHESION MOLECULES (NCAM) IN HEALTHY AND DISEASED RENAL TISSUE

Doctoral Dissertation

Belgrade, 2014

UNIVERZITET U BEOGRADU

MEDICINSKI FAKULTET

Sanja Ćirović

EKSPRESIJA NEURALNIH ADHEZIONIH MOLEKULA (NCAM) U ZDRAVOM I OBOLELOM BUBREŽNOM TKIVU

doktorska disertacija

Beograd, 2014

Mentor:
Prof. Dr Jasmina Marković-Lipkovski,
Medicinski Fakultet Univerziteta u Beogradu

Članovi komisije za ocenu završene doktorske disertacije:

1. Prof. Dr Claudia A. Müller, profesor Medicinskog fakulteta Eberhard Karl Universität, Tübingen

2. Prof. Dr Jovan Vasiljević, profesor Medicinskog Fakulteta Univerziteta u Beogradu

3. Prof. Dr Svetislav Tatić, profesor Medicinskog Fakulteta Univerziteta u Beogradu

Acknowledgement

I would like to express my sincere gratitude to my mentor Prof. Dr. Jasmina Marković-Lipkovski for giving me the opportunity to carry out this research, for her motivation, continuous support and enthusiasm. Her supervision and guidance helped me in all the times during the research and writing of the thesis. I thank her for helping to shape the thesis by critically reviewing it and giving careful and instructive comments. I thank her for all time and energy that she spends making me a better researcher.

I would also like to express my sincere gratitude to my supervisors Prof. Dr Claudia A. Müller for her patience, support and understanding, for her encouragement and for all that she teaches me during my stay in Germany.

I would like also express my sincere gratitude Prof. Dr Gerhard A Müller, for the great collaboration and for the support during realization of the project.

I would also like to thank Prof. Dr Hans-Jörg Bühring for his collaboration and delivery of new mesenchymal antibodies for my research.

I would also like to thank Prof. Dr Gerd Klein for support, encouragement and constructive feedback.

I would also like to thank Prof. Dr. Jovan Vasiljević and Prof. Dr. Svetislav Tatić for their time, support and constructive advices. It is no easy task, reviewing a thesis, and I am grateful for their thoughtful comments.

I would like to thank Prof. Dr. Ljiljana Gojković-Bukarica and M.Sc. Radmila Novaković for they support and encouragement during difficult situations in the course of research.

I would like to express my special appreciation and thanks to my colleagues Dr. Martina Bosic, Dr. Jelena Vještica and Dr Maja Životić, for their help in writing and proof reading my thesis.

I would like to specially thank Ms. Ingeborg Steiert, Ms. Jutta Gamper-Tsigaras and Ms Višnja Vujović for their help in the experimental work throughout the project and technical assistance.

My special thanks to my parents, my husband and my kids for their support in whatever I am doing. To all my friends all around thank you.

Expression of neural adhesion molecules (NCAM) in healthy and diseased renal tissue

Abstract

Introduction: Kidney performs essential physiological roles that include metabolic waste excretion and maintenance of fluid and electrolyte balance. Different factors may lead to renal dysfunction. Kidney diseases are currently a global public health problem. Fortunately, dialysis and transplantation provide life-saving treatments, but these therapies are rife with limitations. Thus, new ways of therapies, such as stem cell treatment are more than required as an alternative and new glimmer of hope to all nephrology patients. Neural cell adhesion molecule (NCAM) is widely expressed during kidney development and it presents potential marker for renal stem/progenitor cells.

Aim: Aim of this dissertation was evaluation of NCAM presence in different types of renal tissue (normal fetal or adult, and pathologically changed), and comparison and correlation of NCAM expression with already defined stem cell markers in order to more closely characterize renal fetal progenitor cells.

Method: Specifically designed primers were used for reverse transcriptase PCR, after mRNA isolation from fetal, neonatal, adult normal, adult tissues with interstitial fibrosis and tumor tissues, to clarify presence of different NCAM on nucleotide level. Also, Western Blot tests were performed in order to identify expression of different NCAM protein isoforms in healthy and kidney with disease. Further, FACS analysis was done on renal cell lines to correlate NCAM expression with adult renal stem cell markers CD24 and CD133. Co-expression and co-localization of NCAM with other cell surface markers was also examined using immunohistochemistry and double immunofluorescent staining.

Results: Our results showed aberrant NCAM expression in renal tumor tissues as well as in tissue with interstitial fibrosis. Interestingly in both types of mentioned tissues NCAM had co-expression with FGFR1, tyrosine kinase receptor, responsible for cell proliferation and aggressive behavior in some epithelial tumors. Considering NCAM expression on fetal samples possible renal progenitor population cell pool of $NCAM^{+}CD24^{+}$ cells was found, which was not the case with $NCAM^{+}CD133^{+}$ cell pool. Also, we had detected that NCAM molecules were post-trasnaltionally modified.

Namely, all NCAM molecules become polysialylated after induction of mesenchymal cells by ureteric bud tip and condensation of same mesenchymal cells. RT-PCR analyses showed that all cell lines and tissues, except tumor tissues express all 3 major NCAM isofirms NCAM-120, NCAM-140 and NCAM-180.

Conclusion: NCAM-120/140/180 isoforms are present in healthy and diseased kidney tissues. Human fetal renal progenitors can be divided at least in two progenitor cell populations: PSA-NCAM^{+}CD24^{+}CD326^{-} population which will evolve to nephron progenitors and NCAM^{+}PSA-NCAM^{-}CD24^{-}CD326^{-} cell pool which will probably become stromal cells. Thus, polysialylation of NCAM could be a trigger of mesenchymal-epithelial transformation during kidney development. In renal tissues NCAM interacts with different molecules, such as FGFR1 or integrin α5β1, and this interaction probably causes different cell signaling. Precise mechanism of NCAM/FGFR1 interaction in tumors and exact role of NCAM in tumor development are a matter of future investigations. But, since we had detected different localization of NCAM/FGFR1 in tumor cells, expression of NCAM/FGFR1 in different cell compartments could be activating various signaling pathways. NCAM+ renal interstitial cells are significantly increased in the initial phase of renal interstitial fibrosis. They display a morphological heterogeneity concerning co-expression of FGFR1, α5β1 integrin and other molecules relevant for renal interstitial fibrosis, and could be responsible for the regulation of repairing process in renal tissue.

Key words: NCAM, PSA-NCAM, renal progenitors, fetal tissue, CD24, FGFR1, integrin α5β1, RCC, interstitial fibrosis.

Ekspresija neuralnih adhezionih molekula (NCAM) u zdravom i obolelom bubrežnom tkivu

Rezime

UVOD: Bubreg ima značajnu fiziološku ulogu u izlučivanju štetnih produkata metabolizma putem urina, kao i ulogu u održanju ravnoteže vode i elektorlita. Različiti faktori mogu dovesti do poremećaja funkcije bubrega. Bolesti bubrega su trenutno globalni problem javnog zdravlja. Dijaliza i transplantacija su trenutno dominantni vidovi terapije koje se primenjuju u lečenju bubrežne isuficijencije, ali uz puno ograničenja. Novi načini terapije, kao što je tretman matičnim ćelijama, su više nego potrebni kao alternativa standardnim metodama lečenja i predstavljaju novi tračak nade za sve pacijente koji imaju neki oblik bubrežne disfunkcije. Neuralni ćelijski adhezioni molekul (NCAM) je široko ispoljen tokom razvoja bubrega i predstavlja potencijalni marker renalnih stem/progenitorskih ćelija.

CILJ: Cilj ove disertacije je evaluacija NCAM ekspresije u različitim tipovima bubrežnog tkiva (fetalno, adultno normalno i adultno tkivo sa intersticijskom fibrozom i tumorsko tkivo), kao i njena korelacija sa ekspresijom već definisanih markera renalnih stem ćelija kako bi se preciznije definisale fetalne renalne progenitorske ćelije.

METOD: Detekcija različitih NCAM izoformi na nivou nukleotida je vršena primenom RT-PCR metode, nakon izolacije iRNK iz fetalnog i normalnog adultnog tkiva, kao i tumorskog i tkiva sa intersticijskom fibrozom. Prisustvo NCAM isoformi na proteinskom nivou, u pomenutim tkivima detektovano je upotrebom Western blot-a i Imunoprecipitacije. Ko-ekspresija NCAM-a sa CD24 i CD133, markerima adultnih renalnih progenitora ispitivana je upotrebom protočne citomertije (FACS) na renalnim ćelijskim linijama. Imunohistohemijskim i dvostrukim imunofluorescentnim bojenjem ispitivana je koekspresija i kolokalizaciji NCAM-a sa drugim ćelijskim markerima.

REZULTATI: RT-PCR rezultati ove doktorske disertacije su pokazale da sve ćelijske linije i ispitivana tkiva, osim tumorskog tkiva eksprimiraju tri glavne NCAM isoforme NCAM-120, NCAM-140 i NCAM-180. Takođe, detektovana je aberentna-prekomerna NCAM ekspresija u tumorskom, kao i u tkivu sa intersticijskom fibrozom. Interesantan nalaz čini pokazana koekspresija NCAM-a sa FGFR1, tirozin kinaznim receptorom, koji ima ulogu u ćelijskoj proliferaciji i agresivnom ponašanju pojedinih

epitelnih tumora. U ćelijama fetalnog tkiva bubrega uočena je koekspresija NCAM-a i CD24. Koekspresija NCAM-a i CD133 nije uočena. Po prvi put smo dvostrukim imunofluorescentnim bojenjem pokazali prisustvo post-translaciono modfiikovanih polisijalinizovanih formi NCAM-a na ćelijama kondezovanog mezenhima u fetalnom tkivu. Uporednom analizom koekspresije NCAM-a i PSA-NCAM, CD24 i CD326 među mezenhimalnim renalnim progenitorima u fetalnom tkivu mogu se izdvojiti bar dve populacije progenitorskih ćelija: PSA-NCAM^{+}CD24^{+}CD326^{-}, kao prekursori budućeg nefrona, i NCAM^{+}PSA-NCAM^{-}CD24^{-}CD326^{-}, kao prekursori stromalnih ćelija.

ZAKLJUČAK: NCAM-120, NCAM-140 i NCAM-180 izoforme su prisutne u zdravom i obolelom tkivu bubrega. U fetalnom bubrežnom tkivu NCAM biva post-translaciono modifikovan (PSA-NCAM). PSA-NCAM je prisutan na svim ćelijama koje predstavljaju prekursore nefrona, sugerišući da je polisijalinizacija NCAM molekula neophodna u toku mezenhimno-epitelne transfrmacije i procesa diferencijacije bubrega. U tumorskom i tkivu sa intersticijskom fibrozom detektovana je koekspresija NCAM sa FGFR1. Precizna uloga NCAM/FGFR1 interakcije u tumorima, ali i u tkivu sa intersticijskom fibrozom još uvek nije definisana i predstavlja veliki izazov za buduća istraživanja. Značajno povećanje NCAM^{+} ćelija u intersticijskoj fibrozi, kao i koekspresija NCAM^{+} ćelija sa FGFR1 i integrinom α5β1 molekulima koji figuriraju u ćelijskoj proliferaciji i signalizaciji, sugeriše da NCAM^{+} intersticijske ćelije mogu biti od koristi prilikom regeneracije bubrega i kao takve imati primenu u budućoj ćelijskoj terapiji bubrežne isuficijencije.

Ključne reči: NCAM, PSA-NCAM, renalni progenitori, fetalno tkivo, CD24, FGFR1, integrin α5β1, RCC, intersticijska fibroza.

Naučna oblast: Molekularna medicina
Uza naučna oblast: Nefropatologija

UDK broj:

Table of Contents

1. Introduction

The kidney has a major role in maintaining of human health, based on essential physiological functions that include metabolic waste excretion and maintenance of fluid and electrolyte balance. Different factors may affect renal function, whereby kidney diseases can arise during development, juvenile, or adult life. Regardless of changes related to congenital or sporadic diseases, tubuli and/or interstitium are frequently damaged and their normal close mutual relationship could be replaced with an increase in renal interstitial space, the progressive loss of peritubular vascularization and hypoxic damage of the tubules, which further results in tubular atrophy. All these changes mostly lead to interstitial fibrosis i.e. chronic renal failure. Also, cellular damage of the functional units of kidney, known as nephrons, is a common attribute among diverse kidney disorders. Progressive destruction of nephrons culminates in kidney failure. Types of renal disease include acute kidney injury (AKI), which is the abrupt loss of renal function that can often become permanent, and chronic kidney disease (CKD), the progressive loss of renal function that culminates in organ failure known as end stage renal disease (ESRD) (1,2). Kidney diseases are currently a global public health problem. Fortunately, dialysis and transplantation provide life-saving treatments, but these therapies are rife with limitations and place considerable burdens on patients, their families and healthcare systems. Thus, it has become imperative to find alternative ways, new therapies to treat existing kidney dysfunctions and to promote kidney health.

Regenerative medicine offers solutions by using stem cells as novel approach for curing injured kidney. The presence of many renal cell types in kidney poses challenges both to understanding and finding appropriate renal stem cells. Nevertheless, the discovery of regenerative renal cells in adult kidneys, especially those in the nephron tubule and PECs in the glomerulus, provides hope that there are already cell templates and conducive environs where kidney integrity can be restored by promoting regenerative mechanisms (2).

1.1. Neural cell adhesion molecule (NCAM)

NCAM was originally described in 1974 as synaptic membrane glycoprotein D2 in the brain (3), but as a cell adhesion molecule (CAM) it was presented for the first time in 1977 (4). NCAM was the first identified Ca-independent CAM of the immunoglobulin superfamily which mediates homophilic and heterophilic binding to adjacent cells and to the extracellular matrix by cis- and trans-interactions; and later recognized to be expressed on the cell surface of almost all neural cell types in the central and peripheral nervous system.

Thus, NCAM (also known as CD56) belongs to the immunoglobulin superfamily (IgSF). Members of IgSF are group of glycoproteins (transmembrane and membrane-anchored), that are characterized by presence of various number of Ig modules. IgSF molecules are the most heterogeneous group of cell surface receptors, with at least 65 proteins involved in cell adhesion (5). The extracellular part of IgSF molecules contains multiple Ig-like modules connected like beads on a string. Ig-like modules are usually followed by another bindings blocks, fibronectin type III (Fn3) modules (6).

In humans, NCAM is encoded by a single-copy gene on band q23 chromosome 11. NCAM gene includes more than 314 kb and contains 19 major exons as well as 6 additional smaller exons. Alternative splicing of NCAM mRNA can result in 27 different NCAM isoforms (7, 8). Nevertheless, most studied are three major isoforms, referred to as NCAM-120, NCAM-140 and NCAM -180 according to their different molecular weights (8, 10). While the isoform NCAM-120 is anchored to the cell membrane via a glycosyl-phosphatidyl-inositol (GPI) linker (11), both NCAM-180 and NCAM-140 are transmembrane proteins with different lengths of their cytoplasmic domains (C-terminus). On the other side, all NCAM isoforms have similar N-terminus, which contain always 5 Ig-like modules and 2 Fn3 domains; in some soluble NCAM isoforms it is possible to detect only one Fn3 domain (Scheme 1). Now it is known that exons from 1-14 encode N-terminus (5 Ig-like and Fn3 domanis), while exons 17-19 encode intracellular region of NCAM molecules (Scheme 2) (12).

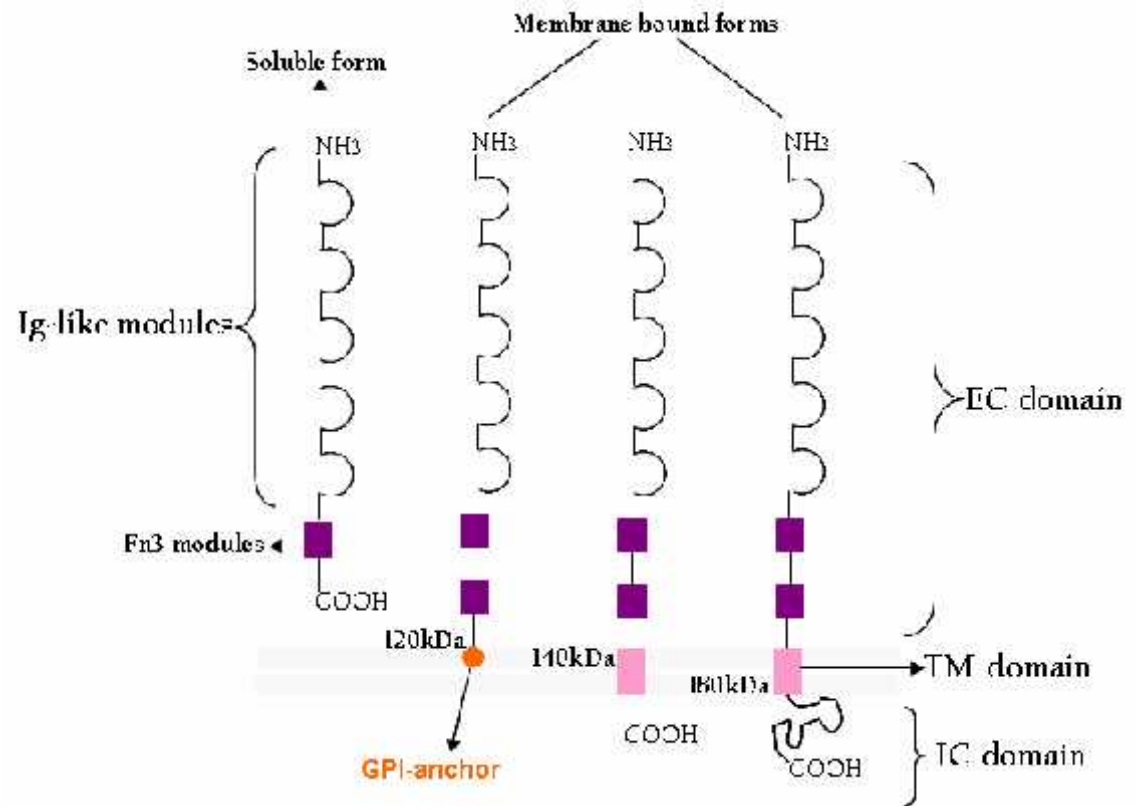

Scheme 1. Graphic display of different isoforms of NCAM. EC- extracellular, TM- transmemembrane, IC- intracellular, GPI- glycosylphosphatidylinositol anchor

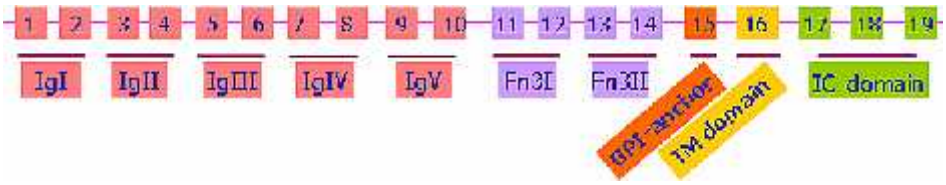

Scheme 2. Graphic presentation of the NCAM gene; exons 1-19 which code 3 major isoforms (12)

NCAM is abundantly expressed during embryonic development, whereas it is found mainly in tissues of neural origin in the adult organism. In past, NCAM was characterized as a mediator of cell-cell adhesion and cell adhesion as one of NCAM function was firstly described. Today there are several models which present how NCAM thru homophilic interaction regulates cell adhesion (Scheme 3). Several studies demonstrated that interactions between NCAM Ig modules, (Ig1, Ig2, Ig3) resulted in zipper like formations that are crucial for homophilic adhesion between two NCAM molecules (13). In addition to cell-cell adhesion, homophilic interaction of NCAM

induces signal transduction, resulting in neuronal differentiation (14, 15) and inhibition of cell proliferation (16, 17). Also, NCAM plays a major role during development of the nervous system, mediating adhesion between neural cells and stimulating neurite outgrowth and asciculation (18-21).

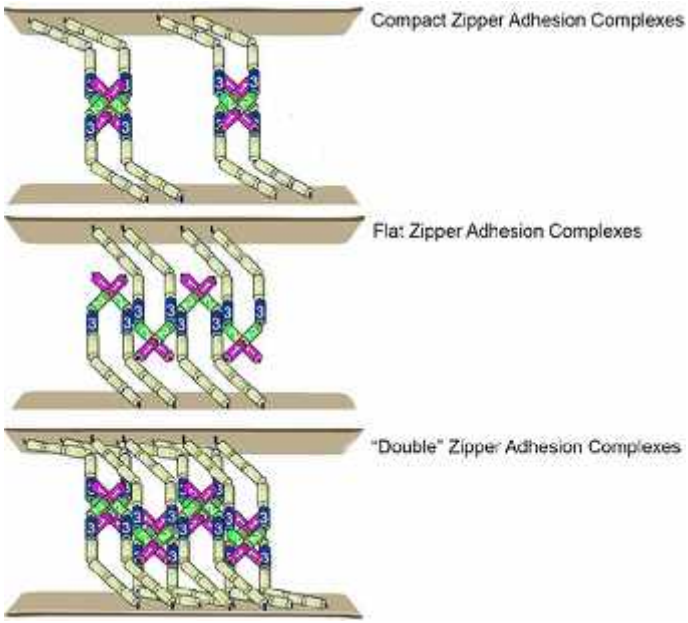

Scheme 3. Schematic presentations of the cell–cell homophilic adhesion models, (designed according to ref.13)

The extracellular and intracellular domain of NCAM can also mediate signaling via heterophilic adhesion. In this type of interaction NCAM interplays with molecules of extracellular matrix such as heparin/heparan sulfate (HSPGs), chondroitin sulfate proteoglycans (CSPG) and different types of collagen (22-25). Also, NCAM mediates signaling transduction through heterophilic dimerization of a broad range of other molecules such as several heterophilic ligands: adhesion molecule L1, fibroblast growth factor 1 (FGFR 1), the glial cell line-derived neurotrophic factor (GDNFR) (26-29).

Variable spectrum of different NCAM roles, as we have seen, is a consequence of NCAM alternative splicing, and its homophilic and heterophilic interactions. But in addition to that, NCAM can be also post-translationally modified by homopolymers of α-2,8-linked N-acetylneuraminic acids (Neu5Ac or NANA), called polysialic acids (polySia, PSA), that are bound at variable numbers to N-glycans on the extracellular fifth immunoglobulin-like domain of the molecule (30). PSA changes of the glycosylation patterns may convert different NCAM isoforms from interactive to anti-

adhesive states (31). The PSA residues can extend beyond the NCAM protein core and provide an enormous hydrodynamic exclusive space of the extracellular part of NCAM that disrupts adhesive properties of NCAM and other interacting adhesive molecules such as cadherins (32). Recent reviews have highlighted that PSA-NCAM is a critical regulator of cell adhesion during neural cell differentiation and migration, neurite outgrowth and correct synaptic targeting of growing axons for regular neuronal circuit formation in the developing nervous system of the mouse embryo (33). In the adult brain, PSA-free NCAM isoforms dominate, whereas PSA-NCAM has been shown to be continuously expressed at sites of synaptic plasticity and neurogenesis. Thanks to all these interactions and modifications NCAM is a crucial molecule in the developing as well as in the adult human brain.

Also, now it is known that NCAM has various roles in other, non neural tissues. Thus, NCAM is considered as specific marker in malignant lymphomas, neuroendocrine carcinomas, Alzheimer's dementia, myeloma and ovarian carcinomas (29, 34-39). Recently it has been shown that in humans, NCAM express 3 major isoforms in healthy adult non neural tissues such as: thymus, testis, pancreas, duodenum and kidney (12).

In kidney, NCAM is widely expressed during development (33), also on rare interstitial cells in adults (40) and on renal tumors (41-44). Thus, in kidney NCAM has a multiple role in mesenchymal-epithelial transformation, migration, proliferation and epithelial-mesenchymal transformation, but the precise molecular signaling mechanisms have not been established yet.

1.2. NCAM and kidney development

The kidney is one of the few organs that undergo mesenchymal-epithelial transition (MET) during development. The metanephric (permanent) kidney develops from a specialized region of the caudal end of the intermediate mesoderm called the metanephrogenic mesenchyme. Reciprocal inductive cellular interactions between the metanephric mesenchyme (MM) and the ureteric bud (UB) are considered to be essential events in the development of metanephric kidney in mammals (45). Thus

interplay between MM and cells at the tip of the branching UB thereby initiates MET of specific multipotent renal progenitor cells (Scheme 4).

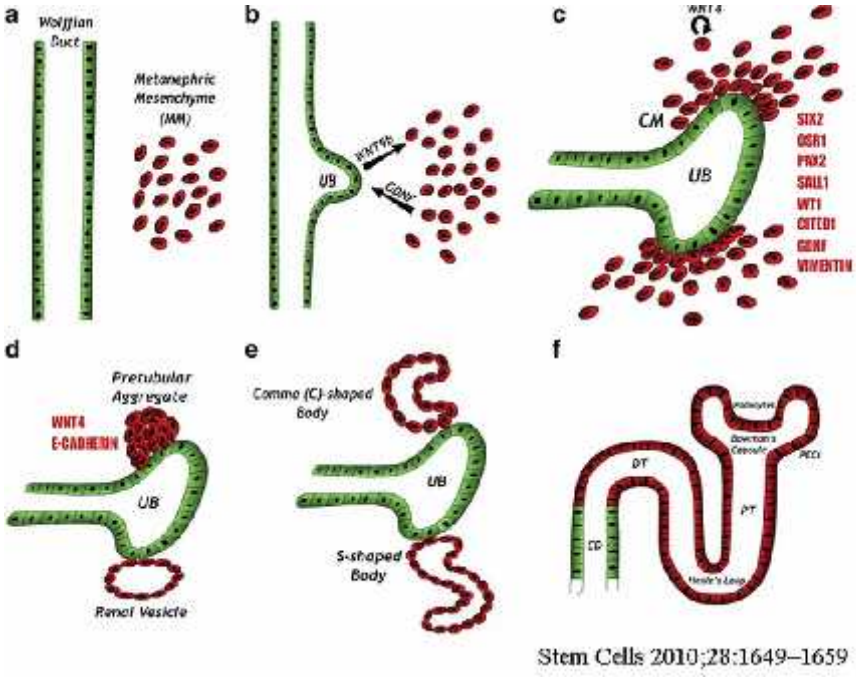

Scheme 4. Mesenchymal-epithelial transition as a result of interactions between MM and UB

The human metanephros, in which renal stem/progenitor cells of the MM are induced to form nephrons until birth, appears as early as at the 5th week of gestation (wg). First, mesenchymal cells induced by cells at the tip of the outgrowing UB start to condense, and form cap mesenchyme. Condensed mesenchymal cells induced by UB start to polarize and form a pre-tubular aggregate (PA), a structure which is known to be one of the first morphologically identifiable stages. Cells in PA continue to grow and form a renal vesicle (RV, the most primitive stage of nephron development: a stage I nephron). RV then elongates, becomes a comma-shaped **(**C) and then an S-shaped body (S) (stage II nephron). Future growth divides S body to distal and proximal part. Distal part of S body makes contact with and fuses with the distal component of the UB, and latter forms the collecting duct. Proximal S body gives rise to capillary loop nephron and Bowman's capsule (stage III and IV). Soon afterwards, endothelial cells invade to make a capillary knot-like outgrowth, the glomerular tuft, which goes on to form the glomerulus (stage V). Together, the Bowman's capsule and the glomerulus comprise the definitive renal corpuscle. The rest of the nephron elongates to form components of the

proximal tubule, the loop of Henle and the distal tubule (Scheme 5). The full complement of glomeruli in the fetal human kidney is attained by 32-34 weeks (46-48).

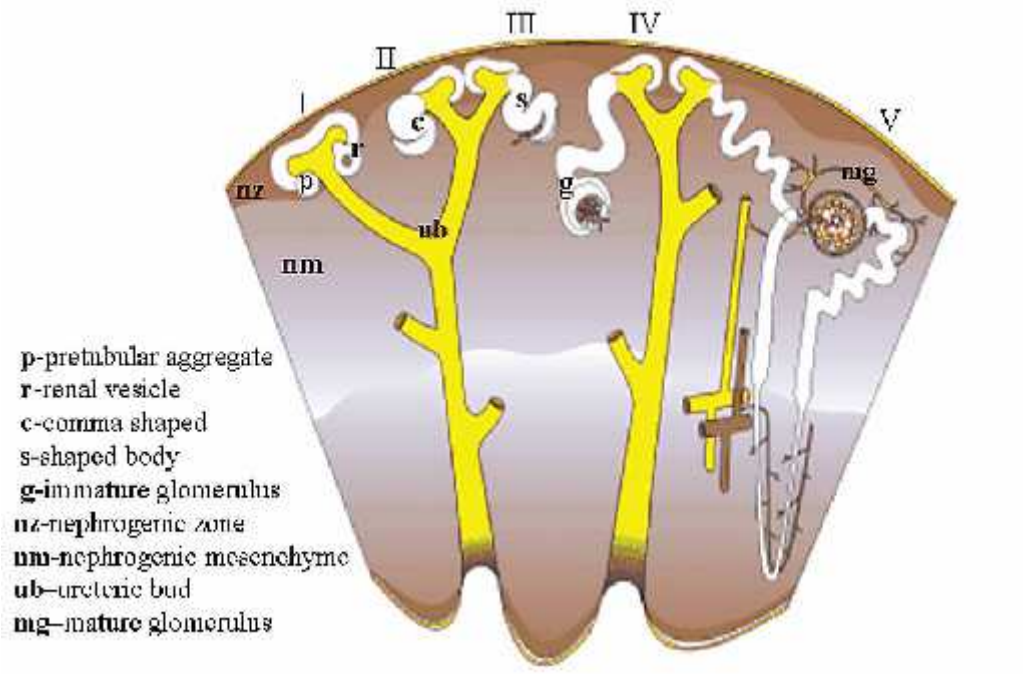

Scheme 5. The development of the nephron, from I-V nephron stage (designed according to www.gudmap.org)

Interestingly, un-induced as well as induced fetal renal MM cells, as well as nephron progenitors (PA, RV, C and S body) are well known to widely express NCAM (33, 49) as specific cell surface antigen up to the prenatal period during kidney development in humans and rats. Induced mesenchymal cells are described to rapidly loose expression of NCAM after MET on immature tubular cells during further differentiation of the nephron (40, 50).

Kidney development, MM-UB interactions and consequent formation of the nephron and the collecting system depend on genetic programs that are highly regulated. Unique renal organogenesis as well as structural complexity of the adult kidney (more than 26 mature cell types) has presented many challenges to the identification and characterization of renal progenitor/stem cells.

1.3. NCAM in renal tumors

Kidney cancers represent about 2% of all cancers in human population. The most common form of renal neoplasms, with the highest mortality rate of the genitourinary cancers in adults is renal cell carcinoma (RCC) (51). In recent decades, the incidence of RCC has been steadily rising by 2-4% each year. In 2010, RCC was diagnosed in 90-95% of all renal neoplasms (52).

RCC originates from tubular structures of the kidney and is classified into four major histological types. Each type differs in origin, genetics, morphology and behavior, metastatic potential and clinical outcome (52-55). Clear cell RCC (cRCC) is the most common type, accounting for about 75-80% of all cases of RCC. Other types are papillary (pRCC, 10-15%), chromophobe (chRCC 5%) and collecting duct (1%) RCC; fifth group presents unclassified RCC (less than 2%). Characteristic of all different RCCs is lack of early warning signs, frequent metastases, and resistance to currently used treatments (54). The prognosis for patients with recurrent and/or metastatic RCC is poor, median survival is 10-13 months and 5-year survival is < 5% after nephrectomy (54-57).

Human RCCs seem to arise from a variety of specialized tubular-epithelial cells located along the nephron; mainly cRCC, pRCC and chRCC originate from proximal and distal tubules. These tubules originate from mesonephros after MET during kidney development. Mesonephros strongly expresses NCAM, so re-expression of NCAM in tumor cell of RCC could be expected. Re-expression of NCAM in RCC was first described several years ago by Daniel et al (44). They showed that NCAM expression is of interest for evaluating the prognosis of patients with cRCCs and for determining a subgroup of patients at high risk for adrenal and CNS metastases. More recently, a study on small group of RCC claimed that NCAM expression is present on RCC regardless to histological type (58). Independent studies of NCAM and of FGFR revealed that both molecules are involved in cell processes such as cell migration, proliferation, epithelial-mesenchymal transformation (EMT), events that transform normal epithelial cell to mesenchymal tumor cell. Also, recent data revealed that NCAM together with FGFR-1 promotes progression of ovarian carcinomas (59, 60).

A better understanding of NCAM role in tumor molecular pathways that lead to tumor appearance and growth may help in the development of new strategies for the early detection and treatment of renal carcinoma.

1.4. NCAM in renal fibrosis

Kidney interstitial fibrosis (IF) can be defined as the accumulation of collagen and related molecules in the renal interstitium. In normal adult kidney basal membranes of the neighboring tubules are closely packed to each other, thus from the morphological point of view renal interstitium in normal kidney represents a virtual space. So, if on routinely stained slides for light microscopy renal interstitium could be seen, this implies some pathological condition. EMT of tubular epithelial cells which are transformed to mesenchymal fibroblasts migrating to adjacent interstitial parenchyma constitutes the principal mechanism of renal fibrosis along with local and circulating cells (61).

Normal human renal interstitium contains rare cells, mainly fibroblasts which could be positive for vimentin or S100-A4 markers. Under normal conditions, the repair process that follows the injury is completed by provisional ECM degradation and by myofibroblast apoptosis, throughout mechanisms subjected to close control. However, in some cases, after kidney damage, activated fibroblasts i.e. myofibroblasts express α smooth muscle actin (αSMA) and then a repair mechanism dysregulation occurs; sustained myofibroblasts play a major role in kidney fibrosis since they produce extracellular matrix rich in collagen fibres, particularly collagen type I and III, that coalesce forming fibrous bundles resistant to degradation (62).

In addition, other renal cells could contribute to interstitial fibrosis such as transdifferentiated tubular (63) or endothelial cells (64) and vascular pericytes (65). Interestingly, Markovic-Lipkovski et al had detected rare neural cell adhesion molecule (NCAM) positive renal interstitial cells that seemed to be increased in incipient phase of renal interstitial fibrosis (40). Considering different hypothesis regarding the origin of interstitial cells in normal kidney, as well as in renal fibrosis (66), it is still a major challenge to investigate molecular markers expressed by these interstitial cells. We

therefore sought to examine co-expression of NCAM and several molecular markers which are relevant for renal fibrosis like fibroblast growth factor receptor 1 (FGFR1), integrin α5β1 and αSMA. FGFRs are a family of four tyrosine kinase receptors and can be activated by their cognate ligands and by direct interaction with NCAM (67). FGFR1 plays multifunctional role in cell proliferation, migration and differentiation (68), and might be involved in epithelial-mesenchymal transdifferentiation (EMT) and renal fibrosis (69). Integrin α5β1 and fibronectin form a prototypic integrin–ligand pair which is functionally very important because it mediates fibronectin fibrilar formation and governs extracellular matrix assembly (70). Strong expression of α5β1 integrin has been previously observed on interstitial cells in patients with IgA nephropathy, suggesting that α5β1 integrin could interact with NCAM and may play a role in the pathogenesis of chronic kidney disease in these patients (71).

1.5. NCAM in renal stem progenitors

Historically, kidney is widely regarded as an organ without regenerative powers, since no new nephrons appear after 36 weeks of gestation in humans (33). Over the past two decades, the phenomenon of renal regeneration has been increasingly investigated and now it is currently speculated that the human kidney can regenerate in some contexts, but the mechanisms of renal regeneration remain poorly understood. Today, numerous groups of researchers re-evaluated problem of identification of multipotent renal stem/progenitor cells. Characterization of renal progenitor cells is important step in developing cell-based therapeutic applications for kidney disease. Two major approaches, which are based on: a) identification of fetal human nephron progenitor cells (hNPCs) or on b) discovery of a hierarchical population of adult renal progenitors cells are currently in focus of investigations.

The fact that NCAM is widely expressed during fetal development and than rapidly lost after birth, classified NCAM as marker for fetal renal stem cells (50). In the human kidney, stem/progenitor cells are induced into the nephrogenic pathway to form nephrons until the 34 week of gestation, and no equivalent cell types can be traced in the adult kidney. (33). In the cited study (33), they proposed several different pools for

renal progenitors. Thus, by FACS sorting in fetal kidney it is possible to found FZD7+NCAM+EpCAM- nephron progenitors, characteristic for C and S body, than NCAM+EpCAM- cell pool, possible stroma progenitors and NCAM-EpCAM+ cells,precursors for UB (33).

Studies that investigate adult renal progenitors and renal repair are increasing every year. In contrary to fetal, adult renal progenitors does not express NCAM/EpCAM cell populations. Nevertheless, adult renal progenitors within the Bowman's capsule which can generate novel podocytes and also proximal tubular cells have been identified (72). This cell express CD24 and CD133 cell surface markers and treatment of acute renal failure with CD24+CD133+ significantly ameliorated the morphologic and functional kidney damage (73). Interestingly, in normal renal tissue a population of CD133+ stem cells able to differentiate *in vitro* and *in vivo* into endothelial and epithelial cells (74). Also, single NCAM+ interstitial cells present in fibrotic tissue may be possible adult renal stem cells (40). Better understanding of renal stem cells, their behavior, origin and their roles in kidney regeneration events, will contribute to create new clinical treatments for kidney disease.

2. Hypothesis/Aim

We expect that NCAM positive renal cells express specific progenitor markers such as CD24, CD133, embryonic transcription factor Six2, GDNF molecule and marker mezenhimalnh stem-cell W8B2, so that these cells may actually be potential renal progenitor cells in the adult kidney and have role in the induction of interstitial fibrosis.

Aim

1. Characterization of the expression of NCAM isoforms in:
    - Fetal kidney tissue
    - Adult healthy kidney tissue
    - Adult - renal tissue with initial interstitial fibrosis
    - Renal cell carcinoma, and
    - Renal - cell cultures

2. Identification and characterization new markers - antibodies to renal cells and tissues, using a new monoclonal antibody W5C4C5, W8B2 - potential of mesenchymal markers as well as potential new antibody for NCAM, W1C3 and 35C9 (obtained in the laboratory of prof. Dr. JH Bühring, University of Tübingen), in order to differentiate potential renal progenitor cells and clarification of NCAM role in the development of kidney.

3. Material and methods

3.1 Human renal tissue

Tissues analyzed in this thesis included different type of renal tissues such as fetal, neonatal and adult samples. Adult samples were divided in: adult normal tissues obtained from not transplanted kidney, adult normal tissues adjusted to tumor, renal tumor tissues and adult tissues collected during routine biopsies. All tissue samples were obtained after informed consent of the parents/patients and the study was approved by the Ethic Committee of the Medical Faculty University of Belgrade (reference number: 29/VI-7). All experiments in this thesis were done partly at the Center for Medical Research, Eberhard Karls University Tübingen and at Institute of Pathology, Medical Faculty, University of Belgrade.

3.1.1. Fetal tissue samples

Twenty one fetal kidneys from 15 to 30 weeks of gestation were obtained during elective or spontaneously occurring abortions at Department of Obstetrics and Gynecology, Medical Faculty of the University of Belgrade. Different kidneys: 15^{th}, 20^{th}, 22^{nd}, 24^{th}, 26^{th}, 28^{th} and 30^{th} week of gestation were analyzed. Two samples of neonatal renal tissue at 36^{th} and 40^{th} week of gestation provided from autopsies at the Institute for Pathology, Medical Faculty of the University of Belgrade were also investigated.

One piece of each sample was conserved in RNAlater (Qiagen Ltd., Germany), a RNA stabilization reagent, for subsequent efficient RT-PCR analysis, the second part of the tissue was put into cell culture medium RPMI 1640 (PAA Laboratories GmbH, Austria) immediately after removal, snap-frozen, and stored in liquid nitrogen or at -80ºC until further analysis, while third part of each sample was put in 4% buffered formalin and embedded in paraffin for immunohistochemistry staining.

3.1.2. Tumor tissue samples

Renal tumor tissue was obtained from 49 patients (29 males, 20 females) undergoing nephrectomy. Among these patients renal cell carcinoma was diagnosed in 36 cases,

oncocitoma in 9 cases, 2 collecting duct carcinoma, one cortical fibroma and one metanephric adenoma. Detailed clinical and pathological information was available for all RCC cases, included histological subtypes, tumor size, nuclear grade (NG) and TNM staging, listed in Table 1. For analyzed oncocitomas clinical features are present in Table 2. The mean age of patients presented in Table 1 and Table 2 was 56.8 years (range 34-87). All renal tumor samples were prepared and stored as it was previously described in the section above (paragraph Fetal tissue samples).

Table 1. Summary of the clinicopathological features in RCC

Case no.	Age	Sex	Tumor size (cm)[#]	Nuclear Grade	Stage
Clear cell RCC					
1	61	F	6	1	pT2NxMx
2	39	M	3,5	1	pT2NxMx
3	58	M	4	1	pT1aNxMx
4	87	F	2,5	1	pT3aNxMx
5	71	M	5,5	1	pT3aNxMx
6	54	M	10	2	pT3bNoMx
7	64	M	9	2	pT3aNxMx
8	46	F	12	2	pT3aNxMx
9	58	M	6	3	pT1bNxMx
10	74	F	5	3	pT3aNxMx
11	44	M	7	3	pT1bNxMx
12	36	M	9	3	pT4N2M1
13	60	F	13,5	4	pT3aNoMx
14	75	F	8	4	pT3aNxMx
15	57	F	8	4	pT3N2Mx
16	64	M	8	4	pT3aNxMx
Multilocular cystic RCC					
1	47	M	4	1	pT1aNxMx
2	34	M	4,5	1	pT1bNxMx
3	44	F	6	2	pT1bNxMx

Papillary RCC					
1	62	M	4,2	1, type I	pT3aNxMx
2	59	M	3	1, type II	pT3aNxMx
3	59	M	6	1, type II	pT3NxMx
4	55	M	4,5	2, type II	pT1bNxMx
5	59	M	3,5	2, type II	pT1aNxMx
6	47	M	4	2, type II	pT1aNxMx
7	59	M	3,5	2, type II	pT1aNxMx
8	50	M	1,5	2, type II	pT1aNxMx
9	55	M	4,5	3, type II	pT3aNxMx
10	65	M	NK	3, type I	pT3bNxMx
11	56	M	10	3, type II	pT3aNxMx
12	48	M	12	4, type II	pT3aNxMx
Chromophobe RCC					
1	43	M	NK	1	NK
2	39	F	5	2	pT1bNxMx
3	60	M	2	2	pT1aNxMx
4	70	F	1,5	2	pT1aNxMx
5	61	M	7	2	pT1bNxMx

- the biggest tumor diameter, NK- not known

Table 2. Summary of the clinical and morphological features in oncocytoma

Case no.	Age	Sex	Tumor size (cm)#
1	61	F	2,0
2	43	F	2,3
3	51	F	2,5
4	60	F	3,5
5	53	M	4,0
6	57	F	6,0
7	59	F	6,5
8	81	F	8,0
9	69	M	9,5

- the biggest tumor diameter

3.1.3. Adult tissue samples

90 kidney biopsy specimens with various forms of glomerulonephritis and glomerulopathies were analyzed in this thesis after the routine diagnostic workup was completed. Paraffin-embedded samples were also further used for immunohistochemistry. The second renal biopsy core was put into cell culture medium RPMI 1640 (PAA Laboratories GmbH, Austria) immediately after removal, snap frozen in liquid nitrogen and stored at -80ºC. In the cases where we had enough tissue, a piece of tissue sample was conserved in RNAlater (Qiagen Ltd., Hilden, Germany), a RNA stabilization reagent, for subsequent efficient reverse PCR (R-PCR) analysis.

Distribution of diagnosis among 90 analyzed biopsies was: lupus nephritis (LN) - 24 cases, focal segmental glomerulosclerosis (FSGS) - 17 cases, membranous glomerulonephritis (MGN) - 13 cases, membranoproliferative glomerulonephritis (MPGN) - 8 cases, renal graft - 8 cases, IgA nephropathy - 6 cases, mesangioproliferative glomerulonephritis (MesPGN) - 5 cases, rapidly progressive glomerulonephritis (RPGN) – 5 cases, minimal change disease - 4 cases.

In addition normal tissue was also obtained from 10 cadaveric kidneys of young healthy donors that were not transplanted and from 4 normal kidney samples adjusted to tumor. These samples were also treated as it was described in section “Fetal tissue.”

3.2. Cell lines

Two human epithelial adherent RCC cell lines were used for analysis of NCAM expression in this thesis. One well characterized clear cell RCC (cRCC) line CRL-1932 (786-0) was obtained commercially from American Type Culture Collection (ATCC, LGC Standards GmbH, Germany), while second cRCC cell line TW33 was established in the laboratory of Professor Gerhard Müller (University of Göttingen, Germany). Different NCAM antibodies tested on these cell lines are presented in Table 3.

Table 3. NCAM antibodies tested on cell lines.

Clone number	Dilution	Source	Binding region	Company/cat. no.*
Eric-1	1:75	Mouse mc	N-terminus	Ancell/208-020
NCAM-OB11	1:100	Mouse mc	C-terminus	Sigma/C9672
EP2567Y	1:150	Rabbit mc	C-terminus	Epitomics/2433-1

*cat.no.-catalog number

Also, embryonic epithelial adherent cell line HEK-293 (ATCC, LGC Standards GmbH, Germany) was used to analyze NCAM expression and expression of other renal cell progenitor markers listed in Table 4.

Table 4. Antibodies tested on cell lines.

Name	Clone	Dilution	Source	Company/cat.no
CD24	8.B.76	1:10	Mouse mc	Santa Cruz/sc-58998
CD133/2	293C3	1:10	Mouse mc	Miltenyi Biotec/130-090-851
FGFR1	M19B2	1:100	Mouse mc	Abcam/ab823
PSA-NCAM	2-2B	1:250	Mouse mc	AbCys S.A./AbC0019
EpCAM (CD326)	9C4	RTU[#]	Mouse mc[@]	"Buehring Lab."[*]
CD34	43A1	RTU	Mouse mc	"Buehring Lab."
W1C3	W1C3	RTU	Mouse mc	"Buehring Lab."

[#]-ready to use supernatant, [@]-mouse monoclonal, [*]-kindly provided by Prof. H.J. Buehring, Tuebingen

The retinoblastoma cell line Weri-Rb-1 was used as positive control (ATCC, LGC Standards GmbH Germany). The cell lines were grown in culture in RPMI1640

medium (PAA Laboratories GmbH, Austria) supplemented with 10% fetal calf serum and refobacin and cultivated at 37°C with 5% CO2.

3.3 Buffers and stock solutions

Phosphate-buffered saline (PBS)

Reagent	*Amount to add (g)**
NaCl	8
KCl	0.2
Na_2HPO_4	1.44
KH_2PO_4	0.24

*- measures for preparation of 1x PBS

PBS can be made as a 1x solution or as a 10x stock. To prepare 1 l of either 1x PBS, dissolve the reagents listed above in 800 ml of H_2O. Adjust the pH to 7.4 with HCl, and then add H_2O to 1 l. Sterilize solution by autoclaving, store PBS on room temperature.

PBS/$MgCl_2$

Reagent	*Amount to add (g)**
NaCl	8
KCl	0.2
Na_2HPO_4	1.44
KH_2PO_4	0.24
$MgCl_2 \cdot 6H_2O$	0.10

*- Measures for preparation of 1L of 1x PBS/$MgCl_2$

Sodium citrate buffer (10mM)

Reagent	*Amount to add*
Trisodium citrate (dehydrate)	2.94 g
dH_2O	1 L

Dissolve trisodium citrate in H_2O and adjust the pH to 6.0 with 1 N HCl. Store at room temperature for 3 or at 4°C for 6 months.

Radio Immuno Precipitation Assay buffer (RIPA)

Reagent	*Amount to add*
NP-40 (20%)	5 ml
Tris HCl 1M	5 ml
SDS (20%)	0.5 ml
NaCl 5M	30 ml
Na-deoxychlorate (10%)	5 ml
dH_2O	50 ml

Tris-Buffered Saline (TBS) 10x

Reagent	*Amount to add*
Tris base	5.6 g
Tris HCl	24 g
NaCl	88 g
dH_2O	900 ml

Adjust the pH to 7.6 with HCl. For a 1X solution, mix 1 part of the 10X solution with 9 parts distilled water and pH to 7.6 again. The final molar concentrations of the 1X solution are 20 mM Tris and 150 mM NaCl.

Tris-Buffered Saline, 0.1% Tween-20 (TBST)

Reagent	*Amount to add*
TBS 10x	100 ml
dH_2O	900 ml
Tween-20	1 ml

FACS buffer

Reagent	*Amount to add*
PBS 1x	500 ml
BSA (10%)	5 ml
Na azide (0.1%)	2.5 ml

Tris/Borate/EDTA Buffer (TBE) 10x

Reagent	*Amount to add*
Tris base	108 g
Boric acid	55 g
EDTA 0.5M pH 8.0	40 ml

Dissolve Tris, Boric acid and EDTA in 800 ml dH_2O and adjust the pH to 8.3 with HCl and then add H_2O to 1 l, autoclave for 20 min. For a 1X solution, mix 1 part of the 10X solution with 9 parts distilled water. Store at room temperature.

2% Agarose gel

Reagent	*Amount to add*
Agarose	2 g
TBE 1x	100 ml

GelRed Staining solution: (keep it in dark)

Reagent	*Amount to add*
Gel Red	15µl
NaCl 1MBoric acid	5ml
dH_2O	45 ml

Solution can be reused 3-4x, store it in dark.

3.4. Immunohistochemistry method

Immunohistochemistry (IHC) staining was used for demonstrating the presence and location of proteins in tissue sections. Fetal, adult and tumor samples were fixed in 4% formalin and embedded in paraffin blocks. Before staining, steps 5 µm thick sections were deparaffinized and dehydrated in xylene and declining series of alcohol (100%, 96%, 70% ethanol). Rehydrated slides were washed in distilled water and blocked for endogenous peroxides with 3% H_2O_2. After blocking, slides were washed 3 times for 5 min in phosphate buffer saline (PBS). Next step in IHC method was heat-induced antigen retrieval with sodium citrate 10 mM, pH 6.0 for 20 minutes in microwave. After cooling for 20 min on room temperature (RT) and rinsing 3 times for 5 min in PBS primary antibodies listed in Table 5 in proper concentration/dilution were applied on slides and incubated for 1 hour on RT. Sections were then again washed 3 times for 5 min in PBS. Further course of IHC staining was carried using EnVision™ Detection System (code K4007, K4009, DAKO, Germany) following staining procedure prescribed by the manufacturer. In brief: HRP labeled anti-mouse or anti-rabbit polymer was incubated for 30 min. After washing, slides were treated with 3,3'-diaminobenzidine (DAB) or 3-amino-9-ethylcarbazole (AEC) as substrate, for 2-10 min at RT and counterstained with haematoxylin (code S3309, DAKO, Germany). Negative controls were performed by omitting the first antibody. Specimens were mounted and coverslipped with aqueous-based mounting medium Faramount (code S3025 DAKO, Germany) and non-aqueous permanent mounting medium, Ultramount (code S1964, DAKO, Germany). The slides were evaluated using the light microscope BX53 with DP12-CCD camera (Olympus, Germany).

Table 5. List of antibodies used in immunohistochemistry staining

No.	Name	Clone	Dilution	Source	Company/ Cat. no.
1	NCAM	123C3.D5	RTU	Mouse mc	Labvision/MS-204-R7
2	WT1	6F-H2	1:50	Mouse mc	Dako/M3561
3	W1C3	W1C3	RTU	Mouse mc	“Buehring Lab.”
4	W5C4C5	W5C4C5	RTU	Mouse mc	“Buehring Lab.”
5	FGFR1	M19B2	1:100	Mouse mc	Abcam/ab823

6	TRA-1-60	TRA-1-60	1:50	Mouse mc	Millipore/MAB4360
7	PSA-NCAM	2-2B	1:100	Mouse mc	AbCys S.A./AbC0019
8	Cadherin 9	/	1:50	Rabbit pc*	Sigma/HPA007167
9	CD34	43A1	RTU	Mouse mc	"Buehring Lab."
10	CD326	9C4	RTU	Mouse mc	"Buehring Lab."
11	CD133	293C3	1:10	Mouse mc	Miltenyi Biotec/130-090-851
12	Aquaporin 1	1/22	1:50	Mouse mc	Abcam/ab9566

*****-polyclonal

3.5. Indirect Immunofluorescence method

3.5.1. Double Immunofluorescence Staining (DIF)

Five µm-thick cryostat sections were treated as it was previously described (75). In brief, frozen sections cut from fetal, neonatal, adult and tumor renal tissue were dried for 1h at RT, fixed in acetone for 10 min. at RT before use for indirect double immunofluorescence labeling. After fixation, slides were incubated for 1h at RT with rabbit monoclonal antibody against NCAM, clone EP2567Y (diluted 1:200), followed by Cy3-conjugated goat anti-rabbit antibody (diluted 1:2000; Dianova). Then, the one of the mouse monoclonal antibody listed in Table 6 in appropriated dilutions was added followed by goat anti-mouse IgG-Alexa 488 (diluted 1:1000, Invitrogen). The cell nuclei were identified by counterstaining with 4,6-diamino-2-phenylindolyl-dihydrochloride (DAPI; 1 µg/ml Sigma-Aldrich, Germany). Negative controls were performed in all experiments by omitting the first antibodies. In each staining experiment cross-binding of the secondary fluorescence labeled antibodies was controlled on specific control slides on which the first or second mAb was omitted. Sections were mounted with Fluoro Preserve Reagent (Calboichem, Germany). All slides were analyzed on epifluorescence microscopy with F-View-CCD camera (Olympus, Germany), on an Axiophot Zeiss immunofluorescent microscope or on a LSM 510 Confocal Microscope with Apotome (Carl Zeiss, Germany). Digital pictures from every fluorescence channel were taken and superimposed for the specific antibody staining, using the software AnalySIS from Soft Imaging Systems (Olympus, Germany)

and the software AxioVision Release 4.8.2 version (Carl Zeiss, Germany) for analysis and documentation. Fluorescence red signal represents NCAM expression, while green signal corresponds to expression of one of antibodies listed in Table 6; yellow to orange signal on merge revealed co-localization of two markers on the single cell.

Table 6. List of Primary mouse antibodies used in DIF staining with NCAM clone EP2567YY

No.	Name	Clone	Dilution	Company/ Cat. no.
1	NCAM	Eric-1	1:100	Ancell/208-020
2	CD24	8.B.76	1:50	Santa Cruz/sc-58998
3	CD133	293C3	1:10	Miltenyi Biotec/130-090-851
4	CD326/EpCAM	9C4	RTU	"Buehring Lab."
5	CD34	43A1	RTU	"Buehring Lab."
6	Ki-67	MIB-1	1:100	Dako/M7240
7	W1C3	W1C3	RTU	"Buehring Lab."
8	W5C4C5	W5C4C5	RTU	"Buehring Lab."
9	W8B2	W8B2	RTU	"Buehring Lab."
10	FGFR1	M19B2	1:100	Abcam/ab823
11	TRA-1-60	TRA-1-60	1:50	Millipore/MAB4360
12	Six-2	H-4	1:500	Santa Cruz/sc-377193
13	PSA-NCAM	2-2B	1:100	AbCys S.A./AbC0019
14	E-cadherin	HECD-1	1:100	Takara/M106
15	Integrinα5β1	SAM-1	1:100	Chemicon/CBL497
16	Cdaherin 9	/	1:100	Sigma/HPA007167
17	Aquaporin 1	1/22	1:100	Abcam/ab9566

3.5.2. Triple Biotin/Streptavidin Immunofluorescente method

Fetal tissue samples were also stained using Biotin/Streptavidin immunofluorescence technique. This staining protocol was used since both primary antibodies were produced

in mouse. After fixation all slides were blocked 15 min. for Streptavidin (Streptavidin/Biotin kit, Vector laboratories, UK), washed and then 15 min. blocked for Biotin (Streptavidin/Biotin kit, Vector laboratories, UK) at RT. After blocking steps, slides were incubated 1 h at RT with PSA-NCAM (diluted 1:400) or TRA-1-60 (1:50) or E-cadherin (1:100). Next step was 30 min. incubation with goat anti-mouse-Biotin (diluted 1:300, BA-9200, Vector laboratories, UK), followed by conjugated Streptavidin-Alexa488 (diluted 1:500, Invitrogen, Germany) for 1h at RT. Then after washing in PBS, slides were incubated over night with one of the previously mentioned mouse mAb (CD24, CD133, CD34, Ki-67, EpCAM, E-cadherin, TRA-1-60) and next day sections were treated with secondary antibody Cy3-conjugated goat anti-mouse antibody (diluted 1:500; Dianova, Germany). Like in DIF method, the cell nuclei were identified by counterstaining with 4,6-diamino-2-phenylindolyl-dihydrochloride (DAPI; 1 µg/ml, Sigma-Aldrich, Germany). Negative controls and cross-binding controls were performed as it is described in DIF staining. Sections were mounted with Fluoro Preserve Reagent (Calboichem, Germany). All slides were analyzed on an Axiophot Zeiss immunofluorescent microscope or on a LSM 510 Confocal Microscope with Apotome (Carl Zeiss, Germany) using the software AxioVision Release 4.8.2 version (Carl Zeiss, Germany) for analysis and documentation.

3.6. Western Blot (WB)

Protein extracts from renal tissues were obtained by dissolving 50 x 20 µm thick frozen tissue sections in 500 µl RIPA (Radio Immuno Precipitation Assay buffer) extraction buffer (1% Triton-X100, 0,5 % sodium deoxycholate, 0,1 % sodium dodecyl sulphate, 150mM sodium chloride and 50mM Tris, EDTA 5mM, pH 8.0) for 60 min. on ice. Protein extracts from cell lines were prepared using 1 x 10^7 cells per 1 ml RIPA buffer. Afterwards the tissue and cell lysates were treated with ultrasound and centrifuged for 10 min. at 13000 rpm. Supernatants were harvested. Roti-Nanoquant protein quantization assay (Carl Roth, Germany) as a modification of Bradford's protein assay was used to determinate protein concentration in samples. Assay was performed according to manufacturer's instructions. Concentration of each sample was determined; samples were frozen at -80°C until further analysis. Samples containing equal amounts

of proteins in lysates were separated on NuPAGE Novex SDS-PAGE 4-12 % Bis-Tris Mini Gels (Invitrogen, USA). Sample preparation and run conditions were prescribed by Invitrogen protocol. After electrophoresis, separated proteins were transferred into 0,45 mm PVDF (polyvinylidene difluoride) transfer membrane (Millipore, USA). Non-specific protein binding sites were blocked with 5% milk solution in 1x Tris Buffer Saline Tween 20 (TBST) for 1 h at RT. Thereafter the membranes were probed with antibodies listed in Table 7 overnight and subsequently washed with 1x TBST for 15 min. Anti-Rabbit antibodies were detected by a goat anti-rabbit IgG antibody conjugated with horseradish peroxidase (HPR), diluted 1:20000 (GeneTex, Inc, USA), anti-mouse antibodies except PSA-NCAM were detected by rabbit anti-mouse IgG/HRP diluted 1:8000 (Dako, Germany). PSA-NCAM antibody was detected with goat anti-mouse IgM/HRP conjugated antibody dilution 1:10000 (Jackson ImmunoResearch, USA). The immmunoreactive bands were visualized on high performance chemiluminesence film (code, 28-9068-35 GH Healthcare Limited, UK), after the membrane was incubated with RapidStep ECL Reagent (code 345818, Calbiochem, USA).

Table 7. List of primary antibodies used for Western Blot

Name	Clone	Dilution	Source	Company/cat.no
NCAM	EP2567Y	1:5000	Rabbit mc	Epitomics/2433-1
NCAM	Eric-1	1:100	Mouse mc	Ancell/208-020
NCAM	OB11	1:100	Mouse mc	Sigma/C9672
PSA-NCAM	2-2B	1:1000	Mouse mc	AbCys S.A./AbC0019

3.7. Immunoprecipitation (IP)

Fetal tissue lysates were tested for IP too. Sigma-Aldrich Protein A sepharose was used as carrier-agarose affinity beads for precipitation of antibody-NCAM, clone EP2567Y (1:100) and for antigen-containing sample-proteins in tissue lysate. Tissue lysates and antibody samples were incubated 3 h at +4°C on MACS-mix, tube rotaror (Miltenyi Biotec, Germany). After that, samples were centrifuged at 12000 g for 2 min. at +4°C. Non-bound sample components are washed away in PBS-MgCa. Lysate-precleaning supernatant and antibody pellet were incubated overnight at +4°C on MACS-mix. Next day samples centrifuged at 12000 g for 2 min and pellet-precipitate was 3x washed in

PBS-MgCa. Further precipitate was re-suspended in 20µl PBS-MgCa and run on electrophoreses, prescribed by Invitrogen protocol, described above in Western blot procedure. As primary antibody PSA-NCAM diluted 1:500 was used, and detected by goat anti-mouse IgM/HRP conjugated antibody dilution 1:10000 (Jackson ImmunoResearch, USA). The immmunoreactive bands were visualized as it is described in Western blot.

3.8. Flow cytometric analysis (FACS)

The adherent RCC and fetal cell lines were harvested by incubation for 2-3 minutes with Trypsin (code T4424, Sigma-Aldrich, Germany). After blocking of non-specific binding 10 min on 4°C with 10 mg/mL polyglobin (Gamunex 10%, Talecris Biotherapeutics, USA), cells were incubated for 15 min, 4°C with 25 µL of proprietary antibodies listed in Table 3 and Table 4. For combined indirect extracellular and intracellular staining, cells were first labeled with non-conjugated antibody and then stained with goat anti-mouse/anti-rabbit secondary antibody for 15 min. After incubation time cells were washed twice in FACS buffer containing PBS supplemented with 0.1 % bovine serum albumin and 2.5 ml of 0.1 % sodium azide and used for flow cytometry. Cells labeled with proprietary mice antibodies were stained with 10 µl of 1:25 diluted F(ab')2 fragment of R-phycoerythrin (PE) conjugated goat anti-mouse antibody (code R0480, Dako, Germany), or with FITC-conjugated goat anti-mouse IgG, dilution 1:200 (code 115-096-146, Dianova, Germany) as the secondary antibody. Cells labeled with rabbit antibody were stained with 10 µl of 1:100 FITC-conjugated goat anti-rabbit IgG (code 111-096-144, Dianova, Germany). Two washing steps were performed before measuring the cells. As negative and positive controls, the mouse monoclonal antibodies W6/32HK and W6/32HL respectively were used. The extracellular and intracellular expression of NCAM and other stem cell markers was assessed on cell lines by BD FACSVerseTM flow cytometry and FACSAria cell sorter (Becton Dickinson, Germany). FACS files were analyzed using the available software BD FACSDiva 6.1.3 (Becton Dickinson, Germany) or FlowJo (Milteny Biotec, Germany).

3.9. RNA extraction

Total RNA extraction from cell lines and tissues was carried out using TRIzol (code 15596-018, Invitrogen, Germany) and RNeasy Mini Kit (code 74106, Qiagen, USA). Amount of cells used for RNA extraction was 1 x 10^6, while tissue samples were between 25-50 mg per sample. In each sample 1 ml of TRIzol was added, vortexed and incubated with of 5 min at RT. After incubation, 200 µl chloroform (code 15593-31, Invitrogen) was added and centrifuged 15 min on 12383 rpm on 4ºC. Liquid phase was

carefully collected. Further steps were performed following the guidelines specified in the RNeasy Mini Kit protocol. The concentrations of isolated RNA were measured on a NanoDrop spectrophotometer (Thermo Scientific, USA). RNA samples were now stored on – 70ºC until further analysis.

3.10. Reverse Transcriptase reaction

Isolated total RNA samples were transcript to cDNA using Super Script III First-Stand Synthesis System (code 18080-051, Invitrogen, Germany). Amount of RNA sample pro sample was 1 pg – 5 µg. All components were centrifuged before use and added in specified volume for each sample:

Component	Volume (µl)
RNA (till 5 µg)	n
10 mM dNTP-mix	1
Oligo $(dt)_{12-18}$(0,5 µg/µl)	1
DEPC-H_20 (fill to 10 µl)	n
End Volume	10

Samples were then incubated 5 minutes on 65°C. Denaturation was ensured putting samples on ice for 60 seconds. cDNA synthesis mix (10 µl/pro sample) was added to the samples after cooling and incubated on 50°C for 50 min.

cDNA Synthesis Mix:

Component	Volume (µl)
10X RT buffer	2
25 mM MgCl2	4
0.1 M DTT	2
RNaseOUT™ (40 U/µL)	1
SuperScript® III RT (200 U/µL)	1

Termination of reaction was done by putting probes on 85°C for 5 min, then 1 min on ice. To remove leftovers of RNA, samples were incubated with Rnase H (1 µl pro

sample) for 20 minutes on 37°C. Until PCR amplification cDNA probes were stored on 80°C. In further PCR analysis we have used maximal 2 µl of cDNA pro reaction.

3.11. RT-PCR amplification

For specific amplification of NCAM-120,140 and 180 kDa mRNA the primers listed in Table 8 were used. NCAM isoforms were analyzed in fetal, adult and tumor tissues. For each amplification 500ng cDNA pro sample was used for PCR reaction. Amplification was performed using Veriti® 96-Well Fast Thermal Cycler (Applied Biosystem, USA) starting with an initial denaturation step at 94°C for 10 minutes and followed by 35 PCR cycles, each of which consisted of denaturation at 94°C for 60 seconds, annealing at 55°C for 60 seconds, and extension at 72°C for 1 min and 30 seconds. The last cycle was terminated by a final extension at 72°C for 10 minutes. A 316 bp fragment of Beta-actin (Table 10) was also amplified by RT-PCR as the internal control.

Table 8. List of specific primers used for amplification of NCAM isoforms and β-actin

NCAM Variant	**Forward primer 5' to3'**	**Reverse primer 5' to3'**	**Product Size**	**NCBI referent sequence**
NCAM -120	GAACCTGATCAAGCAGG ATGACGG	CTAACAGAGCAAAAGAAGA GTC	321bp	NM_0010766882.2
NCAM -140	GTCCTGCTCCTGGTGGTT GTG	CCTTCTCGGGCTCCGTCAGT	264bp	NM_000615.5
NCAM -180	CGAGGCTGCCTCCGTCAG CACC	CCGGATCCATCATGCTTTGC TCTC((REF)	336bp	GenBank AK056258.1
B-actin#	CCATCACGATGCCAGTGG TA	TCAGAAGGATTCCTATGTG GGC	316bp	NM_007393.3

primers of ß-actin control amplification

AmpliTaq Gold DNA polymerase (250 Units, 5U/µl) with GeneAmp 10x PCR Gold Buffer and $MgCl_2$ solution (code 4311806, Applied Biosystems, USA) and GeneAmp®

dNTP Blend/100 mM (code 4303443, Applied Biosystems, USA) were used for all PCR reactions.

PCR mix for NCAM isororms pro sample:

Component	Volume
cDNA	500 ng
10x PCR Gold	5 µl
25 mM $MgCl_2$	4 µl
100 mM dNTP's	0.8 µl
Gold Taq (2,5 U)	0.5 µl
Preimer F (10 pmol/µl)	1.5 µl
Preimer R (10 pmol/µl)	1.5 µl
Water (fill to 50 µl)	/

Each amplification product was run for 30 minute on 80V and 80mA on a 2% agarose (code A9539 Sigma Aldrich, Germany) and stained with GelRed (code 41003, Biotium, USA) 30 min. in dark on RT to monitor for specificity on UV transilluminator.

3.12. Sequencing

DNA quantity of amplified NCAM RT-PCR products was checked by BigDyeTerminator v1.1 cycle Sequencing Kit (code 4337450, Applied Biosystems, USA). Cleanup of PCR products before sequencing was done using ExoSAP-IT (code 78201, Affymetrix, USA).

Sample preparation of cDNA for Sequencing:

Component	Volume
cDNA	20 ng
2.5x RR* Premix	2 µl
5x BigDye SB**	1 µl
Primer F or R (3.2 pmol/µl)	0.32 µl

Water (fill to 10 µl) /

*-Ready Reaction

**-Sequencing buffer

Cycle Sequencing was performed using Veriti® 96-Well Fast Thermal Cycler (Applied Biosystem, USA) starting with an initial denaturation step at 96°C for 1 minute and followed by 25 cycles, each of which consisted of denaturation at 96°C for 60 seconds, annealing at 50°C for 5 seconds, and extension at 60°C for 4 min. The last cycle was terminated by a rapid thermal ramp to 4°C and hold until ready to purify. Cleaning of sequencing single DNA product was done in 96 well sequencing plate using NaOAc/EDTA buffer (code S2080, Teknova, USA). After centrifuge on 1500 rpm for 5 seconds, samples were washed in 100% ethanol and centrifuged at 3000 rpm for 30 min, and then 5 min with 80% ethanol again on 3000 rpm. Purified single-stranded DNA products were sequenced using Sanger sequencing method and their compatibility was compared with NCBI referent sequence for each NCAM isoform: NM_0010766882.2 for 120 kDa, NM_000615.5 for 140kDa and GenBank AK056258.1 for 180 kDa using CodonCode Aligner software (Appendix 1).

3.13. Assessment of NCAM+FGFR1+ cells in renal tumors

Co-localization of FGFR1 and NCAM on the same tumor cell was assessed by number of positive cells with respect to the total quantity of cells assessed by DAPI nuclear staining, expressed on four-value discrete scale (scores 0, 1, 2 and 3):

0 - no $FGFR1^+/NCAM^+$ tumor cells;

1 - less than 30% $FGFR1^+/NCAM^+$ cells;

2 - 30 to 60% $FGFR1^+/NCAM^+$ cells;

3 - more than 60% $FGFR1^+/NCAM^+$ cells.

Co-localization was quantified by the consensus of two observers (J.M.L. and S.C.). Fluorescence green signal represents FGFR1 expression and red signal NCAM expression; while yellow to orange signal on merge revealed co-localization on the single cell.

3.1.4. Assessment of interstitial fibrosis (IF) and number of NCAM+ cells

Immunostaining for NCAM+ interstitial cells was evaluated, by light microscopy in a blinded fashion, as a number of positive cells per field of view on the magnification x400 in the region of fibrosis. Extension of IF in renal biopsy samples was semi-quantitatively assessed applying a scale from 0 to 3 with 0 meaning no IF, 1 – less than 25% of renal tissue with IF, 2 - 25% to 50% of renal tissue with IF, and 3 - more than 50% of renal tissue with IF cells.

3.15. Statistical analysis

Statistical analysis was performed using the IBM SPSS software, version 20.0. After applying Kruskall- Wallis test and Mann-Whitney test, *P* values <0.05 were considered to be significant. Graphs were made using Microsoft Office Excel and R statistical environment software packages.

4. Results

4.1. Cell density in culture affect NCAM expression on HEK-293, CRL-1932 and TW33 cell lines

Flow cytometry tests were done on fetal-tumor (HEK-293) and adult-tumor cell lines (WT33 and CRL-1932). Weri-Rb1, retinoblastoma cell lines were used as positive control for NCAM expression. FACS measuring was repeated on same cell types (3x for each cell type) at different cell density. In the first round cells were prepared for FACS when their density was between 40-50% of flask volume/surface, in the second group measuring was done at cell density over 70%. Cell cultures of TW33 did not show any diversity/difference in low or high density cell cultures groups, also in TW33 culture all live cells were grouped only in one population. Unlike to TW33, HEK-293 and CRL-1932 in high density culture had 2 separated populations (big and small) of live cells.

On HEK-293 fetal cell line, in culture at low density (40-50%) and in bigger population with high density NCAM/clone Eric-1 (16.8%), W1C3 (4.2%) (Figure 1A, 1B) and EpCAM (Figure 4A) were slight positive. Interestingly in HEK-293 cell culture at high density (over 70%, in smaller population/pop2) expression of NCAM, clone EP2567Y was distinctly stronger (23.33% of total cell population), while PSA-NCAM showed weak positivity, 4.83% of total cell population (Figure 2), unlike in big population and in low density culture PSA-NCAM was negative (Figure 5A). Green signal on Fig. 2 represents tested cell surface markers: ep-180/EP2567Y, PSANCAM, negative control with secondary antibody/FMO_R and positive control with antibody W6/HL, while red signal represents unstained cells.

Fetal, HEK-293 cell lines were also tested for renal stem markers, such as: CD24, CD133. Both stem cell markers were negative on HEK-293 cell line (Figure 3A, 3B).

Hematopoietic stem cell and endothelial cell marker CD34 (Figure 4B), as well as tyrosine kinase receptor FGFR-1 (Figure 5B) was also analyzed on HEK-293 cell.

Thus, in our results, after FACS measuring, HEK-293 live cells did not have expression of CD34 or FGFR-1.

Unstained cells as negative control and cells stained only with secondary antibody are presented in Figure 6.

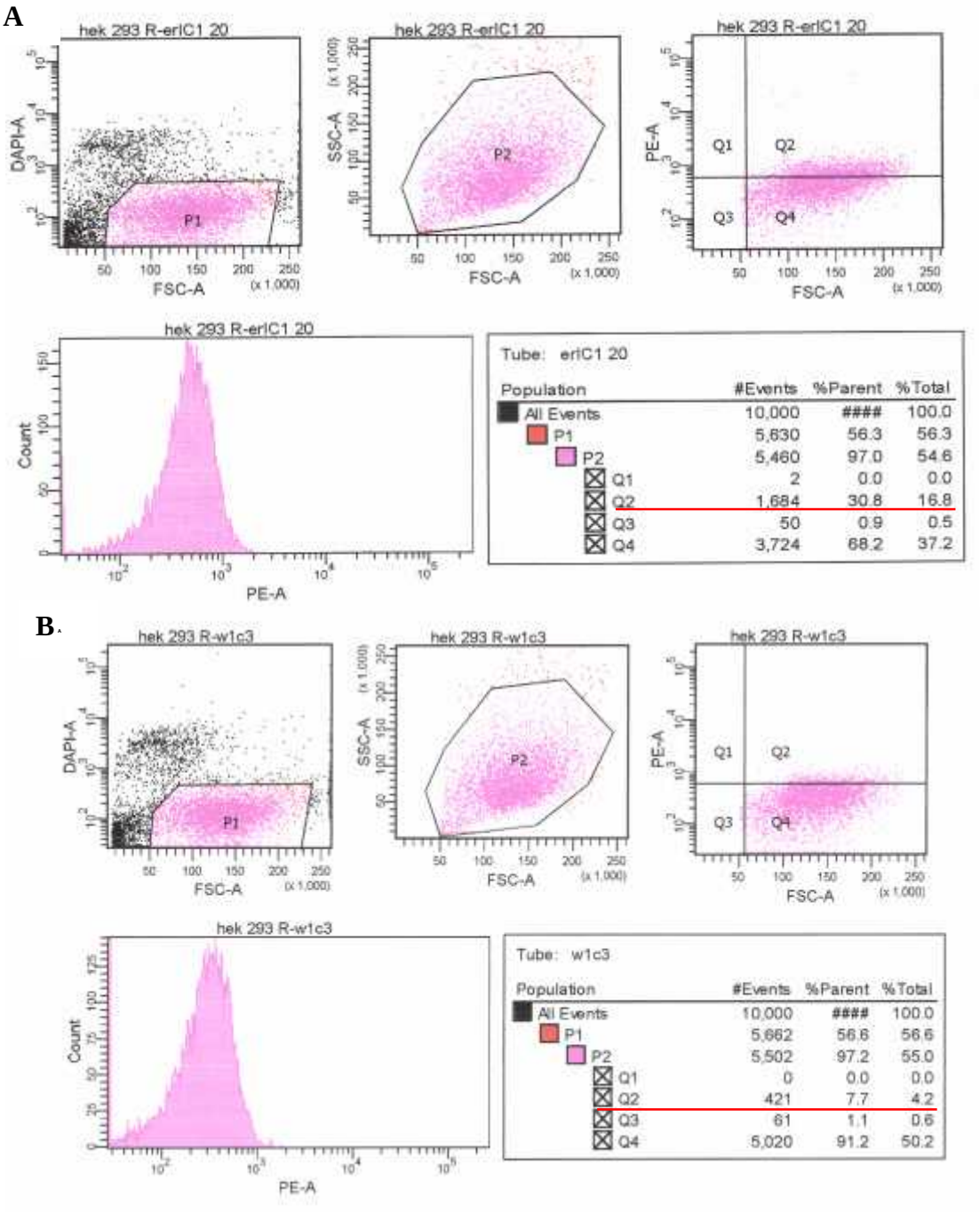

Figure 1. Extracellular FACS analysis on HEK-293 cell line (40-50% density): A) expression of NCAM/Eric-1 and B) W1C3.

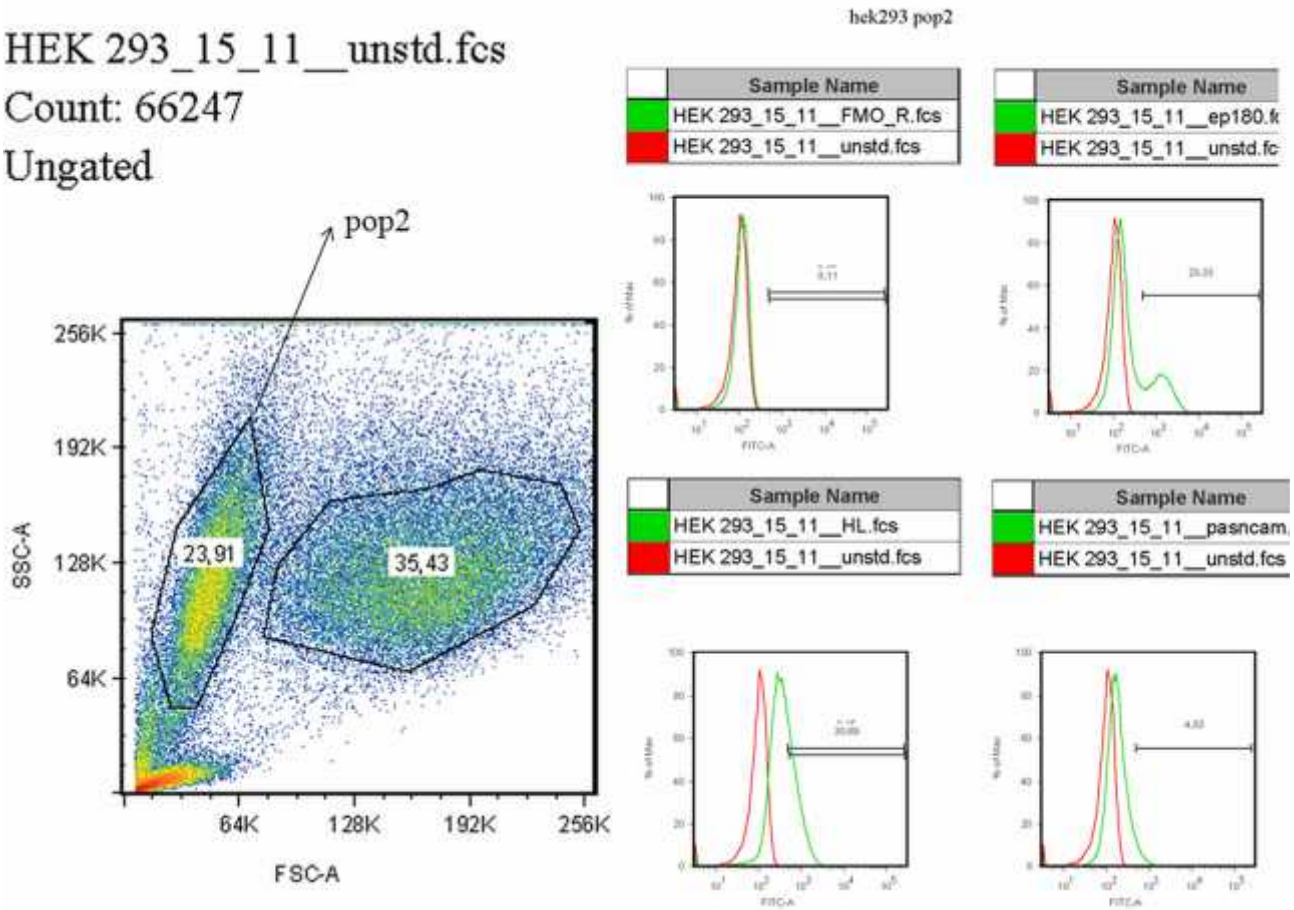

Figure 2. Expression of NCAM, clone EP2567Y and PSA-NCAM in high density population of HEK-293 cell lines.

Tumor cell lines, CRL-1932 had in culture with density over 70% two cell populations, big and small. Expression of NCAM in big population was like in cell culture with density 40 to 50%. Two different NCAM clones (Eric-1, EP2567Y, W1C3 as potential new clone for NCAM and PSA-NCAM were analyzed in CRL-1932. All these markers in bigger populations were negative (Figure 7). While, in small population expression of NCAM/EP2567Y was remarkably stronger 57.07% and other markers (NCAM/Eric-1, W1C3 and PSA-NCAM) had weak expression around 2% of total cells in small population (Figure 8, pop2).

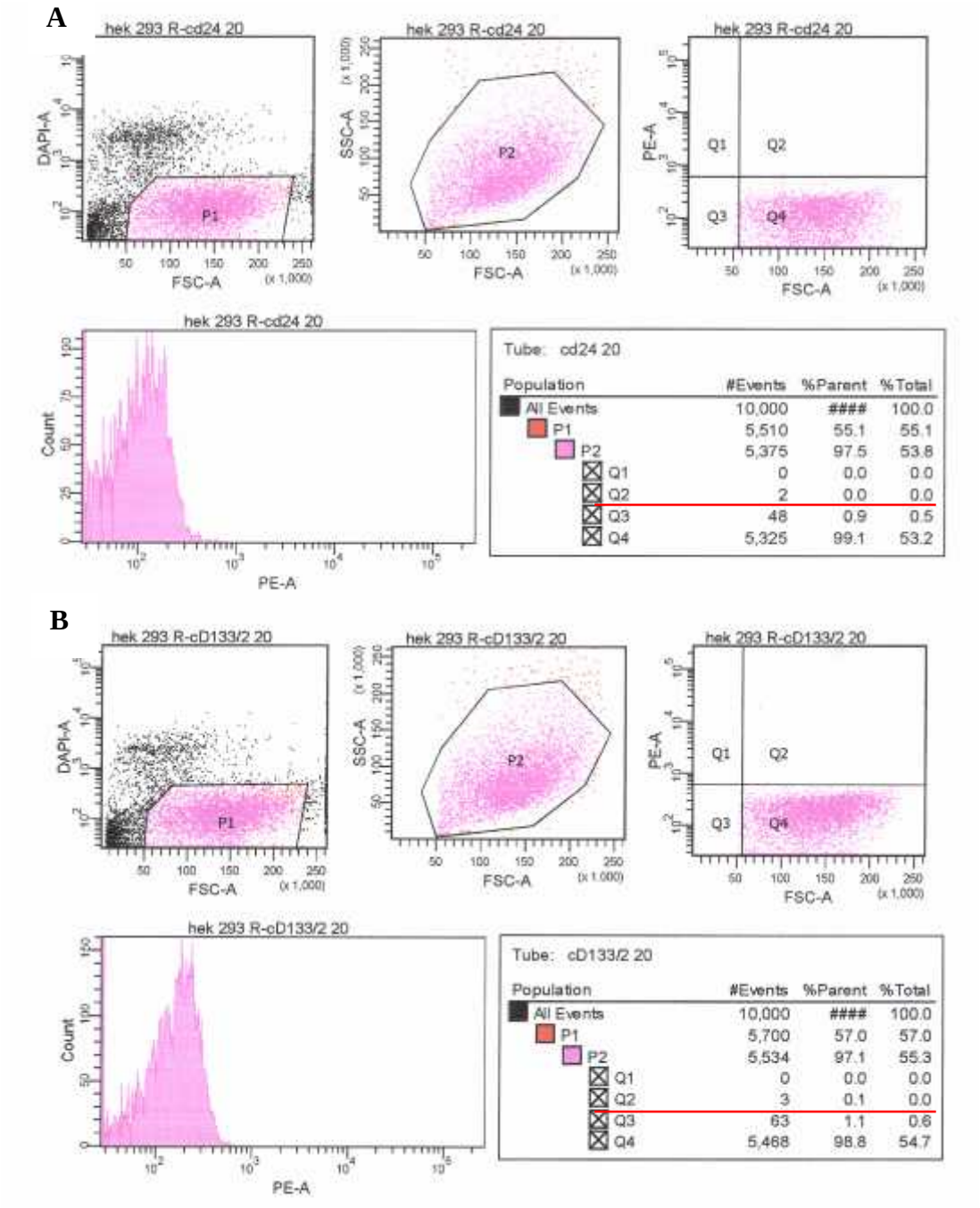

Figure 3. Extracellular FACS analysis on HEK-293 cell line (40-50% density): expression of renal stem markers CD24 (A) and CD133 (B).

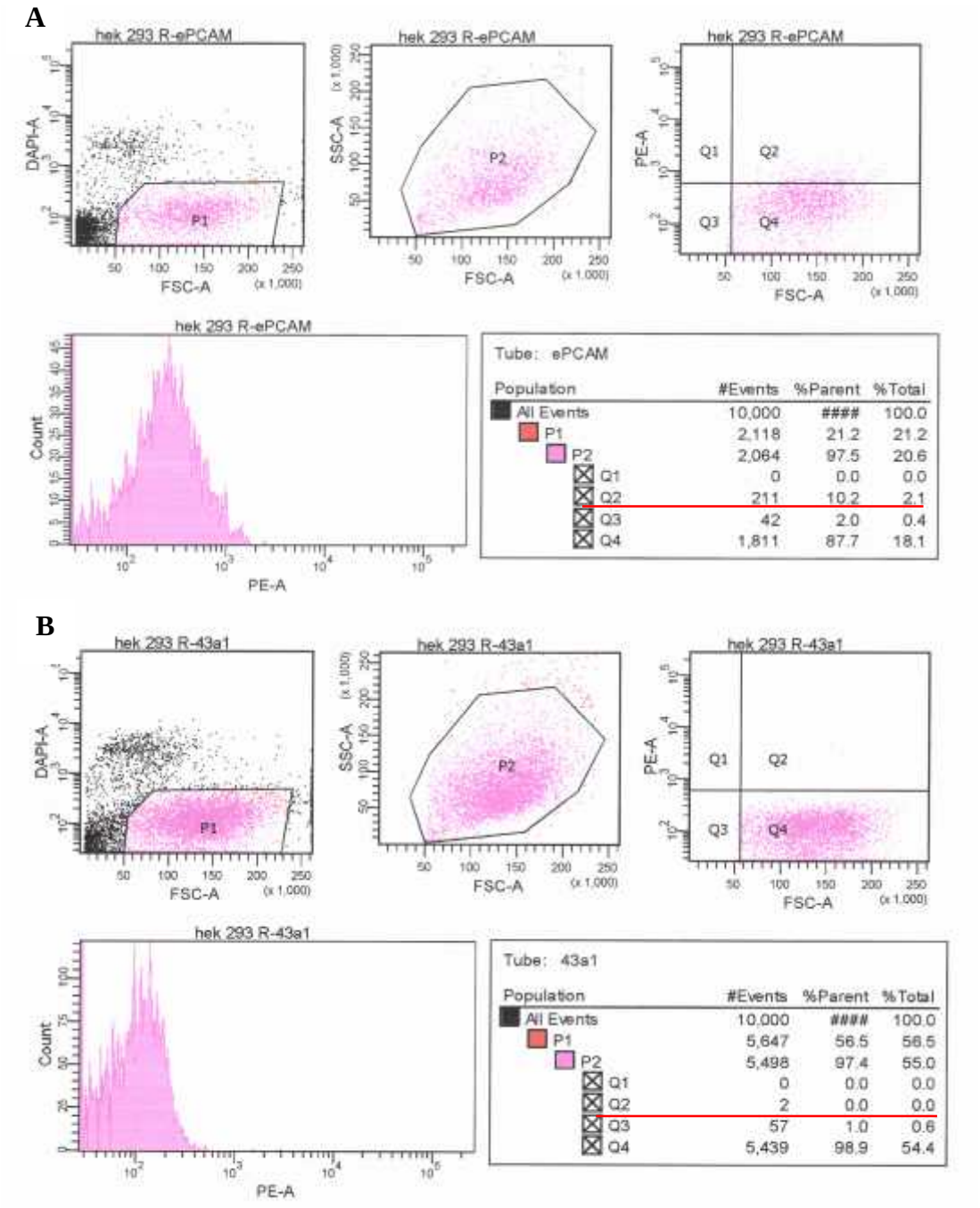

Figure 4. Extracellular FACS analysis on HEK-293 cell line (40-50% density): expression of EpCAM (A) and CD34 (B)

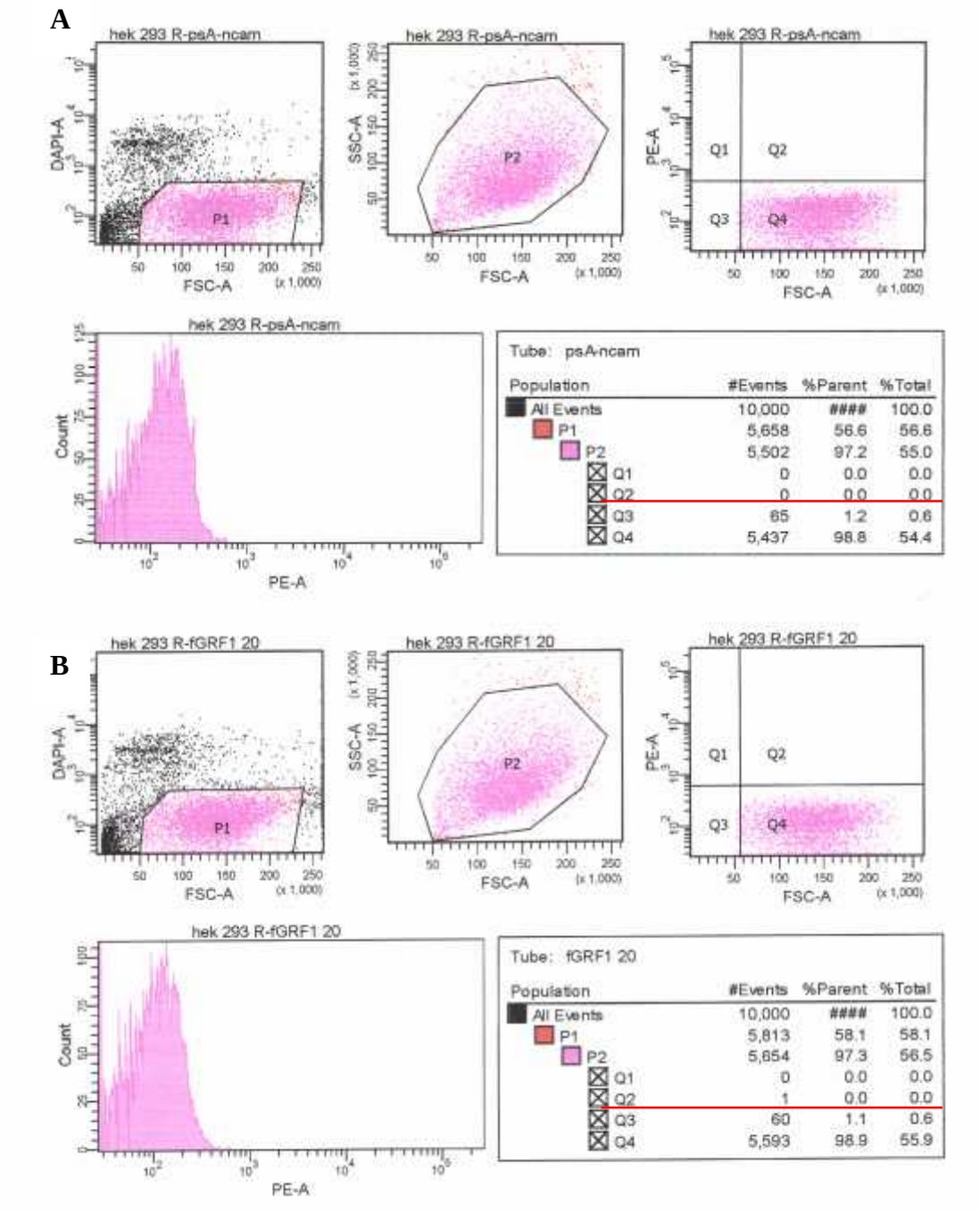

Figure 5. Extracellular FACS analysis on HEK-293 cell line (40-50% density): expression of PSA-NCAM (A) and FGFR-1 (B)

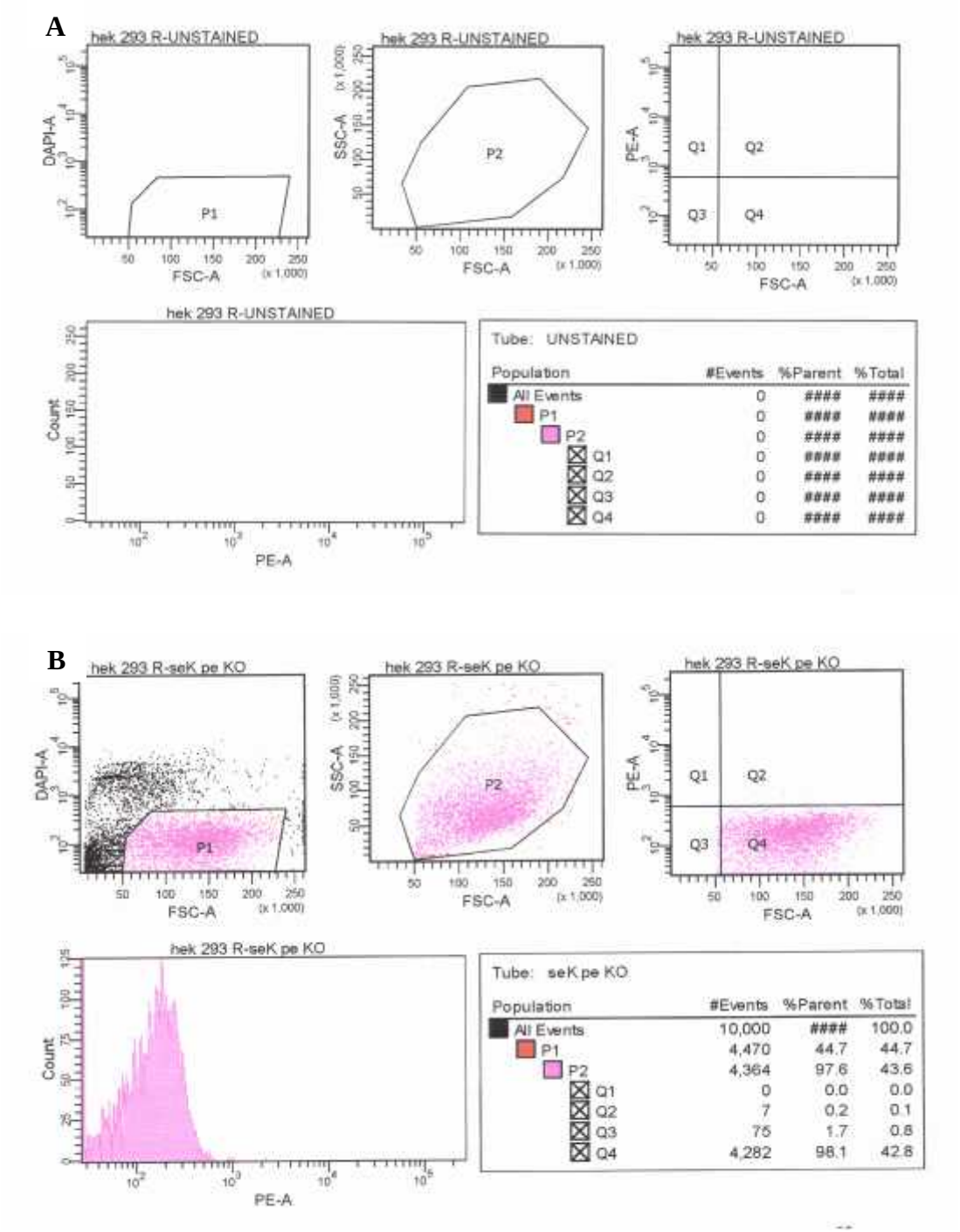

Figure 6. Extracellular FACS analysis on HEK-293 cell line (40-50% density): unstained cells (A) and secondary antibody control (B)

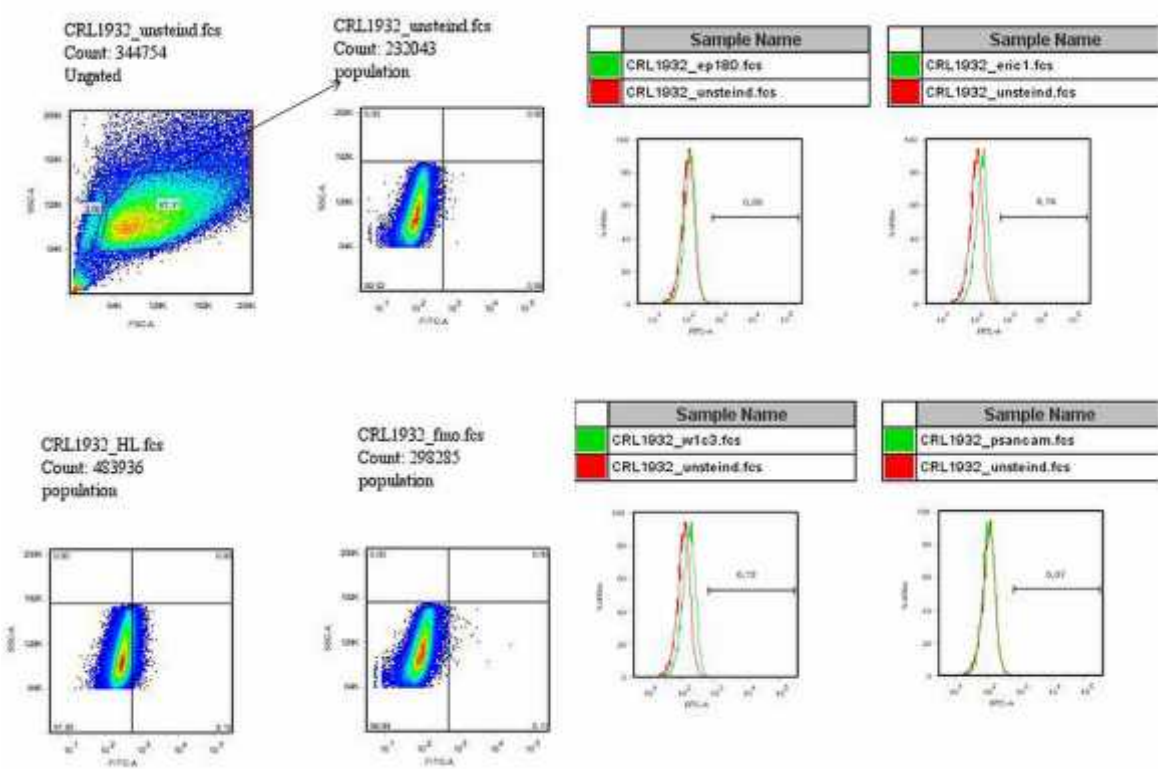

Figure 7. Intracellular FACS analysis on CRL-1932 cell line in bigger population, cell density over 70%

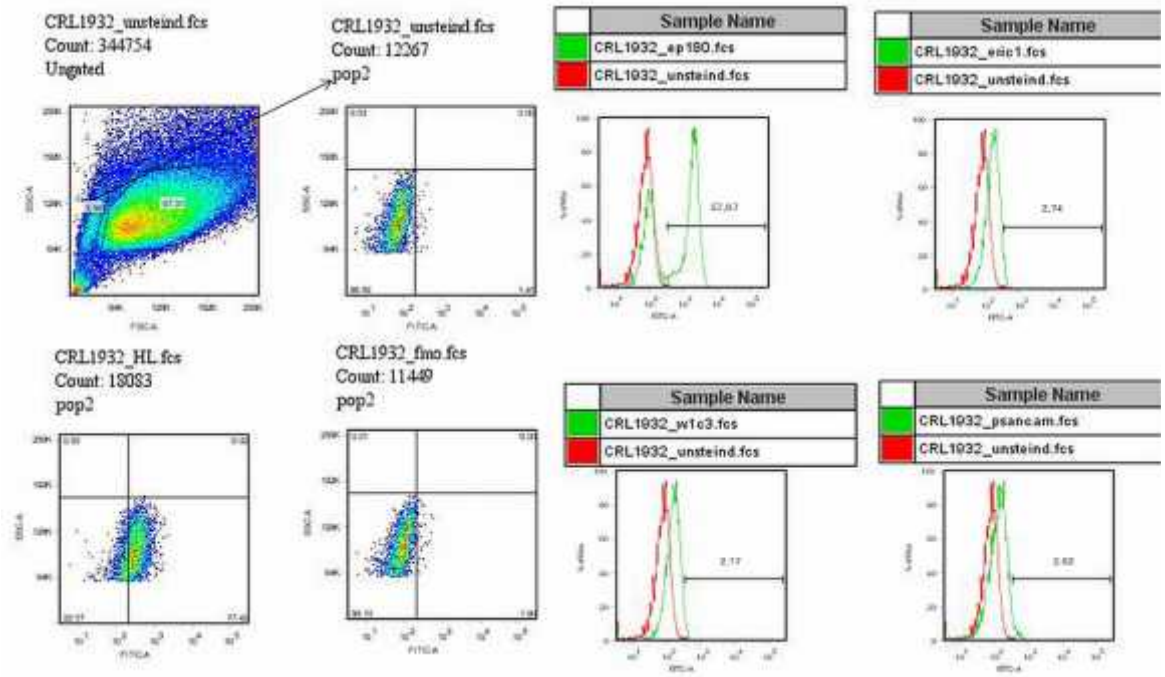

Figure 8. Intracellular FACS analysis on CRL-1932 cell line (cell density over 70%, small population/ pop2)

Nevertheless, TW33 tumor cell lines had one population in cases with density between 40-50% and in culture with density over 70%. In low density culture and in big population of high density CRL-1932 cell culture abtybodies EP3567Y, Eric-1, W1C3 and PSA-NCAM were negative (data not shown). While in high density culture, NCAM/EP3567Y had significantly stronger expression (44.46%) in comperation to other tested maskers (Figure 9).

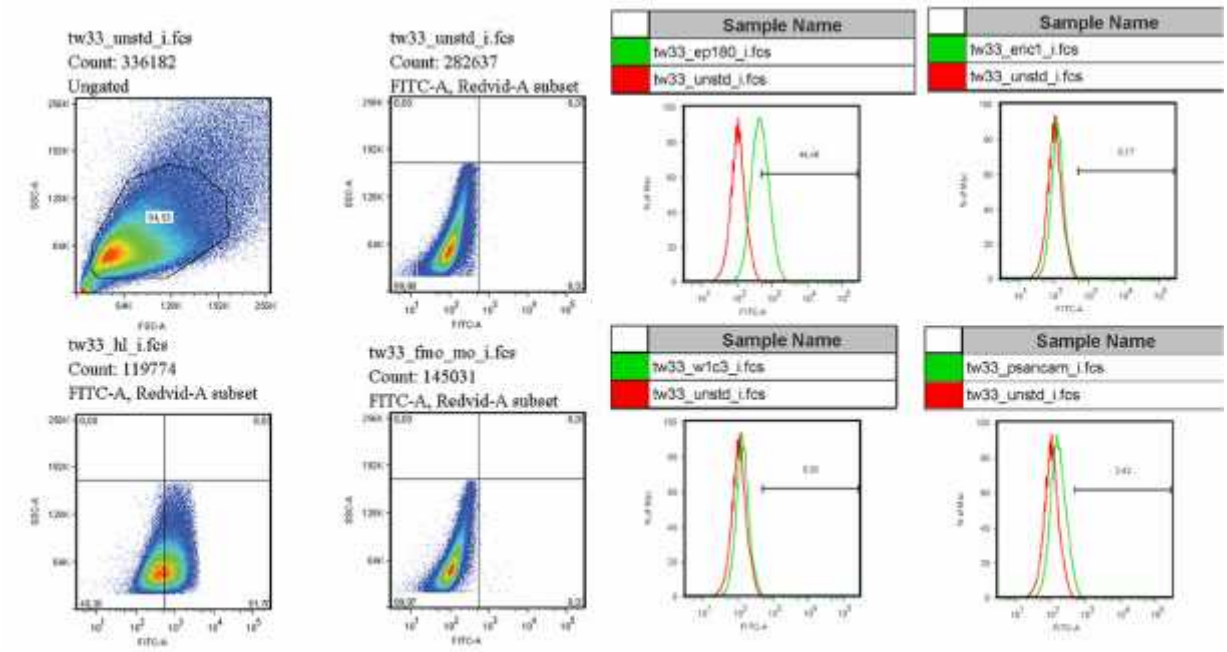

Figure 9. Intracellular FACS analysis on TW33 cell line (cell density over 70%)

To summarize: FACS analysis showed diffuse NCAM expression on cell lines. NCAM EP2567Y was expressed in all tested cell lines (HEK-293, CRL-1932, TW33). Also PSA-NCAM was present on all cell lines (2-4%). While new antibody W1C3 was expressed only on HEK-293 cell lines. Stem cell markers: CD24 and CD133, hematopoietic marker CD34 and tyrosine kinase receptor FGFR-1, were negative on all analyzed cell cultures.

4.2. Localization of NCAM isoforms in fetal and neonatal tissue

Different clones of NCAM antibody, listed in Table 3, as well as new clone for NCAM/W1C3 were tested on cryostat fetal samples by immunohistochemistry in order

to make comparation between them and to distinguish which one is best for future analyses. All 4 antibodies showed reactivity on all metanephric mesenchymal cells between the branching ureteric tree of the inner zones of the developing kidney up to the cortical nephrogenic area, where un-induced as well as condensed (CM) and cap mesenchyme were stained. Beside the mesenchymal cells, presence of NCAM was seen on epithelial cells, differentiated from the condensed mesenchyme into pre-tubular aggregates (PA), renal vesicles (RV), comma- (C) and S- (S) shaped bodies within the inner and outer nephrogenic zone. Indeed, NCAM, all tested clones: EP2567YY, OB-11 (C-terminus), as well as Eric-1 and W1C3 (N-terminus) was detected within nephrogenic zone in all precursor structures of mature nephron (CM, PA, RV, C and S), as well as in nephrogenic interstitium (NI) (Figure 10 A-D, Figure 11, Figure 12-red photo). It looks like the tested antibodies recognized all NCAM isoforms, 120, 140 and 180 (Figure 11). Since no additional labeling could be observed, it implicates no selective expression of the NCAM-120/-140/-180 by different cell populations within the fetal kidneys.

WT1 as marker of undifferentiated renal stem cells progenitors was tested on paraffin fetal samples (Figure 10E), and it showed presence in nephrogenic precursors, start from RV, then C and S shaped body. Interestingly, weak WT1 positivity was detected in some immature glomeruli (Figure 10E). Also, on same samples epithelial markers, such as EpCAM (CD326) and cadherin 9 (CDH9) renal fibroblast markers were analyzed. CD326 was present on epithelial cells of ureteric bud (UB), in nephrogenic zone, as well as in nephron precursors: RV, C, and S and in Bowman's capsule and early tubuli (Figure 10F, Figure 12-green photo). CDH9 was completely negative in nephrogenic zone, only positive signal was detected on the branching ureteric tree and UB of the inner zones of the developing kidney (Figure 10G). Hematopoietic marker CD34 in nephrogenic zone was present only in immature glomeruli and single interstitial cells - precursors of future blood vessels (Figure 10H).

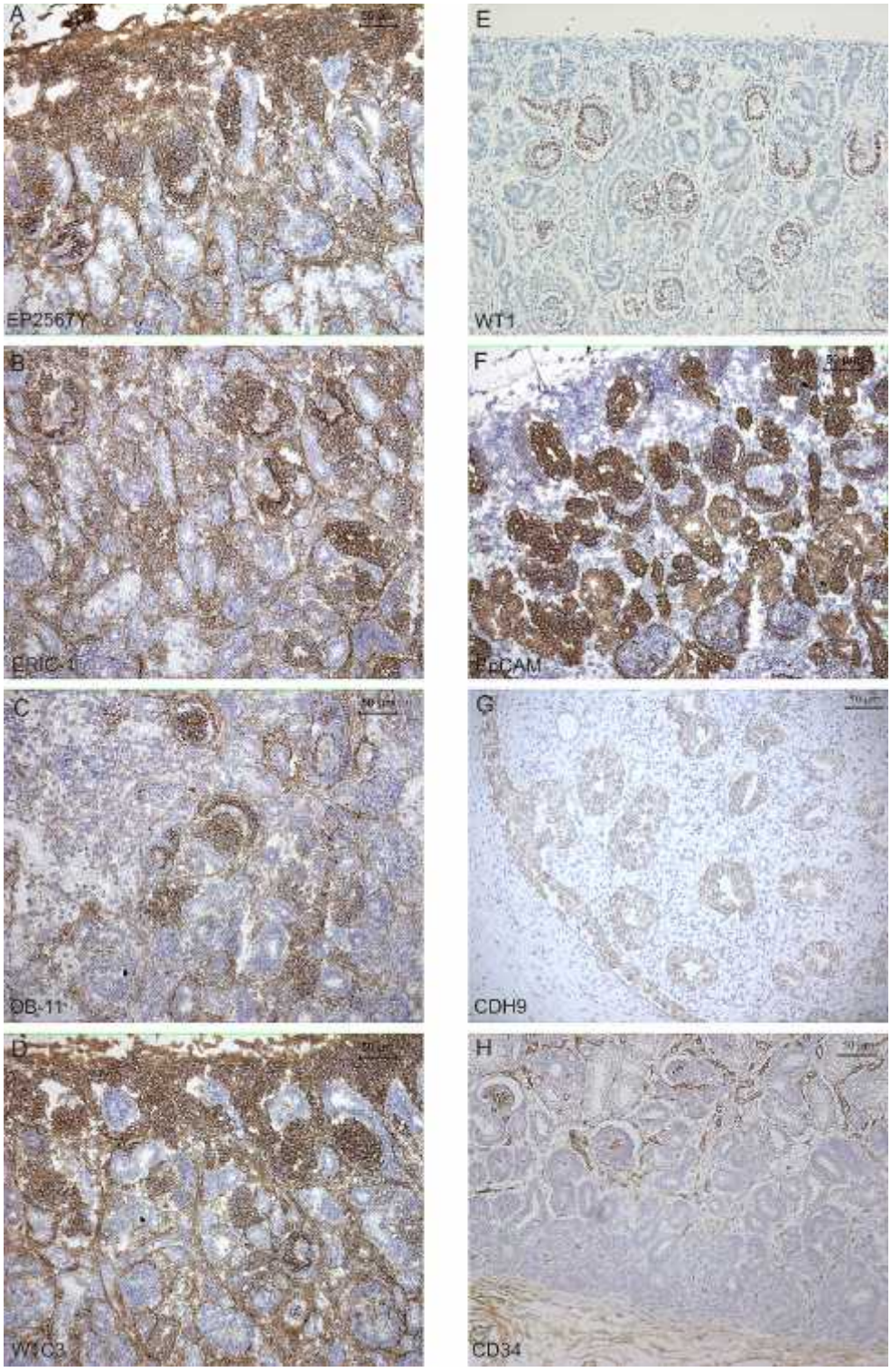

Figure 10. Immunohistochemistry staining on cryostat and paraffin fetal samples in nephrogenic zone: A) NCAM/EP2567Y, B) NCAM/Eric-1, C) NCAM/OB-11, D) W1C3, E) WT1, F) EpCAM-CD326, G) CDH9 and H) CD34.

Immunohistochemistry on all tested NCAM antibodies showed similar staining pattern. Thus, in order to conform their compatibility, DIF staining was performed. NCAM/EP2567Y as rabbit monoclonal Ab was combined with monoclonal NCAM Ab (Eric-1, OB-11 and W1C3). NCAM clone EP2567Y had completely overlapped with Eric-1, OB-11 and W1C3 on induced and un-induced mesenchimal cells (Figure 11). Thus, it is possible that in fetal tissues all three major NCAM isoforms are present. After these experiments NCAM/EP2567Y was used for all double staining with other cell surface markers raised in mouse.

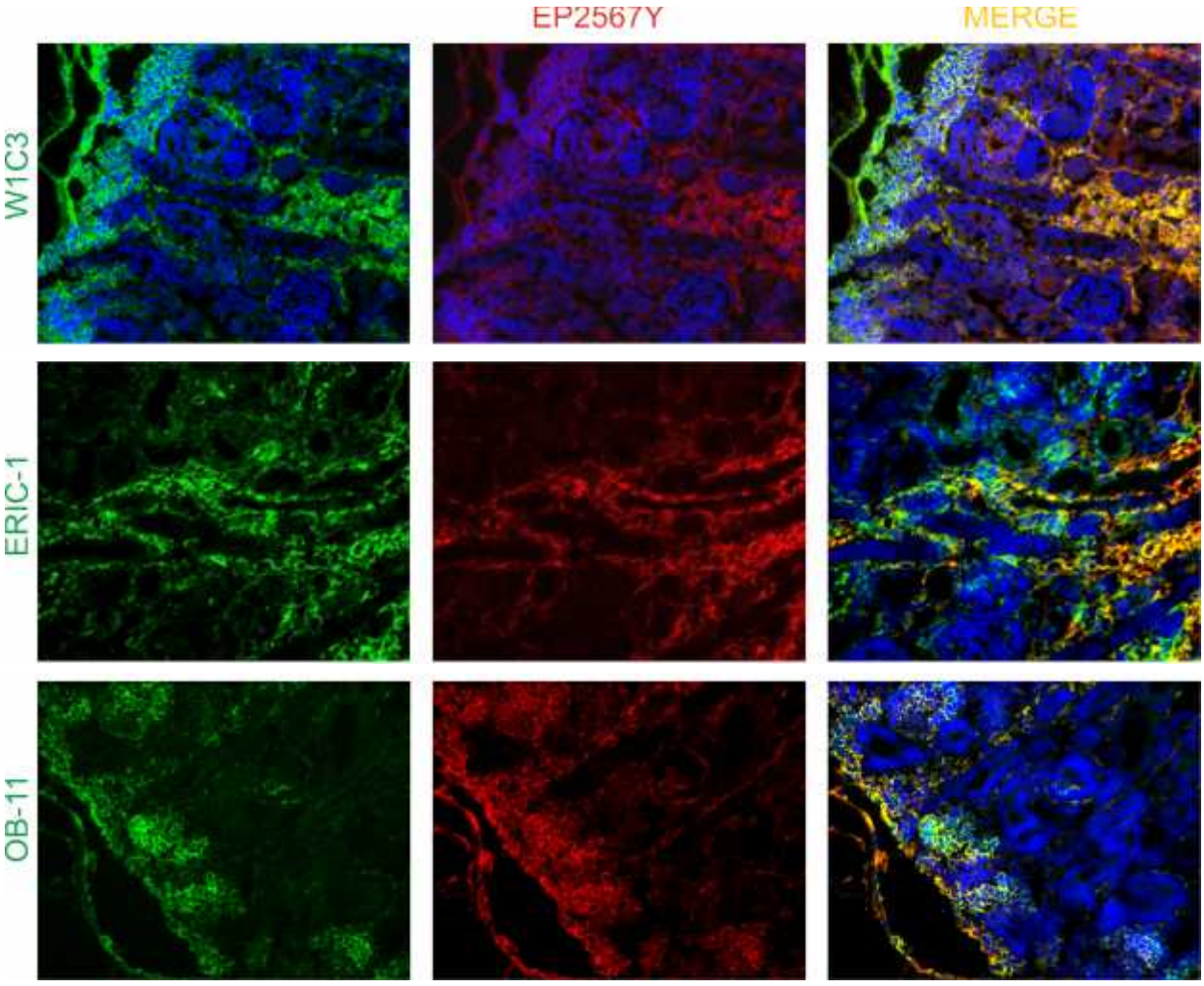

Figure 11. Double imunofluorescent staining on fetal samples conformed that analyzed NCAM clones recognized same structures on fetal tissues.

4.2.1. NCAM+ CD326+ nephron progenitors

To get better understanding of the functional significance of the three major NCAM isoforms during nephron development, double IF was used to examine co-localization of NCAM and other renal progenitor markers. Since NCAM was expressed on all mesenchimal (un-induced and induced) cells in fetal tissues we considered NCAM+X+ cells as marker of early renal nephron progenitors. Thus, first we analyzed NCAM co-expression with EpCAM (CD326). So, we detected co-localization of these 2 markers on all epithelial nephron precursors. NCAM+CD326+ cells were detected on RV (v), C and S body. NCAM+CD326$^-$ was mesenchimal cell in inner (NI) and outer nephrogenic zone (Figure 12). In fetal tissue CD326 is also detected in Bowman's capsule cells and early tubular cells (Figure 12). In medulla of fetal kidney NCAM mesenchimal cells around UB showed no overlapping with CD326, whereas epithelial cells of UB were positive only for CD326 (Figure 12).

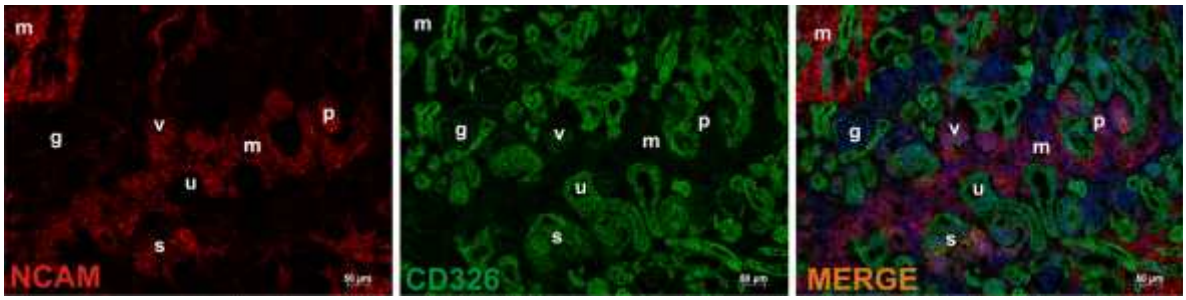

Figure 12. Expression of NCAM+ CD326+ nephron progenitors in nephrogenic zone

Furthermore, NCAM reactivity appeared to be progressively lost on epithelial cells of the distal segment of the S-shaped body during nephron development, but remained on the proximal part of S-shaped bodies. Thus, S body contains two populations NCAM+ CD326+ cells on proximal and medial part of S body, while distal part of the same S body connected with UB had only NCAM$^-$ CD326+ cells (Figure 13).

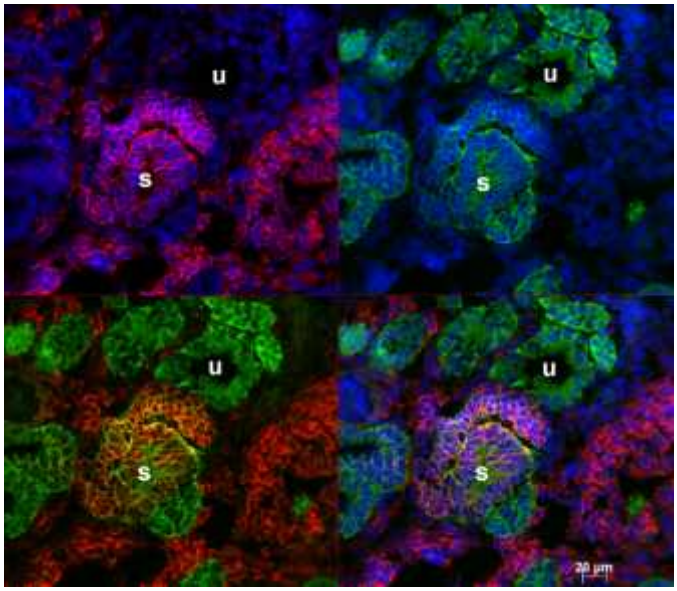

Figure 13. Expression of NCAM+CD326+ and NCAM-CD326+ cells in S-shaped body

NCAM expression in fetal kidney was also compared with Six2 gene specific as undifferentiated mesenchymal renal progenitor. Results obtained by DIF staining reveled co-localization of Six2 and NCAM in condensed mesenchzme (CM).

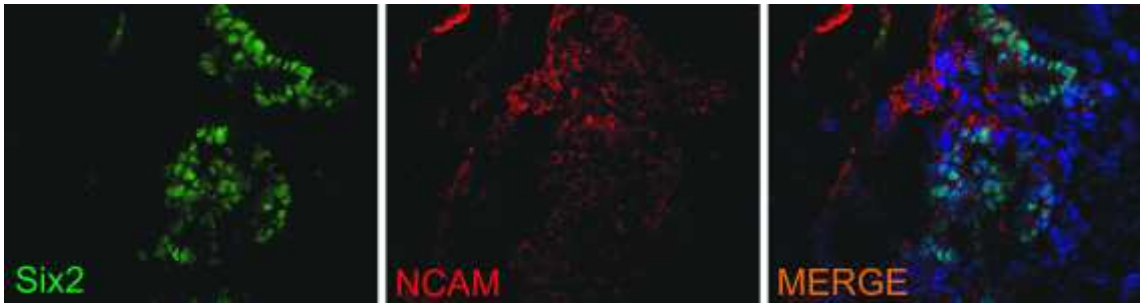

Figure 14. Co-localization of Six2 and NCAM on condensed mesenchzme in nephrogenic zone

4.2.2. PSA-NCAM+ expression in nephron progenitors

As sialynated forms of NCAM could influence function of the molecule and were imunoprecipitated from fetal tissues, localization of PSA-NCAM expression was

investigated in comparison with EpCAM (CD326) and NCAM. In fetal tissue PSA-NCAM showed overlapping with EpCAM in RV, C and S shaped body (Figure 15). This staining has also revealed that condensed and cap mesenchyme as well as in pretubular aggregates were only PSA-NCAM positive, whereas EpCAM appeared on RV and remained on S-shaped bodies. There was no differentiation between co-expression of NCAM/EpCAM and PSA-NCAM/EpCAM (compare Figure 12 and Figure 15).

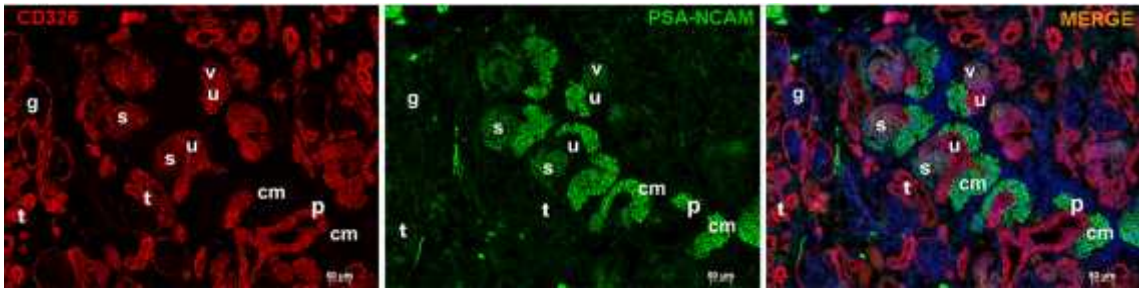

Figure 15. Co-expression of PSA-NCAM and CD326 on nephron progenitors in nephrogenic zone

PSA-NCAM was expressed more restrictedly compared to NCAM (Figure 16) expression which was present on all mesenchymal cells including nephrogenic interstitium (NI) and interstitial cells settled deeply in the cortex, corticomedullary zone and medulla in addition to CM. Thus, PSA-NCAM was present exclusively in condense mesenchyme and its derivates: PA, RV, C- and S-shaped body. Overlapping of PSA-NCAM and NCAM was seen in condense mesenchyme and its derivates, while there was no overlapping of PSA-NCAM and NCAM on interstitial mesenchymal cells (Figure 16).

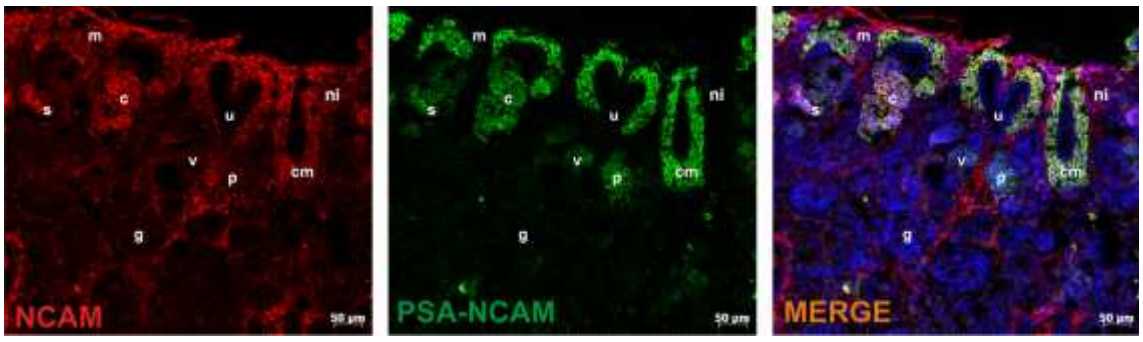

Figure 16. Co-expression of NCAM and PSA-NCAM in nephrogenic zone

Interestingly Ki-67, a marker for cell proliferation, showed co-localization with PSA-NCAM on cells of condensed mesenchyme (cm) as well as on PA (p), RV (v), C- and S-shaped bodies within the nephrogenic zone (Figure 17).

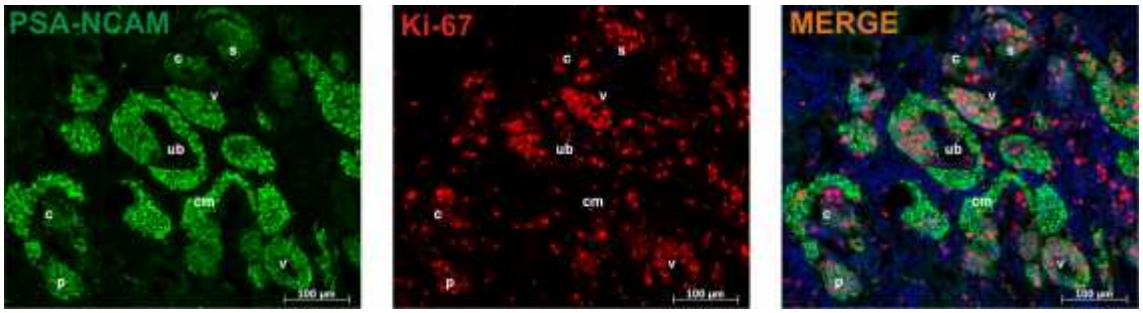

Figure 17. Co-expression of proliferation marker Ki-67 with PSA-NCAM in nephrogenic zone

4.2.3. Co-expression of NCAM and PSA-NCAM with renal progenitor markers

Further imunomorphological analyses were performed on NCAM and PSA-NCAM cells with progenitor markers, such as CD24, CD133 and CD 34 also by DIF labeling.

The progenitor marker CD24 was seen to be co-expressed with NCAM in the outer nephrogenic zone on the condensed and cap mesenchyme. Presence of both molecules was seen on PA and all further stages of nephron development up to the S-shaped bodies (Figure 16, NCAM-red photo, Figure 18, CD24- red photo). However, in nephrogenic zone nephrogenic interstitium was positive for NCAM only, while CD24 was detected in UB tip, branch of UB and early tubules in medulla (Figure 18 - red photo). Co-expression of PSA-NCAM and CD24 (Figure 18 - merged photo) is present in PA, RV, C and S shaped body structures. Thus, the same structures of fetal kidney starting with PA and up to S-shaped body co-expressed CD24, either with NCAM or PSA-NCAM. Since the expression of PSA-NCAM was restricted, compared to NCAM (Figure 16-green), consequently CD24 is expressed mainly in PSA-NCAM expressing cells.

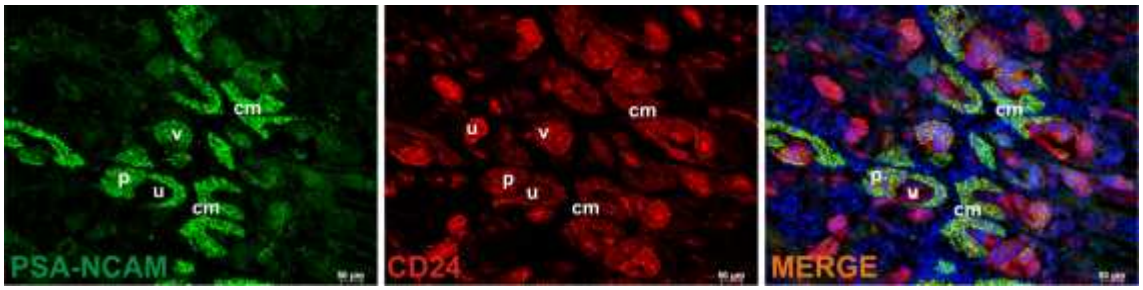

Figure 18. Co-expression of PSA-NCAM and CD24 in nephrogenic zone

Distribution of NCAM, PSA-NCAM, CD24, CD133, CD326 and Ki-67 expression in fetal renal tissue is given in Table 10.

Tabele 10. Results of double immunofluorescent staining on human fetal tissue

	NCAM	EpCAM	PSA-NCAM	CD24	CD133	Ki-67
metanephric mesenchyme (mm)	+	-	-	-	+	-
nephrogenic interstitium (ni)	+	-	-	-	-	-
cap mesenchyme (cm)	+	-	+	-	-	+
pretubular aggregate (pa)	+	-	+	+	-	+
renal vesicle (rv)	+	+	+	+	-	+
comma shaped body (c)	+	+	+	+	-	+
s-shaped body (s)	+	+	+	+	-	+
early tubuli (et)	-	+	-	-	+	+
bowmans capsule (bc)	-	+	-	+	+	-
loop of henle (lh)	-	+	-	-	+	-
distal tubuli (dt)	-	+	-	-	+	-
collecting duct (cd)	-	+	-	-	+	-
ureteric bud tip (ut)	-	+	-	+	-	+
ureteric bud (ub)	-	+	-	+	-	+

To summarized: mesenchymal nephron progenitor cells in human fetal tissues at the level of RV, C and S shaped body had expression of following cell surface markers: NCAM, CD326, PSA-NCAM, CD24 and Ki-67. At these levels/stages of nephron development only negative tested marker was CD133.

On the other hand, TRA-1-60, known as embryonic stem cell marker in analyzed fetal tissue showed expression on the apical side of UB cells. Co-expression or co-localization of TRA-1-60 and NCAM was not detected. Nevertheless, TRA-1-60 positive UB cells were also positive for CD24 (Figure 19A). Thus, CD24 was detected on mesenchymal as well as on epithelial nephron progenitors.

E- cadherin (E-CDH), known as MET gene was also co-localized with TRA-1-60 on UB cells (Figure 19B). Staining with E-CDH reveled that derivate of condensed mesenchyme at level of RV (Figure 19B, green signal) start to expressed E-CDH. So, like CD24, E-CDH is one more marker in fetal tissue which had been expressed on mesenchymal and epithelial nephron progenitors.

Note:

Although it was specified in thesis application, results of co-expression of NCAM with GDNF and 35C9 were not presented because of the technical problems. We were not able to get appropriate GDNF antibody, all tested had huge background, and similar situation was with aliquots of 35C9 antibody.

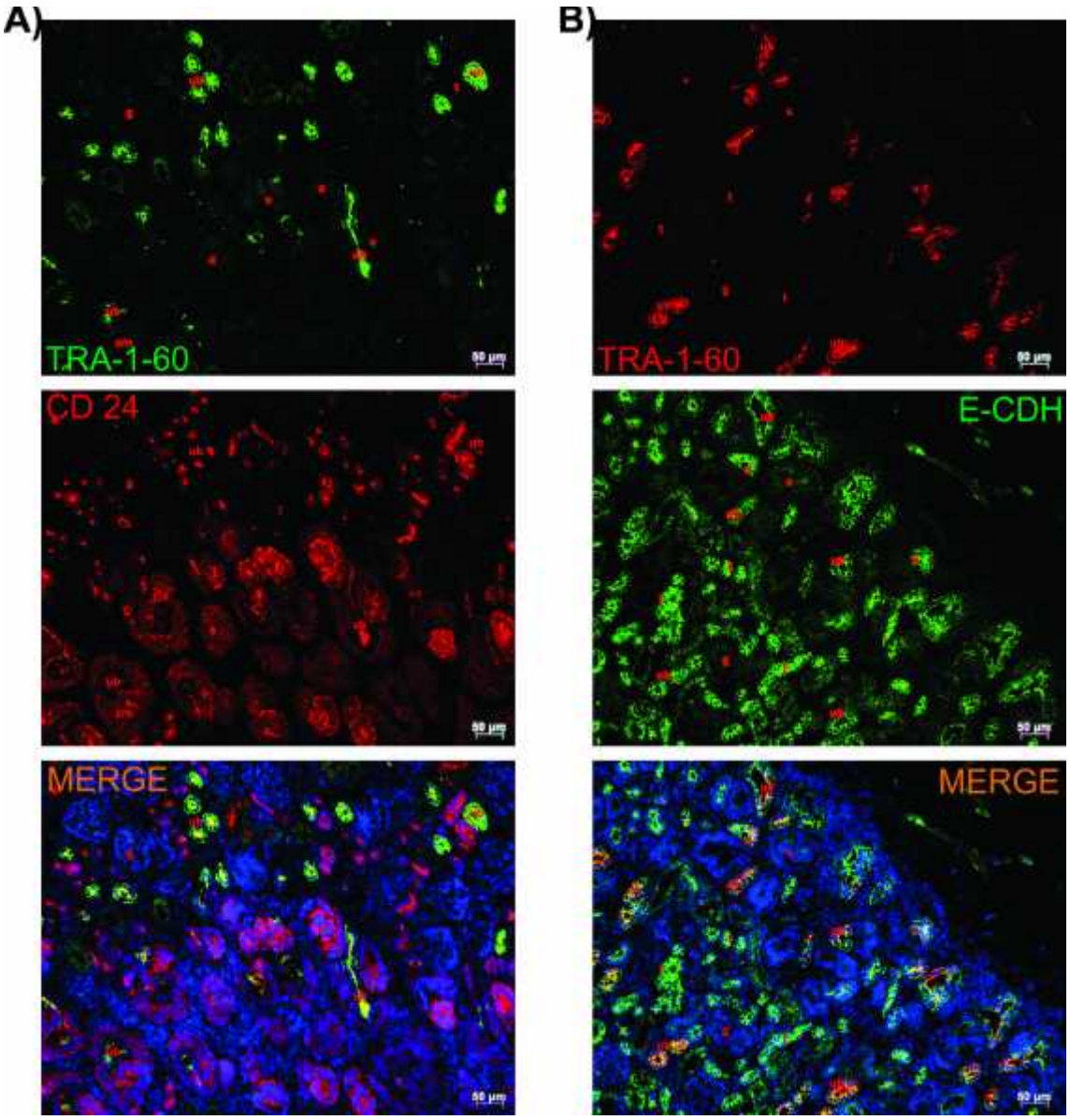

Figure 19. Co-localization of TRA-1-60, CD24 and E-cadherin on epithelial renal progenitors

4.2.4. Neonatal expression of renal progenitors

In neonatal tissue, NCAM is detected on interstitial cells (Figure 20G), while epithelial cells of some tubules remained slightly CD24 positive (Figure 20H). Thus, NCAM and CD24 were expressed on different cell types, although they are closely localized in same areas (Figure 20J).

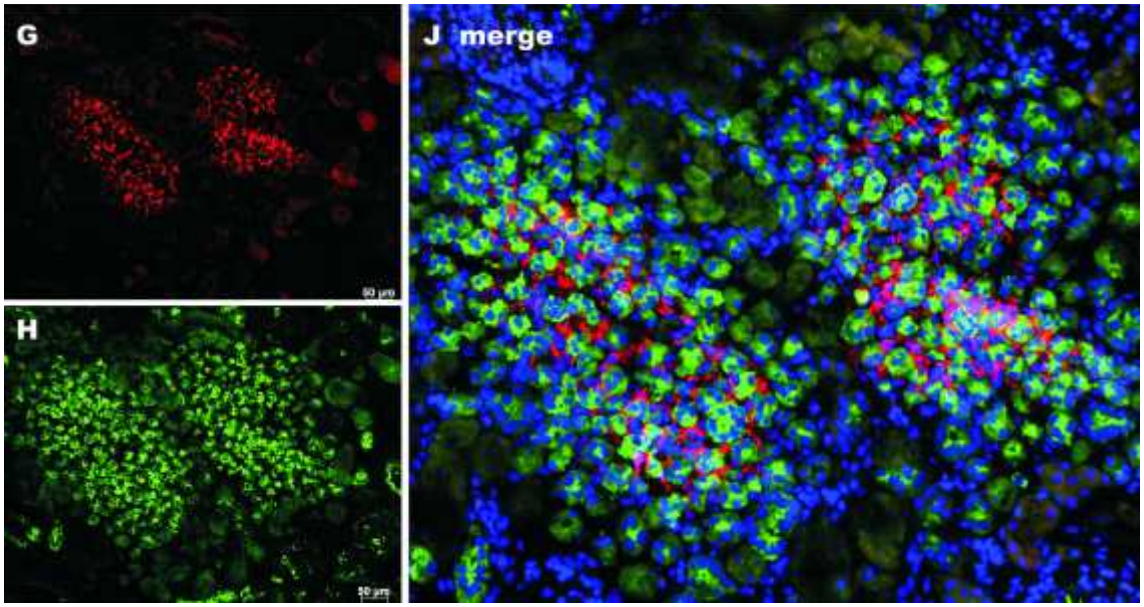

Figure 20. Expression of NCAM and CD34 in neonatal tissue

Expression of CD133 was detected in glomeruli, Bowman's capsule cells and on some tubuli and no co-expression between CD133 and NCAM was detected (Figure 21A) in fetal tissue. Some interstitial cells (deep in tissue) expressed CD133 and NCAM, but they represent different cell population since co-expression of these molecules was not observed (Figure 21B).

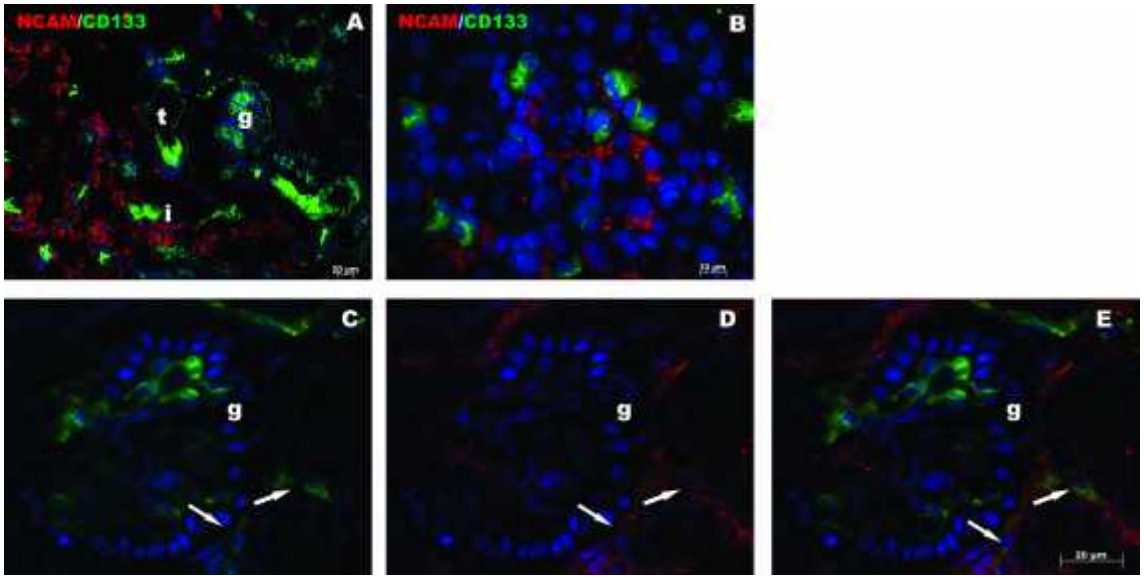

Figure 21. Expression of CD133 and CD34 in neonatal tissues

CD34, known as a marker of hematopioetic stem cells and endothelial precursors was also analyzed in DIF staining with NCAM. CD34/NCAM co-expression was detected in rare cells of the newly formed immature fetal glomeruli as well as on single interstitial cells of the nephrogenic interstitium. Interestingly CD34+ NCAM$^-$ cells were seen to be present in vascular clefts of presumed late differentiation stages of the proximal part of S-shaped bodies, which most likely could contribute to the capillaries of developing glomeruli. (Figure 21C, D, E).

4.2.5. DIF detection of NCAM co-localization with new mesenchymal antibodies

New antibody W5C4C5 was testes by IHC on fetal and adult tissues. Analyses on adult samples were negative, while expression of W5C4C5 in fetal tissues showed broad expression of this marker on mesenchymal cells (Figure 22A). Co-localization with NCAM was detected in all CM derivates and on non induced MM (Figure 22A). Very interesting was detection of W5C4C5 on nerve and its co-localization in adult tissues, (Figure 22B). On the other side, W8B2 expression was detected in some tubular structures in fetal tissues (Figure 22B). No co-localization of W8B2 and NCAM were found.

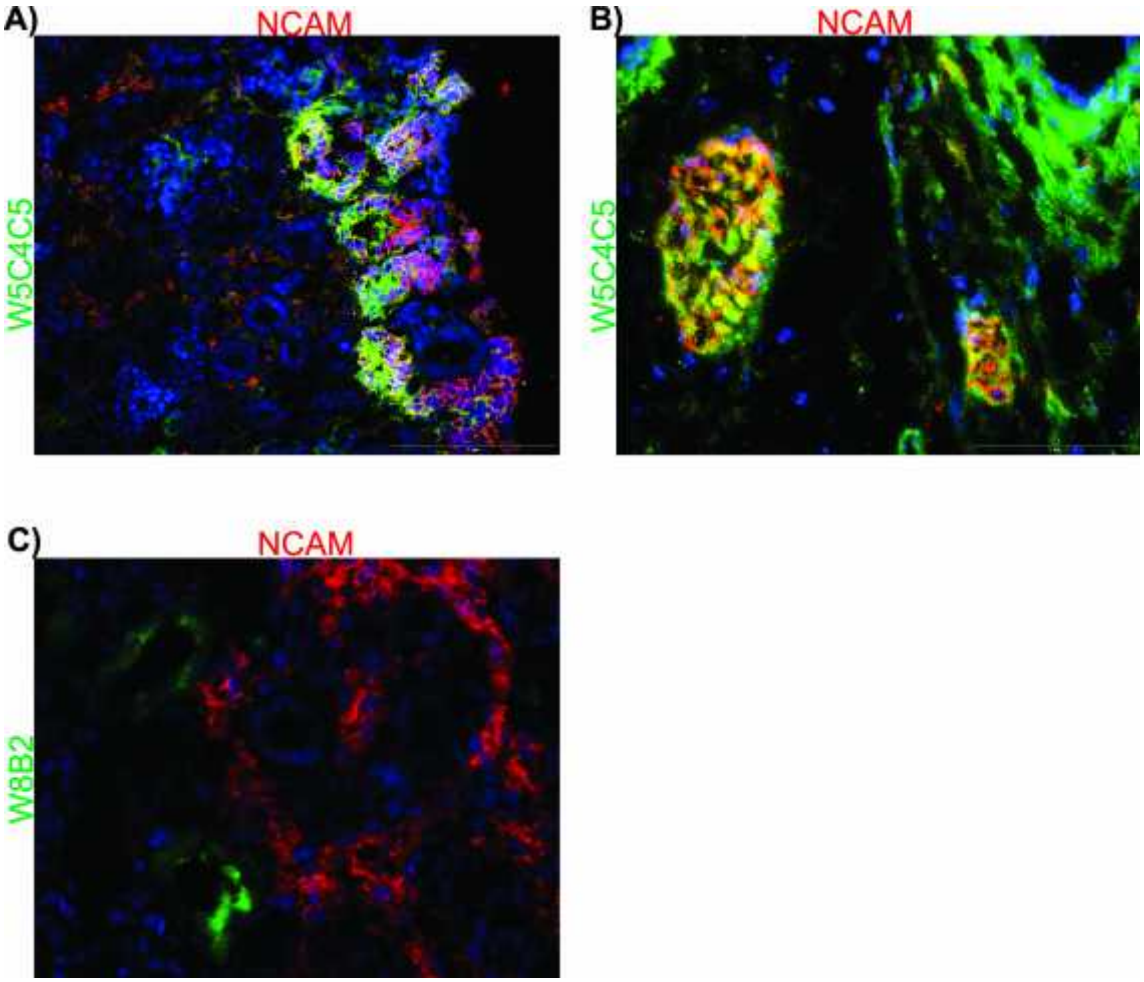

Figure 22. Co-expression of new antibodies W5C4C5 (A, B) and W8B2 (C) with NCAM in fetal tissues

4.2.6. RT-PCR of NCAM isoforms in fetal, neonatal and adult kidneys

The three major NCAM isoforms have been claimed to differ in their intracellular binding to signaling molecules and in influences on the stability of cellular interactions. To investigate the role of NCAM-120, -140, -180 in human kidney development, fetal renal tissue samples obtained from 15 to 30 wg were analyzed by RT-PCR for the expression of the specifically spliced NCAM mRNAs. Isoform specific RT-PCR strategies were developed with specific primers, in exon 20 unique to NCAM-120 mRNA, at the boundary of exons 24/25 as well as in exon 18 for the detection of NCAM-140 and NCAM-180 transcripts respectively. The specificity of the different

NCAM RT-PCRs was verified by sequencing of the amplification products obtained from the human retinoblastoma cell line Weri-RB1 which is known to express all major isoforms (Appendix 1).

NCAM-120, -140 and -180 were detected in fetal samples from 20 to 30 weeks of gestation (Figure 23A, line 1-6). Since equal amounts of mRNA per sample were used for amplification of each isoform, our results suggest that NCAM-140 is dominant in all analyzed fetal samples (Figure 23A, line 1-6). Different signal on agarose gel also suggest that content of each isoform in the same sample is different and it varies from sample to sample. In neonatal tissue all three isoforms were also detected (Figure 23A, line 7). Signal for NCAM-140 was again the strongest, while NCAM-180 was barely detectable (Figure 23A, line 7).

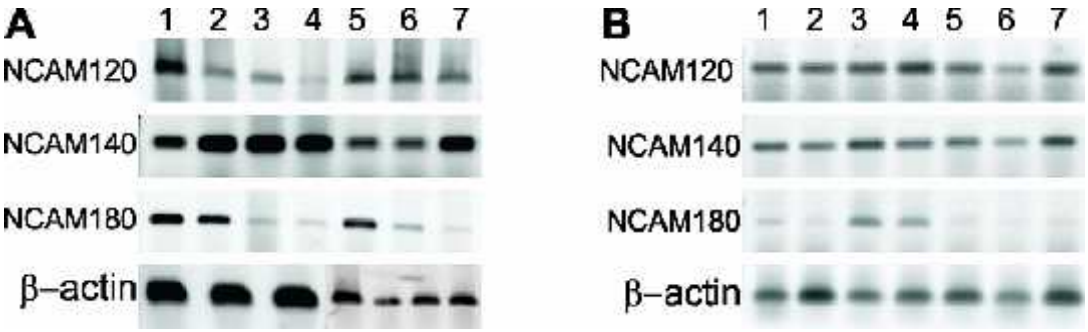

Figure 23. Detection of NCAM-120, -140, -180 in fetal, neonatal and adult tissues. A) line 1- 20th wg, line 2- 22nd wg, line 3- 24th wg. Line 4- 26th wg, line 5- 28th wg, line 6- 30th wg.

For comparison, seven human adult kidneys were additionally analyzed (Figure 23B). In these tissue samples, the same amounts of mRNA per sample were used for amplification of each isoform. Tested tissues showed strong expression of NCAM-120 and -140 kDa isoforms in all analyzed cases (Figure 23B, line 1-7). The largest NCAM isoform, NCAM-180 was clearly present only in 2 cases of adult tissues (Figure 23B, line 3, 4).

4.2.7. Expression of NCAM isoform specific proteins in fetal and neonatal kidney

Presence of different NCAM isoforms in fetal kidneys from the 22th to 28th wg and neonatal kidney of 40 wg were also examined by WB and IP. The antibody EP2567Y derived from an immunization with a synthetic peptide of the C-terminus of NCAM which should recognized NCAM-180 was used in WB.

EP256Y however bound to NCAM-180 as well as a product of about 150 to 140 kDa which could represent a shedded ectodomain fragment after proteolytic cleavage as it has been observed previously. It could, however, not be excluded that the antibody also recognized the 140kDa isoform. WB analyses with this antibody showed presence of NCAM-140 in all fetal and neonatal tissues as shown in Figure 24A. EP256Y seemed to also detect NCAM-180 as well as NCAM isoforms of higher molecular weight up to 250 kDa, suggesting reactivity with heavily polysialylated NCAM molecules (Figure 24A). Analysis of the same blots after stripping and exposure to the PSA-NCAM specific antibody revealed a single broad band with an apparent molecular mass starting at about 150kDa up to more than 250kDa in the fetal tissue samples of the 24th and 28th wg and thus confirmed presence of PSA (Figure 24B). The weak single bands reacting with PSA-NAM antibody were detected in fetal tissue of 22nd wg. In neonatal tissue of 40 wg PSA only a narrow band around 180 kDa was still visible on this blot (Figure 24B).

Since NCAM is not the only molecule who can be polysialilated with NANA in human tissue immunoprecipitation of EP2567Y antibody and tissue lysates for 24th and 28th wg was done. After precipitation analyzed fetal samples were “bloted” with PSA-NCAM. Results of IP conformed that in renal fetal samples at 24th and 28th wg NCAM molecules have been polysialilated (Figure 24C). Since equal amount of protein was used for precipitation wider band on 24th wg suggest that earlier tissue samples had stronger expression of PSA-NCAM.

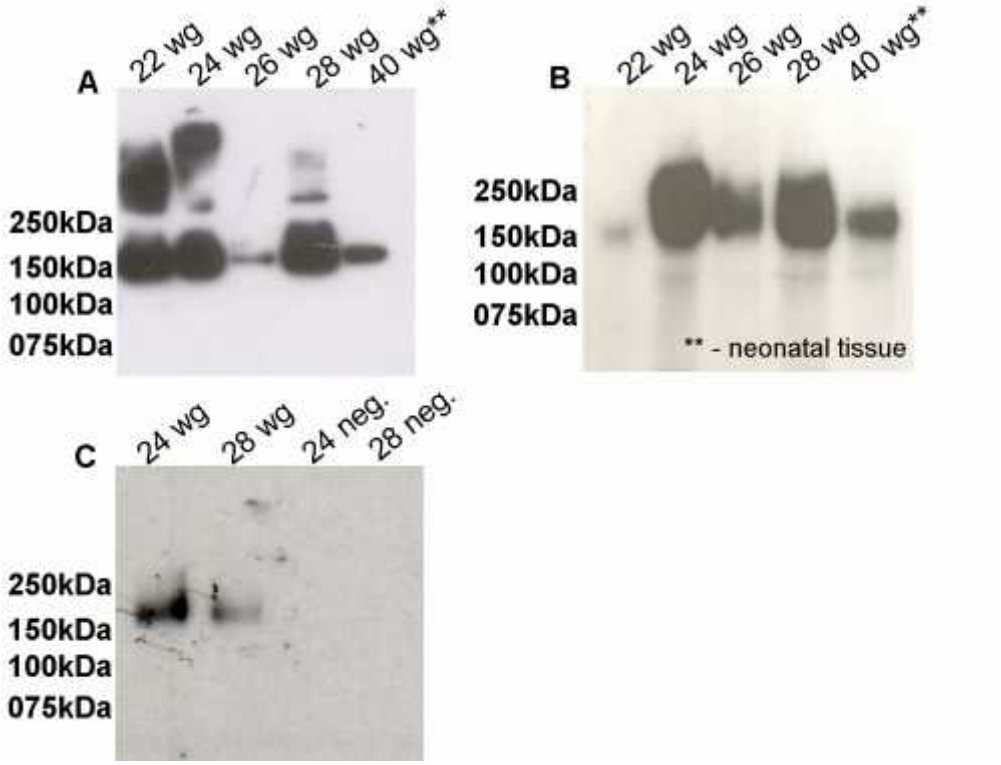

Figure 24. Western blot and immunoprecipitation verification of NCAM and PSA-NCAM expression. A) NCAM/EP2567Y expression in fetal and neonatal tissues; B) PSA-NCAM expression in fetal and neonatal tissues; C) Immunoprecipitates of 24nd and 28th wg by NCAM/EP2567Y blotted with PSA-NCAM; Negative controls – 24 neg and 28 neg.

4.3. Co-expression of NCAM and FGFR1 in RCC

Total number of RCC cases analyzed in our study was 36. From all analyzed RCC cases 30 (83.3 %) had expression of FGFR1, whereas the expression of NCAM was observed in 26 (72.2 %) cases. Co-expression of FGFR1 and NCAM was detected in 26 (72.2 %) cases. All NCAM positive cases were usually FGFR1 positive. Lack of both molecules was found in 6 (16.6 %) cases. Immunohistochemistry showed that staining pattern could be membranous and/or cytoplasmatic of NCAM and FGFR1, thus percentage of positive cells with co-expression of both molecules was evaluated only by triple immunofluorescent technique. In positive RCC cases expression of FGFR1 and NCAM has been detected in the majority of tumor cells. Intensity of staining was variable from case to case and it was not assessed.

Sixteen analyzed cRCC cases revealed FGFR1 expression in 14 (87.5 %) and NCAM expression in 12 (75 %) cases. Co-expression was present in 12 (75 %) cases, since all NCAM positive cases were also FGFR1 positive (Table 11). Interestingly, FGFR1 and NCAM expression in cRCC with lower NG (I and II) was usually membranous and uniformly spread on the cell surface (Figure 25A, 25B, 25E, 25F), while higher NG (III and IV) had predominantly cytoplasmic in addition to membranous expression of these markers (Figure 25C, 25D, 25G, 25H). Three cases of mcRCC were also studied. Only one case of mcRCC had uniform membranous staining of FGFR1 and NCAM, whereas the absence of FGFR1 and NCAM was noticed in 2 samples (Table 11).

Table 11. Summary of the clinicopathological features, FGFR1 and NCAM expression in RCC

Case no.	Age	Sex	Tumor size (cm)[#]	Nuclear Grade	Stage	FGFR1	NCAM	FGFR1/NCAM co-expression
Clear cell RCC								
1	61	F	6	1	pT2NxMx	+	-	no
2	39	M	3,5	1	pT2NxMx	+	+	yes
3	58	M	4	1	pT1aNxMx	+	+	yes
4	87	F	2,5	1	pT3aNxMx	-	-	no
5	71	M	5,5	1	pT3aNxMx	+	+	yes
6	54	M	10	2	pT3bNoMx	+	+	yes
7	64	M	9	2	pT3aNxMx	+	+	yes

8	46	F	12	2	pT3aNxMx	-	-	no
9	58	M	6	3	pT1bNxMx	+	+	yes
10	74	F	5	3	pT3aNxMx	+	+	yes
11	44	M	7	3	pT1bNxMx	+	+	yes
12	36	M	9	3	pT4N2M1	+	-	no
13	60	F	13,5	4	pT3aNoMx	+	+	yes
14	75	F	8	4	pT3aNxMx	+	+	yes
15	57	F	8	4	pT3N2Mx	+	+	yes
16	64	M	8	4	pT3aNxMx	+	+	yes
Multilocular cystic RCC								
1	47	M	4	1	pT1aNxMx	-	-	no
2	34	M	4,5	1	pT1bNxMx	-	-	no
3	44	F	6	2	pT1bNxMx	+	+	yes
Papillary RCC								
1	62	M	4,2	1, type I	pT3aNxMx	+	+	yes
2	59	M	3	1, type II	pT3aNxMx	+	+	yes
3	59	M	6	1, type II	pT3NxMx	-	-	no
4	55	M	4,5	2, type II	pT1bNxMx	+	+	yes
5	59	M	3,5	2, type II	pT1aNxMx	+	+	yes
6	47	M	4	2, type II	pT1aNxMx	-	-	no
7	59	M	3,5	2, type II	pT1aNxMx	+	+	yes
8	50	M	1,5	2, type II	pT1aNxMx	+	+	yes
9	55	M	4,5	3, type II	pT3aNxMx	+	+	yes
10	65	M	NK	3, type I	pT3bNxMx	+	+	yes
11	56	M	10	3, type II	pT3aNxMx	+	+	yes
12	48	M	12	4, type II	pT3aNxMx	+	+	yes
Chromophobe RCC								
1	43	M	NK	1	NK	+	-	no
2	39	F	5	2	pT1bNxMx	+	-	no
3	60	M	2	2	pT1aNxMx	+	+	yes
4	70	F	1,5	2	pT1aNxMx	+	+	yes
5	61	M	7	2	pT1bNxMx	+	+	yes

- the biggest tumor diameter, RCC- renal cell carcinoma, FGFR1- fibroblast growth factor receptor 1, NCAM- neural cell adhesion molecule, NK – not known

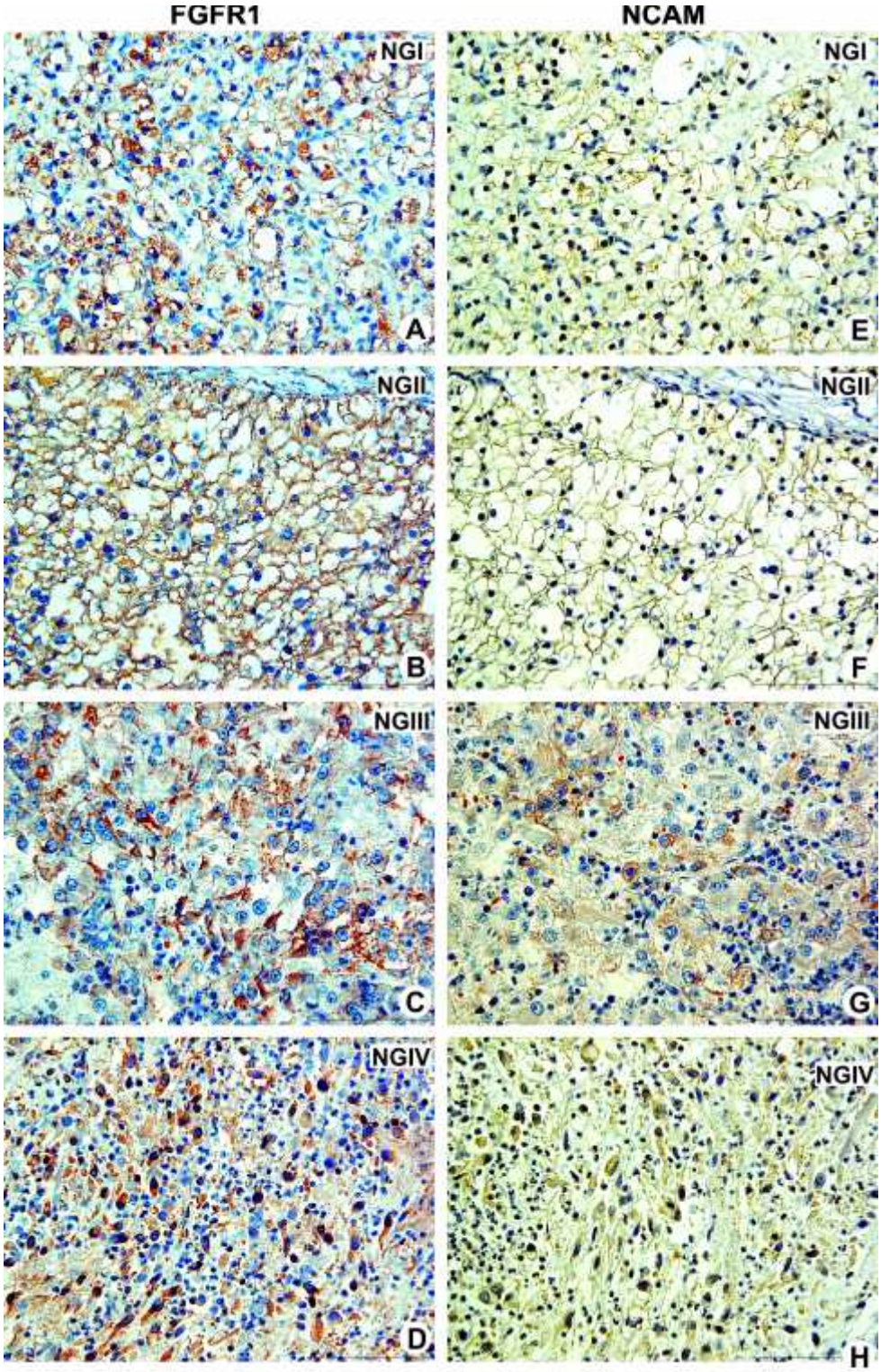

Figure 25. Co-expression of FGFR1 and NCAM in clear cell RCC. Lower NG had exclusively membranous expression of FGFR1 (A, B) and NCAM (E, F). In contrast, higher NG showed cytoplasmatic expression of FGFR1 (C, D) and NCAM (G, H) in addition to membranous; magnification 400x. Abbreviations: NG-nuclear grade

In 12 pRCC cases, 10 (83.3%) had co-expression of FGFR1 and NCAM. Two pRCC, with NG I and II lacked both molecules (Table 11). In contrast to cRCC, expression of FGFR1 and NCAM in pRCC appeared to be mainly cytoplasmatic regardless to NG (Figure 26).

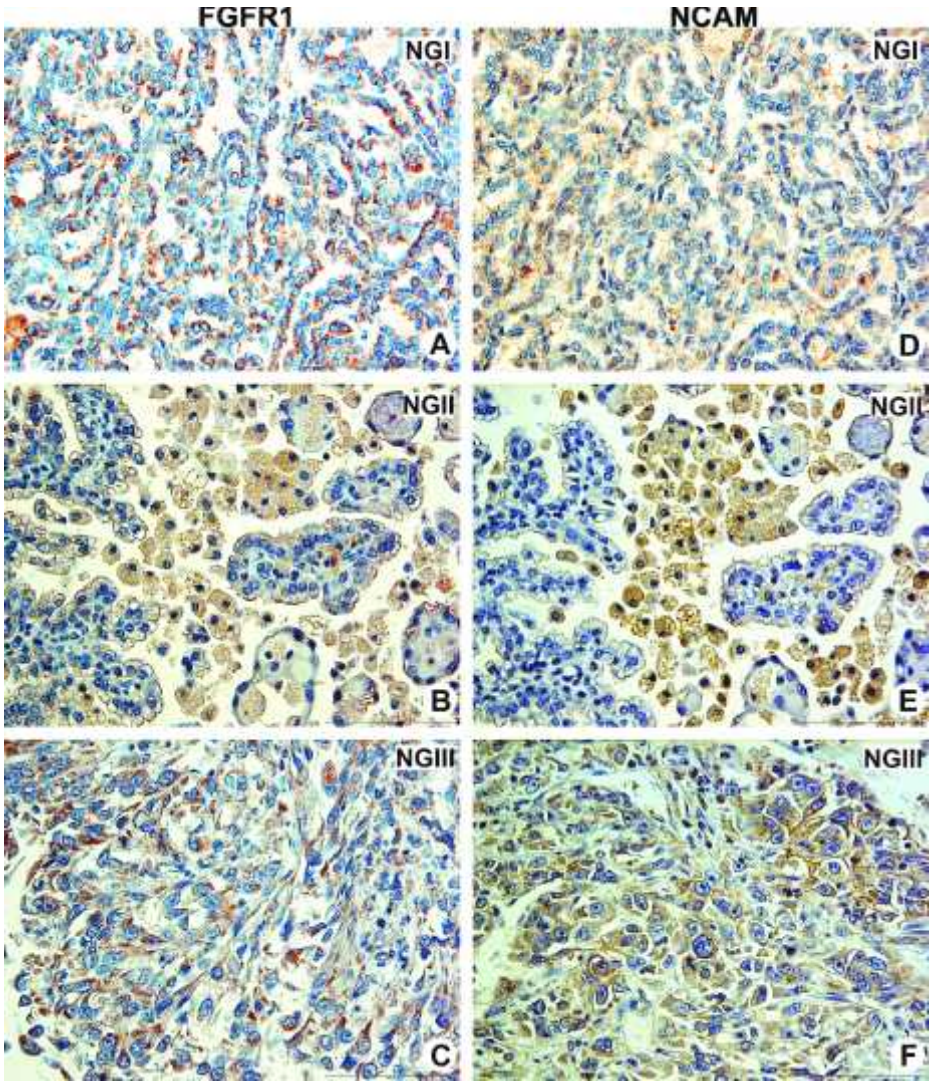

Figure 26. Co-expression of FGFR1 and NCAM in papillary RCC. FGFR1 (A-C) and NCAM (D-F) showed dominant cytoplasmatic expression in addition to membranous in all nuclear grades; magnification 400x.

All 5 chRCC cases expressed FGFR1, while weak NCAM expression was observed in 3 cases (Figure 27A, 27B) with predominantly cytoplasmatic staining.

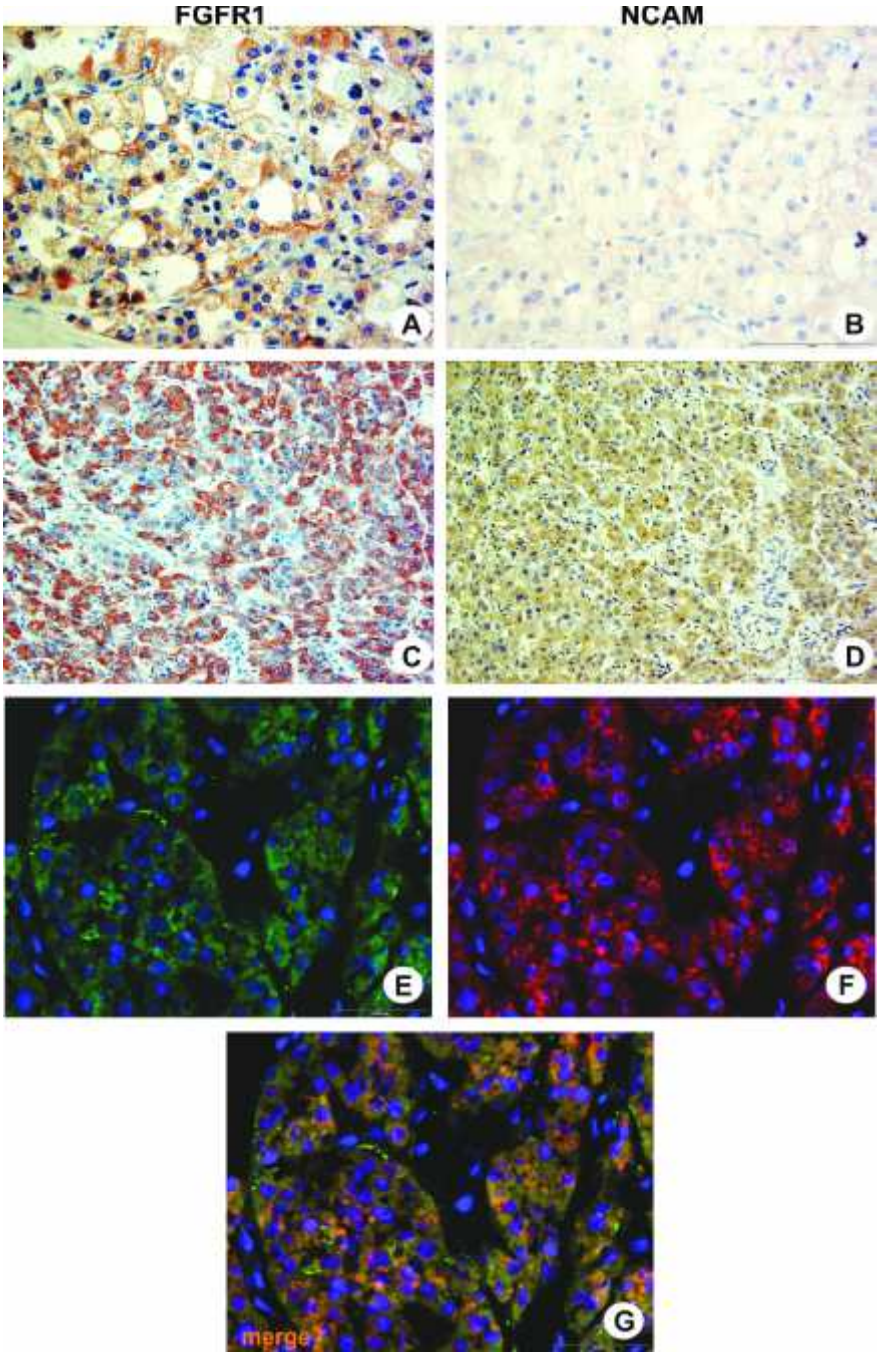

Figure 27. Immunohistochemistry and immunofluorescent staining pattern in chromophobe RCC and in oncocytoma. Chromophobe RCC showed mainly cytoplasmatic and membranous FGFR1 expression (A), while NCAM (B) had weak predominantly cytoplasmatic pattern in these RCC. In oncocytoma both methods revealed clearly cytoplasmatic expression of FGFR1 (C, E) and NCAM (D, F). Co-localization of FGFR1 and NCAM in oncocytoma, yellow to orange merge, G. Magnification 400x, cell nuclei blue, stained with DAPI.

Statistical analysis of the data obtained by immunohistochemistry showed that co-expression of FGFR1 and NCAM in RCC was present regardless of histological type and all other clinicopathological data listed in Table 11 ($p<0,05$).

4.3.1. FGFR1/NCAM co-localization in RCC detected by double immunofluorescence

Results obtained by triple immunofluorescent staining clearly showed co-localization of FGFR1 and NCAM, i.e. expression of both markers on single renal tumor cell (Figure 28, merged photos). By triple immunofluorescent technique, NCAM positive cells better corresponded to FGFR1 positive cells in comparison to immunohistochemical staining where FGFR1 was usually stronger than NCAM (compare Figures 25-27 to Figure 28). Using this technique, it was much easier to see that cancer cells of RCC with higher NG, in addition to cytoplasmatic, had aggregated membranous FGFR/NCAM co-localization (Figure 28I, 28L, 28O, white arrows). The semi-quantitative approach showed that number of $FGFR1^{+}/NCAM^{+}$ RCC cells was increasing with nuclear grade in cRCC and pRCC, since the majority of cases with lower NG (I-II) had co-localization score 0-2 (Figure 28, A-F), while in high NG RCC (III-IV) co-localization score was 3, meaning that more than 60% of tumor cells had FGFR1 and NCAM expressed on the same tumor cell (Figure 28, G-O).

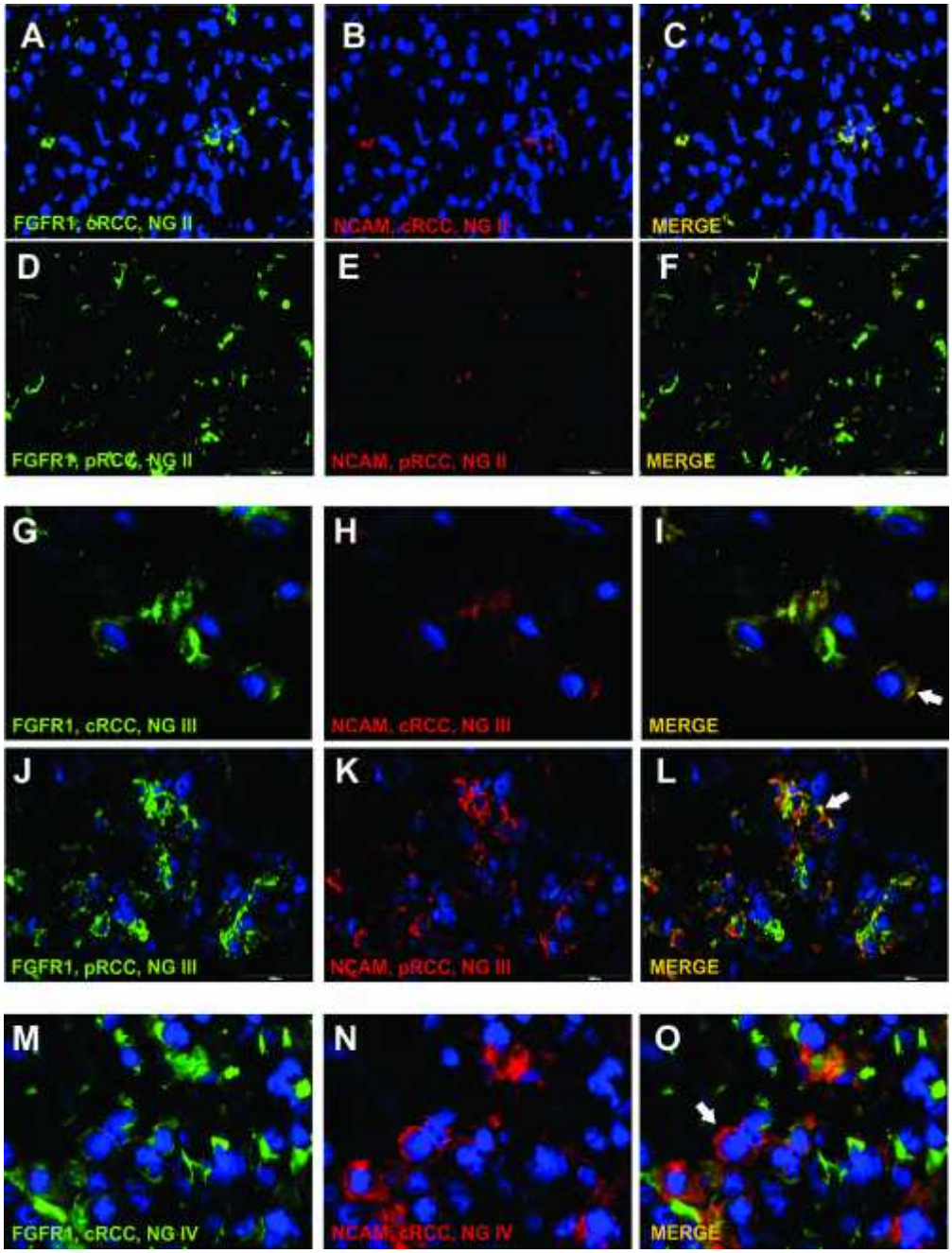

Figure 28**.** Co-localization of FGFR1 and NCAM in clear cell and papillary RCC. Lower NG tumors (I-II) had co-localization score between 0 and 2 (Figure 4C, 4F). In tumors with higher NG (III-IV) co-localization score was 3 (I, L, O).

Legend: cRCC - clear cell RCC, pRCC - papillary RCC, NG - nuclear grade, green - FGFR1, red - NCAM, yellow to orange - merge of FGFR1 and NCAM, blue - nuclei stained with DAPI.

4.3.2. FGFR1 and NCAM expression in oncocytoma and other renal neoplasms

Both techniques - immunohistochemisry (Figure 27C, 27D) and immunofluorescence (Figure 27G-J) - clearly revealed exclusive cytoplasmatic expression of FGFR1 and NCAM in 9 oncocytoma cases (Table 12).

Table 12. Summary of the clinicopathological features, FGFR1 and NCAM expression in oncocytoma

Case no.	Age	Sex	Tumor size (cm)#	FGFR1 cytoplasmatic	NCAM cytoplasmatic	FGFR1/NCAM co-expression
1	61	F	2,0	+	+	Yes
2	43	F	2,3	+	+	Yes
3	51	F	2,5	+	+	Yes
4	60	F	3,5	+	+	Yes
5	53	M	4,0	+	+	Yes
6	57	F	6,0	+	+	Yes
7	59	F	6,5	+	+	Yes
8	81	F	8,0	+	+	Yes
9	69	M	9,5	+	+	Yes

- the biggest tumor diameter, FGFR1- fibroblast growth factor receptor 1, NCAM- neural cell adhesion molecule

Absence of FGFR1 and NCAM expression was found in one case of cortical fibroma and in two samples of collecting duct carcinoma, while the single case of metanephric adenoma showed expression of FGFR1 and NCAM.

4.3.3. NCAM and Aquaporin1 expression in renal tumors

Aberrant NCAM expression in all RCC types and in oncocytoma was compared to Aquaporin 1 (AQP1). AQP1 expression was characteristic only for mature proximal tubuli.

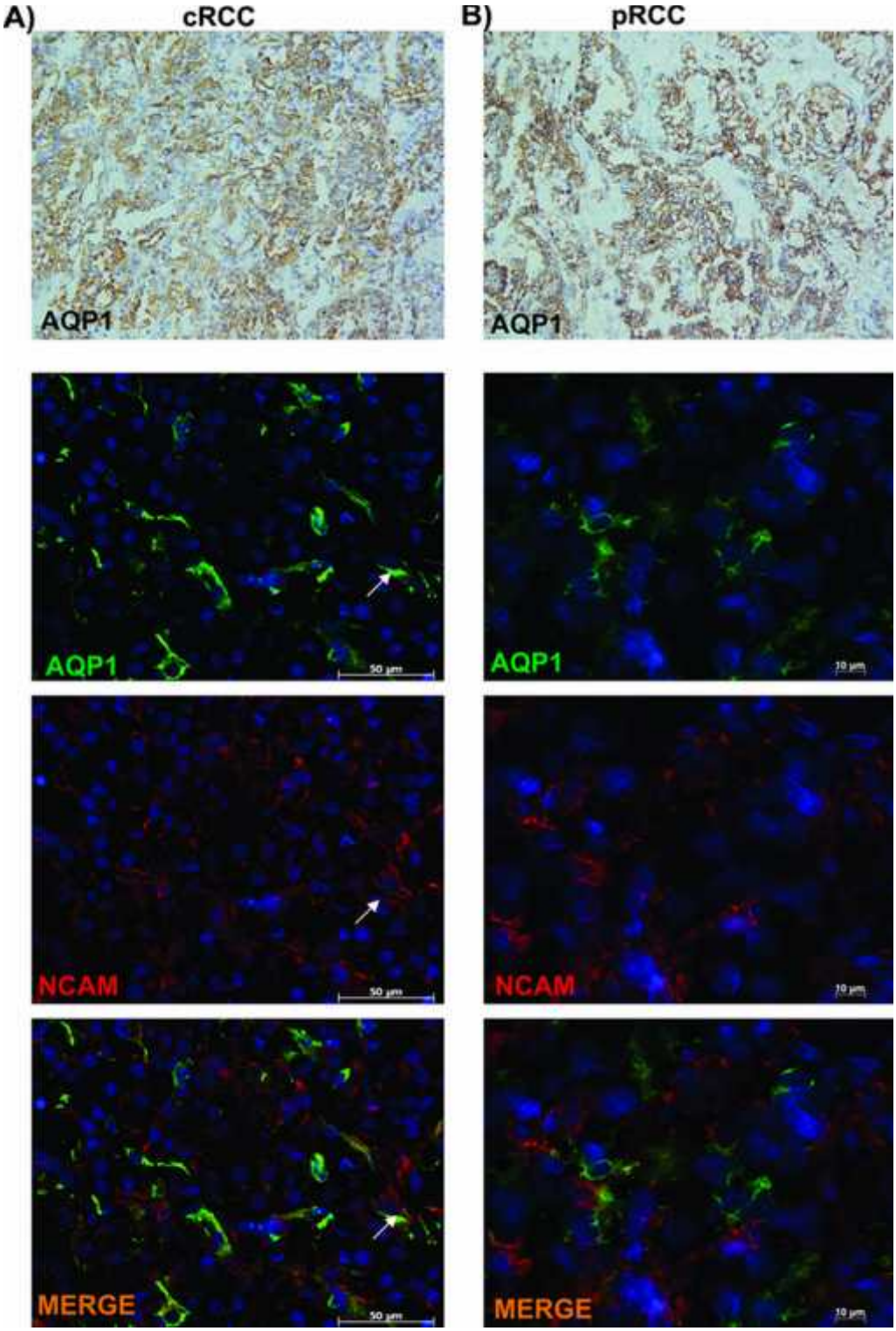

Figure 29. Expression of NCAM and AQP1 in clear cell and papillary RCC. A) Only rare cells in cRCC showed NCAM+AQP1+ cells (white arrow). B) Interestingly in pRCC cells co-localization of NCAM and AQP1 was not detected.

Ontogeny of cRCC and pRCC origin indicated that these two RCC types arise from proximal tubuli. Thus, it was not surprising results that AQP1 was detected on cRCC and pRCC (Figure 29), but not in chRCC, collecting duct carcinoma and oncocytoma.
Interestingly were findings by DIF staining, which showed that only few NCAM+AQP1+ cells in cRCC (Figure 29A, white arrow), in this type tumor cells mainly express one of analyzed markers (Figure 29A). On the other hand, in pRCC NCAM+AQP1+ cells were not found. Tumor cells in pRCC express NCAM or AQP1 (Figure 29B).

4.3.4. Presence of NCAM 120, 140 and180 isoforms in renal neoplasms

Five different tumor types, which had FGFR1 and NCAM expression by immunomorphology, were studied for NCAM 120 and 140 mRNA. All analyzed RCC cases: cRCC, pRCC, chRCC, as well as two benign tumors, oncocytoma and metanephric adenoma, revealed presence of NCAM 140 (Figure 30A). NCAM 120 was present only in chRCC and in both benign renal neoplasms (Figure 30B). Two RCC cases, cRCC and pRCC, were negative for NCAM 120.

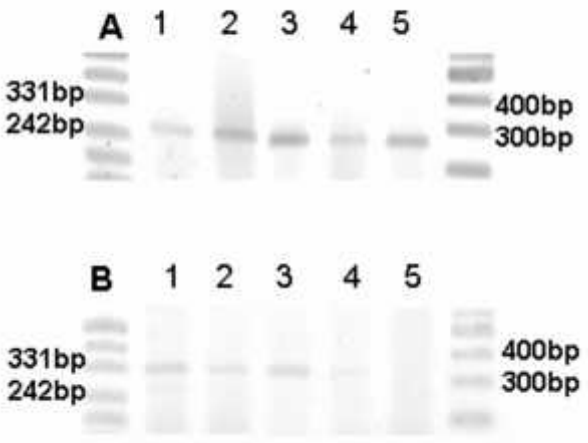

Figure 30. RT-PCR expression of NCAM 140 (A) and 120 (B) isoforms in various renal neoplasms.
Legend: line 1 - metanephric adenoma, line 2 - oncocytoma, line 3 – chromophobe RCC, line 4 – papillary RCC, line 5 – clear cell RCC.

4.4. NCAM+ cells in renal interstitial fibrosis

Renal interstitial NCAM+ cells were rarely present in tubulointerstitial compartment of human non-transplanted kidney obtained by cadaveric donors, used as a control group. Analysis of the 90 kidney paraffin embedded biopsy specimens showed increased number of NCAM+ interstitial cells in 41 cases (45.6%). The distribution of NCAM+ interstitial cells among different forms of glomerulonephritis and glomerulopathies is showed in Figure 31: NCAM+ cells were increased in 66.7% LN, 53.8% FSGS, 53.8% MGN, 12.5% MPGN, 40% RPGN, 40% MesPGN, 16.7% IgA nephropathy, 25% of renal grafts.

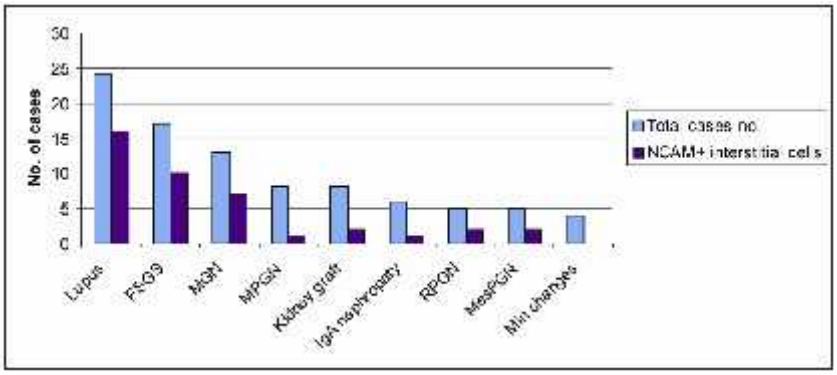

Figure 31. Distribution of NCAM+ interstitial cells among various renal diseases

Statistically significant increase of NCAM positive renal interstitial cells was present mainly in incipient interstitial fibrosis, assessed as scale 1, compared to all others scales of fibrosis ($p<0.001$), showed in Figure 32.

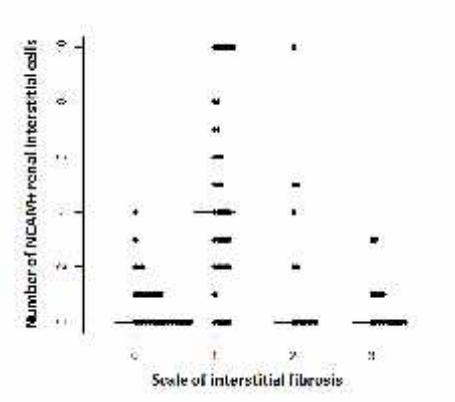

Figire 32. Number of NCAM+ renal interstitial cells in different stages of interstitial fibrosis

4.4.1. Presence of NCAM isoforms in kidneys with and without fibrosis

Thirteen renal biopsies samples were analyzed using specific primers for all the three NCAM isoforms, (Figure 33a, 34b and 34d). RT-PCR were done on eight control renal tissues and three cases with interstitial fibrosis (Figure 33a: line IV, VIII and X). Line X belongs to case which represents lupus nephritis with diffuse incipient interstitial fibrosis since no tubular atrophy is present (Figure 33b), with increased number of NCAM positive cells, shown in Figure 33c.

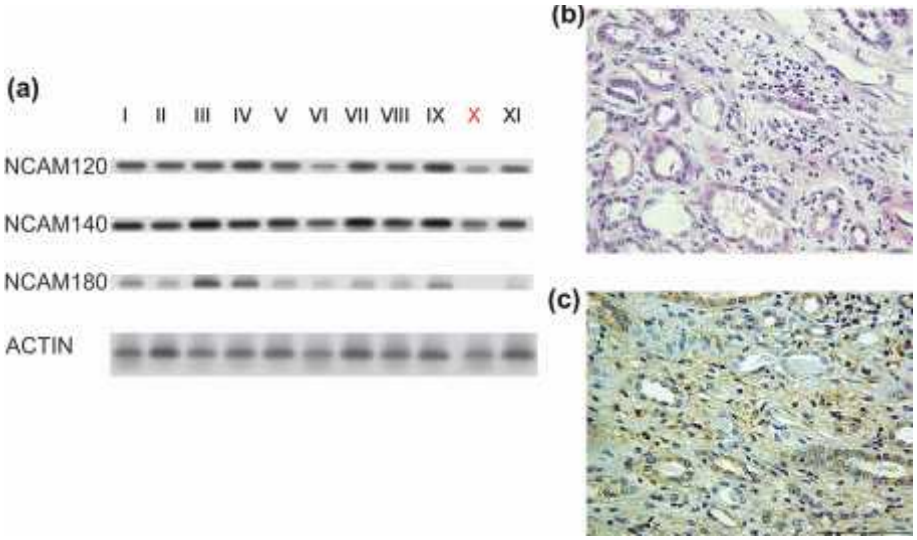

Figure 33. RT-PCR: 3 NCAM isoforms in different renal biopsies samples.

In addition, two more cases with significant increase of NCAM expression were analyzed for 3 different NCAM isoforms: first, FSGS with focal incipient fibrosis (Figure 34a) and results of RT-PCR (Figure 34b), and second, MPGN with incipient fibrosis (Figure 34c) and results of RT-PCR (Figure 34d).

Unfortunately we did not find any difference between presence of NCAM isoforms (120, 140 and 180) in kidneys with and without interstitial fibrosis, with the exception of one sample with diffuse interstitial fibrosis where PCR band of NCAM180 was absent (Figure 33a: line X; Figure 33b and 33c).

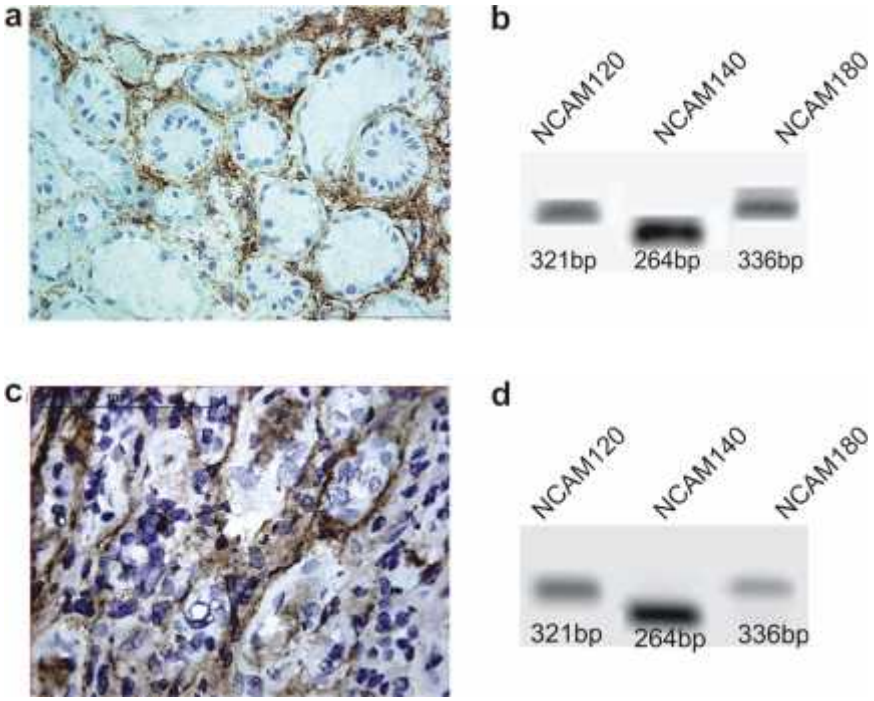

Figure 34. Detection on NCAM 120, 140 and 180 in FSGS and MPGN

4.4.2. Co-expression of NCAM+ renal interstitial cells and FGFR1 integrin α5β1 and cadherin 9

Using immunoperoxidase staining we revealed presence of few relevant markers for fibrosis on renal interstitial cells, such as FGFR1 (Figure 35a) and α5β1 integrin (Figure 35b) and cadherin 9 (CDH9, Figure 35c, red star). Therefore, further analysis using double immunofluorescence staining was applied to clarify whether NCAM+ renal interstitial cells could co-express these markers in normal renal tissue and in kidneys with fibrosis.

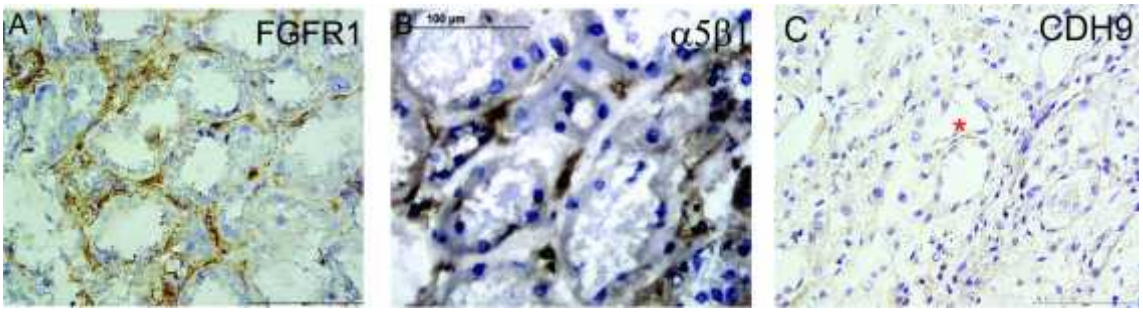

Figure 35. Expression of FGFR1, integrin α5β1 and CDH9 on interstitial cells. Red star- rare CDH9 cell in initial interstitial fibrosis

Double immunofluorescence technique of normal control tissue samples revealed that rare NCAM+ renal interstitial cells could co-express FGFR1 (Figure 36A), or α5β1 integrin (Figure 36B). However, there was great heterogeneity between NCAM+ renal interstitial cells, since not all NCAM+ cells co-expressed these molecules.

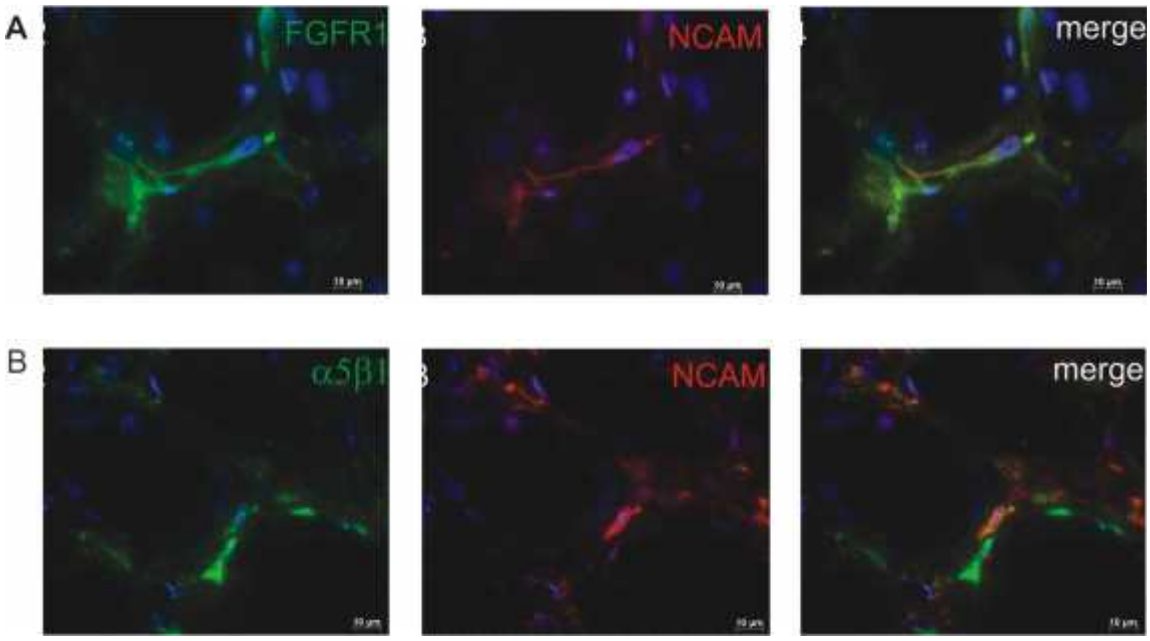

Figure 36. Co-localization of NCAM with FGFR1 and α5β1 integrin on same interstitial cell

Furthermore, we showed that increased NCAM+ renal interstitial cells in incipient fibrosis, could also co-express FGFR1, or α5β1 integrin (Figure 37). There was a great variability between co-expression of these three markers and NCAM on renal interstitial cells from case to case associated with fibrosis. For instance, in some cases with initial phase of fibrosis, rare NCAM+/FGFR1+ renal interstitial cells were detected like in control tissue. In contrast, other renal biopsy specimens with incipient fibrosis almost all NCAM+ renal cells co-expressed FGFR1 (Figure 37, a1-a3). In the renal tissue with fibrosis, increased number of cells coexpressing NCAM and α5β1 integrin (Figure 37, b1-b3) in comparison to normal tissue was observed.

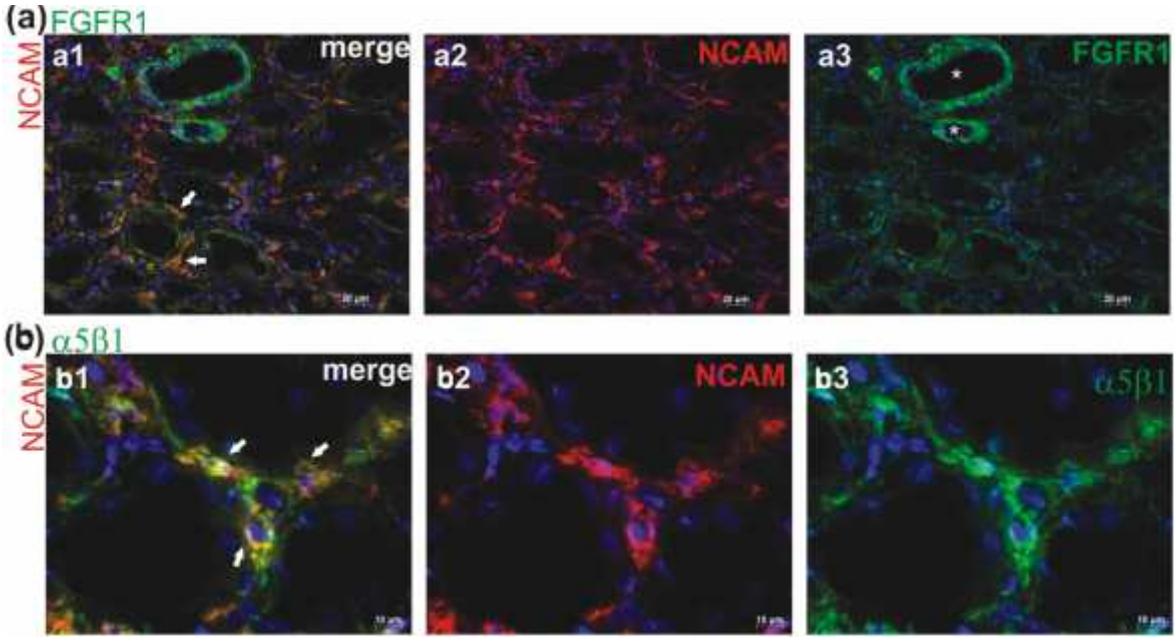

Figure 37. Co-expression of NCAM with FGFR1 and α5β1 integrin in interstitial fibrosis

In addition, in some cases of initial interstitial fibrosis we detected rare NCAM+CDH9+ interstitial cells (Figure 38A, white stars). Very interesting was also founding PSA-NCAM+ NCAM+ cells in tissue with fibrosis (Figure 38B), having in mind that PSA-NCAM was detected only in fetal renal tissues. Also new mesenchymal marker W8B2 was expressed and co-localized with NCAM on rare interstitial cells (Figure 38C, white arrow).

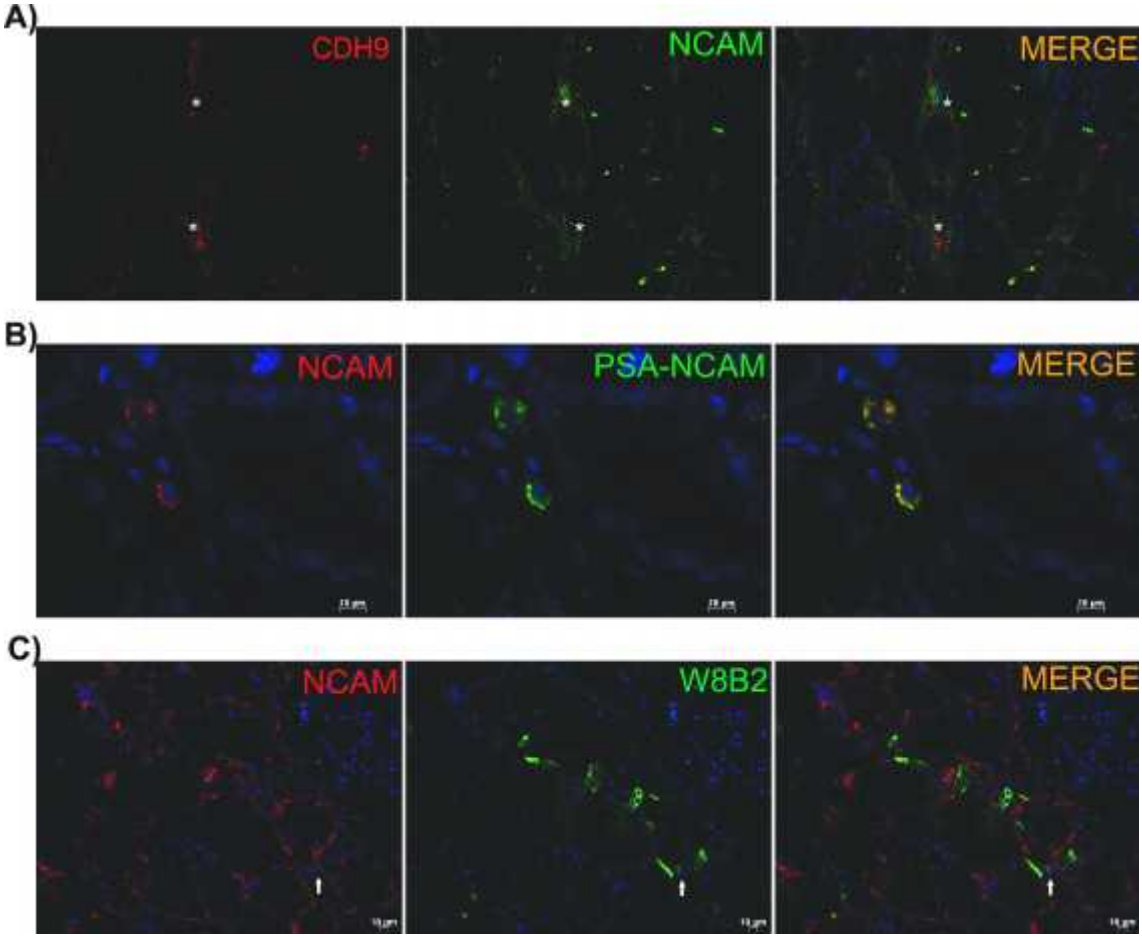

Figure 38. Co-expression of NCAM with rare CDH9+, PSA-NCAM+ and W8B2+ cells in initial interstitial fibrosis.

5. Discussion

5.1. Discussion considering NCAM expression in fetal and neonatal tissues

Significance of NCAM expression on renal progenitor cells in correlation to adult renal stem markers: CD24, CD133 on the same progenitor cells was investigated in fetal and in neonatal tissue. PSA-NCAM co-expression with NCAM and other cell surface markers known to be present on renal fetal and adult progenitor (CD24, CD133) cells was also evaluated. Since NCAM is not expressed on UB or differentiated epithelia, it is likely to be used for the identification of metanephric mesenchyme-derived progenitor nephron populations (NCAM+X+) if the second marker is clearly not detected on MM and stromal cells. This definition is most suitable for the NCAM+CD326+ fraction among the human fetal kidney cells (33).

Using special designed primers for each NCAM isoform, our RT-PCR analysis on fetal, neonatal and adult kidney tissue shows presence of all three isoforms in the fetal as well as in the adult tissue, indicating that there is no evidence of a one specific embryonic NCAM isoform in kidney. Similar results was also detected on mouse embryonic kidney, hrere immunobloting analyses showed presents of 3 distinct bands on 120, 140 and 180 kDa, unlike to embryonic spinal cord were broad band from 170-250 kDa was detected (50). Our results correspond also to a previous study done by Gattenloehner et al (12). Present molecular genetics evidence of the predominant NCAM isoforms 120 kDa, 140 kDa, and 180 kDa present in humans was also corresponding with our immunofluorescent results. Namely, immunohistochemistry and double immunofluorescent analysis with NCAM antibodies like Eric-1 and W1C3 which recognize N-terminal domain of NCAM, common to all isoforms, as well as OB11 and EP2567Y which recognised C- terminus, had strong and similar expression pattern on MM cells (Figure 10A-D, Figure 11). Although lack of NCAM-180 expression in the neonatal sample, less intensive expression of NCAM-180 in adult tissue in comparison to the expression of NCAM-120/140 in the same samples and clear expression of NCAM-180 in all tested fetal tissues, may suggest that 180 kDa isoform is a predominant NCAM isoform during renal development.

Immunohistochemistry staining of NCAM, WT1 and CD326 showed that co-expression of these 3 molecules on nephron progenitors could be detected at level of RV, C and S shaped body (Figure 10E-F). New studies indicated that WT1 is necessary for FGF signalling in renal progenitor and cell surviving (76). In contrast, co-expression of NCAM with CD34 and CDH9 was not observed. CD34 positive cells were localized peri-tubular mainly on endothelial cells, while CDH9 was expressed exclusively in UB cells in fetal tissues. This result is very interesting taking into account that CDH9 was known as marker of renal fibroblast (77) Nevertheless, since in fetal tissue CDH9 was restricted to UB it could be considered as UB marker in fetal epithelial renal progenitors.

In neural development it has been shown that mainly NCAM-140 and 180 kDa modulate cell migration and neuron growth; NCAM-180 is found in postsynaptic densities of mature neurons (78), while NCAM-140 is expressed in growth cones and axon shafts of developing neurons (79) and that NCAM-120 expression is primarily in glia (80). However, all NCAM isoforms may support synaptogenesis (81). Looking back on immunomorphological profile un-polysialylated NCAM molecules in fetal tissues are present on MM cells in renal stromal-future components of renal medulla in adult kidney, according to our results and previous studies (33, 50). These MM cells, which surround UB tree and follow its growth, and which are not induced by UB tip did not show any co-expression of NCAM with any other self surface progenitor markers: CD24, CD133, CD34, Ki-67 and did not had polysialylation of NCAM. Indicating these facts, it can be suggested that NCAM+ renal mesenchymal progenitor cells which “escort” UB have the same purpose in fetal kidneys as in neural development, suggesting that NCAM molecules are responsible for cell migration in this stage of kidney development.

Results on fetal cell lines HEK-293, showed that cell lines with density over 70% expressed NCAM (23.33%). Interestingly, low density cell cultures had almost 2 times less NCAM expression (16.8%). High density cultures had two populations of cells, and in these cases bigger population had similar NCAM expression like cells in low density culture. These finding showed that HEK-293 line had diffuse NCAM expression which was in correlation with growing conditions, indicating that NCAM cell to cell assembling was present only when cells are “overcrowded”. On the other

hand, expression of CD24, CD133, CD34 and FGFR1 were negative in both tested group, while CD326 shored low positive signal (2.1%). These results are contrary to observation of Metsuyanim et al on human fetal kidney cell lines (HFK), which showed over 30% of NCAM+ cells and strong expression of CD326, CD24 and CD133 (over 60%), while CD34 was >15% (33). Thus, HEK-293 cell line was not good "model culture" for investigation of NCAM and renal progenitors in kidney. In addition recently findings of the same group of investigator showed that HFK cell cultured in serum free medium (SFM) had lower NCAM expression (5-20%), these SFM cells were able to form compact colonies of small round/cuboidal cells, while HFK in serum containing medium yield dispread fibroblast shaped cells (82).

FACS analysis of renal fetal progenitor surface markers demonstrated two different progenitor pools in the nephrogenic zone of fetal tissue: $NCAM^{+}EpCAM^{-}$ pool of mesenchymal cells and $NCAM^{-}EpCAM^{+}$ pool of epithelial cells in UB (33). Using DIF staining, we tried to further determinate localization of these cells. Our results show that $NCAM^{+}EpCAM^{-}$ cells are first expressed in CM. Further differentiation and localization shows that NCAM molecules on $NCAM^{+}EpCAM^{-}$ cells became polysialylated in CM. PSA-$NCAM^{+}EpCAM^{-}$ cells simultaneously with polysialylation start to express CD24. So we could say that in nephrogenic zone NCAM+ cells which have been induced by UB tip, have "new" renal progenitor pool of PSA-$NCAM^{+}CD24^{+}$ nephron precursor cells.

Polysialylation of neural cell adhesion molecule (PSA-NCAM) modulates cell-cell homophilic binding and signalling during brain development (83) In the developing neural system, NCAM polysialylation is required for cell proliferation and migration (84, 85) and plays a role in neurogenesis, axonal pathfinding and nerve branching, since negatively charged residue of NANA provide hydrodymamic space and induced anti-adhesive effect on affected cells (86, 87). The $NCAM^{+}$PSA-$NCAM^{+}CD24^{+}$ cells in CM which also have proliferate activity (positive staining with Ki-67), and they represent earlier renal progenitor cells for all future components of mature nephron. If we suppose that PSA-NCAM molecules in kidneys play the same role as PSA-NCAM in neural development, our morphological analysis of PSA-NCAM expression suggests that polysialylated NCAM is required for further migration of renal progenitor and

development of metanephros. Presence of Ki-67+ cells on PSA-NCAM+, but never on NCAM+ cells only, also suggests that PSA-NCAM is correlated with cell proliferation.

Also, the expression of PSA-NCAM on morphologically younger nephron precursors, followed by the expression of EpCAM, suggests that this post translational modification of NCAM molecules could be a trigger for mesenchymal-epithelial transformation (MET) in NCAM+ fetal nephron progenitors.

CD24 is a sialoglycoprotein, mainly known to be present on immature cells, as well as on renal stem (progenitor) cell markers. Strong expression of CD24 and absence of EpCAM expression in condense mesenchyme and pretubular aggregates, indicating that CD24, similar like PSA-NCAM is an earlier marker of MET than CD326 (EpCAM), which is detected on nephron precursors in I stage of metanephron differentiation, known as renal vesicle. Co-expression of CD24 with PSA-NCAM is another proof that polysialylated NCAM is also a renal stem marker. CD24 may have an important role in the commitment and transition of kidney mesenchymal cells to an epithelial phenotype, upregulation of CD24 may also represent an important regulatory step in the transition of a differentiated epithelium to a mesenchymal phenotype, as seen in the model of epithelial injury and in specific forms of cancer (88). Although the role of CD24 in renal development is currently unclear, expression of CD24 on cells in UB tip and its co-expression with TRA-1-60 and E-cadherin on these structures suggest that combination of these three surface markers may present epithelial renal progenitor pool (TRA-1-60^{+}E-CDH^{+}CD24^{+} cells) in fetal tissue. Thus, we could conclude that in fetal kidney tissue exist both mesenchymal and epithelial progenitor cell pools, and that CD24 at one point of kidney development was present in both, epithelial and mesenchimal renal progenitor populations.

In fetal tissues TRA-1-60 is widely expressed on apical side of UB cells. The TRA-1-60 epitope was identified as an isoform of the proteoglycan, podocalyxin and its linked to dedifferentiation in embryonic carcinoma cells and one of a few antigens that are widely used in human stem cell research as positive indicators of a true pluripotent human stem cell (89-91). TRA-1-60 was also present in adult kidney and recent studies showed its up-regulation in tubuo-interstitial diseases, and co-expression of TRA-1-60

with Pax-2 and Ki-67 suggesting its role in reparation of distal tubules in diseased kidney (92).

E-CDH as we mentioned was co-expressed with TRA-1-60 on UB cells, but it is interesting to note that on mesenchymal nephron progenitors E-CDH was present on CM derivates, start on the level of renal vesicle, in human fetal tissues. Similar expression pattern of E-CDH have been already shown, indicating that E-CDH protein is marker of MET (33). Interestingly E-CDH similar like CD24 was expressed on both renal progenitor population pools.

Polysialylation of NCAM molecules on nephron precursors may be the first stage in MET, since looking from morphological aspect PSA-NCAM is not present on structures before condensation of induced mesenchyme. Considering immunostaining profile, polysialylation of NCAM molecules starts at first stage of metanephron development, in CM, and it remains till S shaped body, the last step before formation of mature fetal glomeruli. Absence of polysialylated modification in uninduced mesenchymal cells in medulla and in nephrogenic interstitium and on the other side PSA-NCAM expression at the beginning of nephron development, i.e. stage of CM suggests that NCAM polysialylation is necessary for further nephron differentiation. Considering that lack of PSA-NCAM expression in neonatal, normal adult and cRCC tissue (44) indicates PSA-NCAM as a potential renal fetal/embryonic form of NCAM molecule.

Characterization of new marker, W1C3 by imunohistochemisrty and double immunofluorescence showed co-expression (Figure 10) and co-localization (Figure 11) with NCAM, suggesting that W1C3 is a new clone for NCAM. Nevertheless, FACS analysis on HEK-293 cell line showed four times lower expression of W1C3 (4.2%) in contrast to NCAM (16.8%) in same population. Nevertheless CD56+ subset of mesemchymal stem cells (MSCs) showed increased expression of W1C3 antigen (93). However, knowing that HEK-293 line was not the best “model” for analyses of renal progenitors, W1C3 should be further tested on HFK lines and for precised identification of W1C3 protein mass spectrophotomerty is necessary. W5C4C5 is one more new mesenchymal marker which was DIF tested in relation to NCAM expression. W5C4C5 antibody showed broad co-localization pattern with NCAM in fetal samples, while in adult tissue it was completely negative, except in nerve where also had overlap with

NCAM. These findings suggest that like W1C3, W5C4C5 could be potential new clone for NCAM. And like in W1C3 cases its identification requires mass spectrophotomerty testing/ screaning. In addition W8B2 antigen was also tested in relation to NCAM. Screening of the mesenchymal stem cell antigen 1 (MSCA-1), specific antibody W8B2 on HEK-293 cells transfected with the full-length coding sequence of tissue non-specific alkaline phosphatase TNAP showed specific reactivity with transfected but not with parent cell line. Show that MSCA-1 is identical to TNAP, an ectoenzyme known to be expressed at high levels in liver, bone, and kidney as well as in embryonic stem (ES) cells (94). DIF analyses did not showed any co-expression of W8B2 with NCAM in fetal tissues. Thus, MSCA-1 was not detected on NCAM+ mesenchymal cells.

5.2. Discussion considering NCAM expression in renal tumors and cell lines

Renal epithelial tumors comprise a heterogeneous group of tumors. Renal cell carcinoma (RCC) has different histologic origin, metastatic potential, and clinical outcomes; typically does not proliferate rapidly nor does it invade the surrounding tissues, but it does metastasize. According to the classification in 2002 RCCs have five subtype classifications, i.e., clear cell RCC, papillary RCC, chromophobe RCC, collecting duct carcinomas, and unclassified RCC. This classification reflects the location within the nephron from which the tumors originate. Epithelial cells of the proximal part of the renal tubule give rise to clear cell and papillary RCC, while the collecting tubule of the nephron gives rise to chromophobe RCC and collecting duct carcinomas (95). RCC represents 80% of renal tumors in adults and is characterized by lack of early warning signs, by frequent metastasis, and by resistance to currently used treatments (95, 96). Cancer cells are characterized by indefinite proliferation, invasiveness and metastases. These characteristics are usually related to one another. Namely, cancer cells that proliferate rapidly tend to invade and metastasize. Therefore, identification of molecular markers of tumor aggressiveness is urgently needed. In a variety of human malignancies, tumor progression is associated with changes in cell adhesion molecule (CAM) expression (97).

Significant number of studies revealed that not only that NCAM is essential during neural and widely expressed in renal development, NCAM molecule also have major role in initiation and regulation of NCAM mediated tumorigenesis in various tissues. Thus, it has been known that NCAM is expressed in myeloid leukemia (35). Also, immunohistology studies indicated NCAM as marker of neuroendocrine and neuroectodermal tumors, as well as differential-diagnostic and prognostic marker of multiple myeloma (36, 39). In renal cell carcinoma NCAM was first time described in 2003. In this study NCAM expression was detected in subgroup of aggressive cRCCs. In particular, NCAM expression correlated strongly with the occurrence of metastases in the CNS and adrenal gland, while survival of patients with NCAM-expressing RCCs was lower than the survival of other patients (44). Much more recently study from 2012 also investigated NCAM expression on RCC. Results obtained in this study also indicated that aggressive RCC behavior is related to NCAM expression. Nevertheless,

this study pointed that NCAM expression is not characteristic for any particular RCC subtype, thus NCAM is not useful marker for differential diagnostic of RCC (58).

In this thesis, we described for the first time co-expression of FGFR1 and NCAM in different renal tumors. Co-expression of these two markers was analyzed by immunohistochemistry in cRCC, pRCC and chRCC, in collecting duct carcinoma, oncocytomas and in few other malignant and benign renal neoplasms. Co-expression of both molecules was detected in the majority of studied renal tumors and moreover, co-localization of these molecules on the same renal tumor cells was revealed by triple immunofluorescent technique.

First functional interaction between FGFR1 and NCAM has been reported in neurons (27). Thereafter, interplay between these two molecules in different non-neural cells was reported, indicating that interaction of NCAM with FGFR results in stimulation of FGFR signaling in various cell types (29, 98). It has been shown that NCAM-mediated activation of FGFR leads to different cellular responses (99). Recent publication on experimental cell cultures showed that NCAM-dependent FGFR signaling promotes cell migration and invasion in epithelial ovarian carcinoma (60). The mechanism of FGFR1 activation by NCAM is not well clarified. In particular, FGFR membrane-proximal Ig3 module is known to bind to NCAM membrane-proximal Fn3 module (100). Also further analysis showed that FGFR Ig2 module is involved in direct binding to the F3 (1-2) domains of NCAM and that Ig2 module has two binding sites for NCAM (67). Several speculative models for molecular mechanisms of NCAM interplay with FGFR1 were formulated based on this data (67,100).

Immunofluorescent technique was used to determine whether NCAM and FGFR1 were present on same tumor cells. Thus, co-localization of NCAM and FGFR1 on the same renal tumor cells detected by triple staining could indicate that functional interplay between NCAM and FGFR1 could occur in renal tumor tissues. Nevertheless, semi-quantitative analysis of triple immunofluorescence showed that number of $FGFR1^{+}/NCAM^{+}$ cells was increased with nuclear grade in cRCC and pRCC suggesting that NCAM/FGFR1 interaction may be related and leads to aggressive behavior of these tumors.

Staining pattern of NCAM expression was usually similar to the FGFR1 in different RCC types. Lower grade RCC (I-II) had uniformly membranous expression of

NCAM and FGFR1. Thus, we could say that membranous expression of both molecules in lower grade RCCs could fit to “Kochoyan’s model” (67) suggesting that when NCAM is not involved in cell adhesion between two neighboring cells, molecules are uniformly spread on cell membrane, and FGFR molecules do not bind significantly to NCAM. In these cases FGFR and NCAM molecules do not interact with each other, suggesting that this model could be the key for low aggressive potential of these RCC. Our results are somehow in concordance with recently obtained data based on human ovarian carcinoma cell lines. In this study, ovarian carcinoma cell lines which prominently express FGFRs were transfected with NCAM without Fn3 module (NCAM-ΔF2). *In vitro* experiments showed that cells with NCAM-ΔF2 failed to promote cell migration and invasion (60), suggesting that physical interaction between FGFR1 and NCAM is required for aggressive tumor behavior. Also, same cell line in mice formed tumors with smooth margins within the ovary, indicating that absence of NCAM/FGFR interaction is responsible for poorly invasive potential of developed tumor (60).

However, cRCC with higher NG (III-IV) and all pRCC (NG I-IV) in addition to membranous had cytoplasmatic expression of both markers, while in chRCC membranous and cytoplasmatic expression of FGFR1 was followed by weak mainly cytoplasmatic NCAM expression. Interestingly, triple immunofluorescent technique in RCC with high nuclear grade showed aggregated colocalized expression on cell membrane of both molecules (Figure 28G-O). Thus, we found that expression of FGFR1 and NCAM in tumor cells with higher nuclear grade leads to accumulation of both molecules in cytoplasm and on membrane. Previous data show that when NCAM is involved in cell-cell adhesion, NCAMs may aggregate/accumulate themselves forming *cis*-dimers. These dimers via *trans*-homophilic bindings mediated cell-cell adhesion making so-called “zipper” formations (13), presumed aggregation of NCAMs lead to subsequent aggregation of FGFR molecules (67). Thus, Kochoyan et al proposed a second model of NCAM/FGFR interaction: FGFR is expected to bind to and becomes activated by NCAMs only when NCAM is clustered through a *trans*-homophilic binding mechanism (67). It might be that this model could be applied to RCCs with high nuclear grade, suggesting that aggregations of NCAM and FGFR1 on cell membrane could activate NCAM/FGFR1 interplay which is then responsible for migration and

invasive potential of these RCCs. Study on ovarian carcinoma mentioned above (60), also pointed to crucial role of NCAM/FGFR interaction in aggressive tumor behavior. Same cell lines were now transfected with full-length NCAM. Thus, cells which now had Fn3 domain which is necessary for FGFR binding to NCAM showed migrations and invasion of tumor cells *in vitro* and *in vivo* experiments (60), conforming the role of NCAM/FGFR interaction in aggressive tumor behavior.

Results considering oncocytoma and metanephric adenoma, showed exclusively cytoplasmatic co-localization of FGFR1 and NCAM. Since in both benign renal tumors no membranous staining was detected, it seems that membranous expression is crucial event for NCAM and FGFR1 interplay leading to tumor invasiveness while the lack of NCAM/FGFR1 membranous expression is characteristic of renal benign tumors. In the present study NCAM expression was detected in less number of RCC in comparison to FGFR1. Expression of NCAM in renal tumors was also evaluated previously (41, 44). Daniel et al detected membranous NCAM expression in cRCC only, and no staining in pRCC and chRCC. They claim that NCAM expressing tumors behave aggressively and metastasize preferentially to NCAM-expressing organs like CNS and adrenal gland (44). Other, recently published data on NCAM expression in RCC, revealed cytoplasmatic NCAM staining not only in cRCC but also in pRCC and chRCC, and they did not find any association between NCAM expression and histological RCC type, nuclear grade or stage (41). It remains unclear, why cited studies (41, 44) had presented different staining pattern knowing that in both studies monoclonal antibody for NCAM (CD56, Novocastra) which recognized external domain of NCAM molecule had been used. On the other hand, in our study we revealed both staining patterns, membranous and cytoplasmatic, using monoclonal NCAM antibody specific for external (Fn3) domain. Lower grade tumors (I and II) cRCC and mcRCC had membranous, while high grade cRCC, all pRCC, chRCC in addition to membranous had also cytoplasmatic pattern. Thus, switch from NCAM negative to NCAM positive RCC could be a crucial event for tumor aggressiveness and invasiveness, as it was shown in the experiments by Lehembre et al (99), which clarified the importance of NCAM expression for epithelial mesenchymal transition in the development and progression of epithelial tumors.

NCAM expression was detected by RT-PCR and immunostaining. NCAM-140 was present in all analyzed malignant and benign renal neoplasms. NCAM-140 plays role in growth cones and axon shafts of developing neurons and modulates cell adhesion, neuron growth and cell motility (101). Recent study showed that NCAM-140, which has transmembrane domain, was expressed on various human malignancies, inducing antiapoptotic/proliferative pathways and specifically phosphorylated calcium-dependent kinases that are relevant for tumorigenesis (41). However, NCAM-120, which does not have transmembrane domain, was present only in chRCC, oncocytoma and metanephric adenoma. Functions of these two isoforms still have not been cleared up in renal neoplasms and remain to be further investigated.

FGFR1 was present in great number of all analyzed renal neoplasms. Actually, FGFR1 was present in high percentage of RCC, corresponding to recently published data which showed expression of FGFR1 in 98% of primary RCC (102). Interestingly, FGFR1 regulates different processes in invasive and non-invasive urothelial carcinomas in cell culture experiments. FGFR1 expression in non-invasive urothelial carcinoma promotes proliferation and survival, while in invasive urothelial carcinoma FGFR1 mediates invasion (103). We clearly revealed by imunohistochemistry and by precise immunofluorescent technique on cryostat sections variable FGFR1 expressions on different cell compartments: membranous in lower grade mcRCC and cRCC (NG I-II); cytoplasmatic in addition to membranous in higher grade cRCC (NG III-IV), and in all pRCC and chRCC; cytoplasmatic in all oncocytomas. Thus, variable FGFR1 expression on various renal tumors could indicate different role of FGFR1 signaling in these tumors.

Our results showed that most of analyzed renal tumors co-expressed NCAM and FGFR1 and moreover co-localization of both markers on same tumor cell. Co-expression of NCAM and FGFR1 is not related to histological type, origin, size, stage and nuclear grade. Localization of NCAM and FGFR1 expression in different cell compartments in various renal tumors suggests that NCAM/FGFR1 interaction possibly has multipurpose and different function in tumor oncogenesis in kidney.

FACS analyses on tested tumor cell lines, CRL-1932 and TW33, showed very interesting pattern of NCAM expression. Namely, low density cell cultures (CRL-1932) were almost negative for NCAM expression and they showed only one cell population

of alive cells. On the other hand, high density cultures (over 70%) had 2 populations of cells. In these cultures smaller population strongly expressed NCAM (CRl-1932 – 57.67%), while bigger cell population had very weak NCAM expression. On the other hand TW33 cell lines in both group (low and high density) had only one cell population) and expression around 40%. Previously study on RCC cell lines also showed diffuse NCAM expression on 6 different RCC cell lines (58). Thus, in overcrowded cultures RCC cell lines could have two different cell phenotypes. These finding suggest that cells will used NCAM for cell-cell assembling only when they are "overcrowded".

In addition, aquaporin 1 (AQP1) expression was correlated to NCAM in renal neoplasm. AQP1, a water channel and regulator of endothelial cell migration is expressed in different epithelial tissues, on endothelium and in some urinary tract neoplasms. It is also considered as a differentiation marker for proximal renal tubular cells, from which clear cell and papillary renal cell carcinoma originate. In the normal kidney, AQP1 is only expressed in epithelial cells of proximal tubules and in the descending limb of Henle, but not in other nephron segments, collecting ducts or urothelial cells, whereas aquaporin-2 is selectively expressed in collecting ducts (104).

Recently investigation showed that beside function as water-transporting proteins AQP1 regulates the expression of β-catenin, probably by maintaining the post-translational level of β-catenin, further they demonstrated that AQP1 exerts its migration enhancer function through modulating the expression of FAK. Thus, true FAK pathway AQP1 promote MSCs migration. The systemic administration of AQP1-MSCs into a rat fracture model showed that significantly more AQP1-MSCs migrated to the fracture site, suggesting the potential therapeutic use of genetically modified AQP1-MSCs in cell therapy applications (105).

In this thesis, AQP1 expression was seen in the majority of all cRCC and pRCC. No significant difference was found comparing type 1 and type 2 pRCC carcinomas. All oncocytomas were completely negative. Chromophobe renal cell carcinomas and collecting duct carcinomas were negative. Interestingly in cRCC only rare tumor cells had co-localization of NCAM and AQP1, while in pRCC NCAM+ tumor cells were AQP1 negative and opposite. Fetal tissue in early gestation weeks does not express AQP1 in nephron progenitor cells (data not shown). Therefore, AQP1 shows RCC

subtype-specific expression and could be useful diagnostic marker for cRCC and pRCC carcinomas. Immunohistochemistry study on 202 paraffin embedded RCC samples showed that AQP1 expression decreased significantly in higher grades of cRCC carcinomas, compared to lower grades of this tumor group. This was seen in clear cell renal cell carcinomas but not in papillary renal cell carcinomas. Thus, AQP1 is reliable markers for clear cell renal cell carcinomas of lower grades but not for higher grades, (106). Still, absence of NCAM and APQ1 co-expression suggests that NCAM+ and AQP1+ RCC cells belong to various cancer cell niches.

5.3. Discussion considering adult tissue (normal and tissue with interstitial fibrosis)

The kidney derived, as it was note in introduction in interaction between UB and MM cells. Thus these two progenitor cells pools will differentiate into more than 26 different cell types in the adult kidney. MM cells widely expressed NCAM during kidney development, but this expression is restricted to feotal and early postnatal stage (50). While on adult normal tissue NCAM expression is reserve for nerve and rare single interstitial cells (40). It has been widely accepted that, in contrast to other human organs, normal renal tissue contains a few fibroblasts (62) and some other interstitial cells, such as scarce NCAM+ cells with dendritic morphology, considered as renal progenitor cells (40). However, the contribution of NCAM+ interstitial cells, as well as their immunomorphological characteristics has not been fully elucidated.

Renal fibrosis, whether the origin is inflammatory or immunological, obstructive, metabolic or systemic is inevitably progresses to end-stage renal disease. Glomerular inflammation, mesangial expansion and sclerosis have all been considered important factors in the development of chronic kidney disease (CKD). In the majority of patients with CKD, however, the progression of renal insufficiency is most closely correlated to the degree of tubular atrophy and interstitial fibrosis. Fibrosis can be considered aberrant wound healing, in which there is progression rather than resolution of scarring following injury and fibroblasts are central to this process. Fibroblasts have distinct phenotypes depending on the disease and site from which they are isolated. Fibroblasts in the interstitium of kidneys with chronic progressive disease take on a contractile myofibroblastic phenotype and are responsible for the formation of the fibrillar collagen-rich extracellular matrix (ECM) that fills the interstitium leading to nephron loss and declining kidney function. The presence of myofibroblasts is, therefore, recognized as a predictor of fibrotic progression in both experimental models and human renal diseases (62). Renal interstitium of fibrotic kidney contains a large morphological heterogeneity of cells, mainly fibroblasts and myofibroblasts (66, 107).

In this thesis, NCAM+ cells were confirmed in less than a half of the analyzed human biopsy specimens, where they were usually associated with interstitial fibrosis. These results are in correlation to previously findings by Markovic-Lipkovski et al (40).

Increase of NCAM+ cells was found in incipient renal fibrosis, usually in the areas of peritubular slight fibrosis without tubular atrophy, whereas in the majority of cases in advanced fibrosis they were almost absent. Previous study (108) has also revealed increased density of NCAM+ interstitial cells in early phase of repairing process after ischemic tubular injury in rats, with rapid decline few days after injury. Nevertheless, it is possible that rare NCAM+ cells which are increased in initial phase of fibrosis represent residue of previously mentioned NCAM+EpCAM- progeniror cells in fetal tissues, suggested as stromal precursors (33). Altogether, it could implicate a regulatory role of NCAM+ cells in the initial phase after injury, suggesting that these interstitial cells exhibit transient phenotype. Thus, immunophenotyping of NCAM+ cells could help us to clarify their origin, putative role and fate. Therefore, we further investigated whether NCAM+ renal interstitial cells express other molecular markers relevant for fibrosis, such as FGFR1, CDH9 and α5β1 integrin.

NCAM+ renal interstitial cells, like renal fibroblasts, display a large degree of heterogeneity, even in normal human adult kidneys. In fact, in some renal tissues, it was impossible to find interstitial cells coexpressing NCAM with FRGR1, or α5β1 integrin, while in others NCAM+/FGFR1+ or NCAM+/α5β1+ integrin cells were detectable. FGFR1 receptor is involved in initial activation and proliferation of fibroblasts that are responsible for collagen production (98), and could be directly activated by interaction with NCAM molecule which additionally promotes FGFR1 recycling, resulting in sustained FGFR1 signaling that is important for fibroblast migration (98, 100). However, NCAMs which mediate cell-cell adhesions, by forming NCAM *trans*-homophilic binding via “zipper”-like structures, have been expected to bind and activate FGFR1 (109, 110). This could be the underlying mechanism of the strict and abundant overlapping between NCAM and FGFR1 molecules observed in the areas with incipient fibrosis in some cases in our study. However, the dendritic morphology of NCAM positive interstitial cells allows them to communicate easily with each other, suggesting that strict increase of NCAM expressing cells is not necessary for FGFR1/NCAM interplay. Especially if we know that in neural cells NCAM/FGFR interaction can be modified by other molecules present in cell or in extracelular matrix. Thus, previously noted study (100) showed by nuclear magnetic resonance that adenosine triphosphate

(ATP) binding site to NCAM overlaps with FGFR, so ATP can inhibit NCAM/FGFR interaction.

All major NCAM isoforms can cooperate with FGFR1 (111), and after applying PCR we have not detected any difference concerning major NCAM isoforms on normal and fibrotic renal tissues. Receptor α5β1 integrin, present on mesenchymal derived cells (112), is known to be involved in extracellular matrix assembly, cell adhesion, migration, proliferation and differentiation (70, 99, 113, 114). Since it has been significantly increased in fibrotic kidneys (40, 113), we were encouraged to search for renal interstitial cells co-expressing NCAM and α5β1 integrin. Considering that co-expression of NCAM and β1 integrin is essential for mesenchymal cell motility (99, 114), NCAM+/α5β1 integrin+ interstitial cells could also represent migratory cells easily involved in the renal cell cross-talk. In neural cells NCAM regulates important aspects of integrin-dependent cell migration, axonal/dendritic outgrowth, and synaptic targeting. In brief NCAM interact functionally with integrins and activate convergent signaling pathways leading to ERK MAP kinase. NCAM induces recruitment of tyrosine kinase Fyn to its intracellular domain, which turn activates of FAK, ERK, and the transcription factor cAMP response element binding protein (CREB), which stimulates neurite outgrowth. FAK is a key intracellular regulator of migration in nonneuronal cells, acting by increasing turnover of focal adhesive contacts at the cell's leading edge (115). Furthermore, since α5β1 integrin expressed by fibroblasts promotes acquisition of myofibroblastic phenotype (113), it could probably implicate the same fate of NCAM+/α5β1 integrin+ cells, suggesting that this phenotype might be transient.

The origin of NCAM+ renal interstitial cells remains unclear. Very likely, they represent resident cells which persist after the embrionic kidney development from metanephric nephros that widely expresses NCAM (33). On the other hand, abundant expression of α5β1 integrin in cultured bone marrow progenitor cells (116), as well as expression of α5β1 integrin in addition to CD34 on some NCAM+ interstitial cells (40), could further support our previous idea that the subpopulation of NCAM+ could originate from bone marrow and could be renal progenitor cells. It is tempting to speculate that NCAM positive renal interstitial cells, under particular pathological conditions, could represent transdifferentiated cells derived from tubular epithelium, since NCAM could be re-expressed in these cells after injury (33, 117) and because the

expression of α5β1 integrin could be acquired *de novo* in migrating epithelial cells during wound healing (63, 118).

In addition, in this thesis, for the he first time rare NCAM+/CDH9+ interstitial cells were detected. CDH9 was first time described in brain and together with cadherin-7 and -10 belong to type-II classic cadherins in humans. Together with all other type II class cadherins, CDH9 interact with catenins and it is involved in cadherin-mediated mechanisms of development, morphogenesis and cell-cell interactions/adhesion (119). Initial RT-PCR analyses in renal tissue had revealed that the mRNA for CDH9 was transcribed in the adult human kidney and that CDH9 play a role in cell-cell interaction as shown by a cell aggregation assay (77). Further, all RCC cell lines tested were negative for CDH9 on the mRNA and protein levels and in RCC tissue CDH9 was expressed in stromal, but nor on tumor cells. These findings indicated that CDH9 is exclusively expressed by renal fibroblasts (77). Thus, we could suggest that NCAM+CDH9+ interstitial cells are one type of renal fibroblast involved in tissue regeneration and wound healing.

Furthermore, in this study also for the first time NCAM+/PSA-NCAM+ interstitial cells were detected in incipient interstitial fibrosis. We have seen that in fetal human tissues polysialilation of NCAM molecules is necessary for proper kidney development. Also, in neural development, interactions between heavily polysialylated NCAM molecules, due to a weaker one dimensional zipper formation, favors NCAM signaling. Thus, expression of PSA by NCAM may function as a ‘switch’, regulating whether NCAM is involved in adhesion or signaling. This notion is grounded by the facts that removal of PSA inhibits NCAM-stimulated neurite outgrowth (100). Interestingly expression of PSA-NCAM during embryonic period and absence of typical dendritic morphology in NCAM+/PSA-NCAM+ cells in initial phase of interstitial fibrosis suggest that these cells may be rump from nephron precursors.

One more, very interesting result obtained in this work was detection of new marker W8B2 in initial interstitial fibrosis. W8B2 was also detected in some tubular cells in fetal tissues, but it did not co-localized with NCAM. In contrary in interstitial fibrosis rare NCAM+/W8B2+ cells were detected. W8B2, mesenchymal marker, is identical to tissue non-specific alkaline phosphatase (TNAP), enzyme which probably

had function in matrix mineralization (94). Rare NCAM+/W8B2+ cells are one more type of interstitial cells and they should be father investigated.

To summarized, detection of five different types of NCAM+ interstitial cells is one more conformation of huge heterogeneity of NCAM+ interstitial cell. Co-expression of NCAM with FGFR1, integrin α5β1, CDH9 and PSA indicated NCAM role in different types of cell signaling which are related to cell proliferation, migration, differentiation. Thus, NCAM+ interstitial cells could be involver in repairing process after injury. Recently, Harari-Steinberg et al showed that HFK cell lines ($1 \times 10^5 – 5 \times 10^5$) cultured in SFM and which expressed NCAM+ after performed grafting experiments on the chorio-allantoic membrane (CAM) of a chick embryo succeed to form tubular structures in 4/6 grafts; while the same numbers of NCAM negative cells completely failed to generate similar structures (82). Tubular structures obtained on this way, were tested by immunohistochemistry for tubular epithelial markers. Thus, staining conformed that NCAM+ progenitors undergo MET and form tubular epithelial cells, demonstrates their enriched and broad intrinsic differentiation capacity that NCAM negative progenitor lack. The same study also revealed that *in vitro* cultured NCAM+ human nephron progenitor cells (hNPCs) improve the outcome of chronic renal injury (82).

Further studies are necessary to explain why NCAM expression is increased only in the initial phase of repairing process and to clarify molecular mechanisms that determine whether physiological repair or pathologic fibrosis would occur. They have to highlight the manifold and diverse role of heterogeneous morphology of NCAM positive renal interstitial cells, revealed in this thesis, as well as their influence on renal fibrosis which probably depends on other molecular markers that NCAM positive cells could share.

6. Conclusions

1. Appling RT-PCR, three major NCAM isoforms mRNA transcripts (120, 140, 180 kDa) have been detected both in healthy fetal and adult renal tissues, as well as in adult kidneys with interstitial fibrosis. However, adult renal cell tumours expressed only 120 and 140 kDa isoforms.

2. PSA-NCAM was presented on nephron progenitors, starting from CM up to S shaped body, whereby it was not detected in neonatal and adult healthy tissues, suggesting that post-translational modification with polysialic acid was characteristic of fetal renal tissues and PSA-NCAM could be an embryonic NCAM form of renal tissue.

3. Polysialylation of NCAM molecules on mesenchymal nephron precursors may be the first sign of MET initiation, since from morphological aspect, PSA is necessary for condensation of induced mesenchyme.

4. Compared to widespread NCAM expression on metanephric mesenchyme cells, either those induced or uninduced by uretheric bud, PSA-NCAM was detected only on mesenchymal nephron precursors, cells induced to form further mature nephron formations. It could suggest that NCAM polysialylation was important for normal nephron differentiation, since mesenchymal cells in medulla and in interstitium did not exhibit NCAM polysialylation.

5. New cell surface markers W1C3 and W5C4C5 stained same cells as NCAM in fetal and adult healthy renal tissues, implicating that W1C3 and W5C4C5 detect the same molecules in tissues as NCAM.

6. NCAM was expressed in majority of analyzed RCC. $NCAM^+$ tumor cells in RCC were also $FGFR1^+$. Co-expression of NCAM and FGFR1 is not related to histological type, origin, size, stage and nuclear grade.

7. Different patterns of NCAM and FGFR1 co-localizations within tumor cell compartments of various tumor types could suggest diverse roles that might have an influence on biological tumor behavior.

8. NCAM+ renal interstitial cells are significantly increased in the initial phase of renal interstitial fibrosis. They display a morphological heterogeneity concerning co-expression of FGFR1, α5β1 integrin and other molecules relevant for renal interstitial fibrosis, and could be responsible for the regulation of healing process in the kidney. However, their precise roles have remained to be further clarified.

7. References

1. McCampbell KK, Wingert RA. Renal stem cells: fact or science fiction? Biochem J. 2012; 444: 153-168.
2. Li Y, Wingert RA. Regenerative medicine for the kidney: stem cell prospects & amp; challenges. Clin Transl Med. 2013; 2: 11.
3. Jorgensen OS, Bock E. Brain specific synaptosomal membrane proteins demonstrated by crossed immunoelectrophoresis. J Neurochem. 1974; 23(4):879-80.
4. Brackenbury R, Thiery JP, Rutishauser U. Adhesion among neural cells in chick embryo an immunological assay for molecules involved in cell-cell binding. J Biol Chem. 1977; 252:6835-6840.
5. Walmod PS, Pedersen MV, Berezin V, Bock E. Cell adhesion molecules of the immunoglobulin superfamily in the nervous system. In: Lajtha A, Banik N (eds) Handbook of neurochemistry and molecular neurobiology, vol 7, Neural protein metabolism and function. Springer, New York, 2007; pp 35-152.
6. Yoshihara Y, Oka S, Ikeda J, Mori K. Immunoglobulin superfamily molecules in the nervous system. Neurosci Res. 1991; 10:83-105.
7. Walmod PS, Kolkova K, Berezin V, Bock E. Zippers make signals: NCAM-mediated molecular interactions and signal transduction. Neurochem Res. 2004; 29: 2015–2035.
8. Cunningham BA, Hemperly JJ, Murray BA, Prediger EA, Brackenbury R, Edelman GM. Neural cell adhesion molecule: structure immunoglobulin-like domains cell surface modulation and alternative RNA splicing. Science. 1987; 236:799-806.
9. Walsh FS, Putt W, Dickson JG, Quinn CA, Cox RD, Webb M, Spurr N, Goodfellow PN. Human N-CAM gene: mapping to chromosome 11 by analysis of somatic cell hybrids with mouse and human cDNA probes. Brain Res. 1986; 387:197–200.
10. Nguyen C, Mattei MG, Mattei JF, Santoni MJ, Goridis C, Jordan BR. Localization of the human NCAM gene to band q23 of chromosome 11: the

third gene coding for a cell interaction molecule mapped to the distal portion of the long arm of chromosome 11. J Cell Biol. 1986; 102: 711–715.

11. Goridis C, Brunet JF. NCAM: structural diversity, function and regulation of expression. Semin Cell Biol. 1992; 3:189–197.

12. Gattenlöhner S, Stühmer T, Leich E, Reinhard M, Etschmann B, Völker HU, Rosenwald A, Serfling E, Bargou RC, Ertl G, Einsele H, Müller-Hermelink HK. Specific detection of CD56 (NCAM) isoforms for the identification of aggressive malignant neoplasms with progressive development. Am J Pathol. 2009; 174(4):1160-1171.

13. Soroka V, Kolkova K, Kastrup JS, Diederichs K, Breed J, Kiselyov VV, Poulsen FM, Larsen IK, Welte W, Berezin V, Bock E, Kasper C. Structure and interactions of NCAM Ig1-2-3 suggest a novel zipper mechanism for homophilic adhesion. Structure. 2003; 11(10):1291-1301.
14. Doherty P, and Walsh FS. CAM-FGF receptor interactions: a model for axonal growth. Mol. Cell. Neurosci. 1996; 8, 99-111.
15. Kolkova K, Novitskaya V, Pedersen N, Berezin V, Bock, E. NCAM-stimulated neurite outgrowth depends on activation of protein kinase C and the Ras-mitogen activated protein kinase pathway. J. Neurosci. 2000; 2238-2246.
16. Crossin KL, Tai MH, Krushel LA, Mauro VP, Edelman GM. Glucocorticoid receptor pathways are involved in the inhibition of astrocyte proliferation. Proc. Natl. Acad. Sci. 1997; 94: 2687-2692.
17. Krushel LA, Tai MH, Cunningham BA, Edelman GM, Crossin KL. Neural cell adhesion molecule (N-CAM) domains and intracellular signaling pathways involved in the inhibition of astrocyte proliferation. Proc. Natl. Acad. Sci. USA. 1998; 95: 2592-2596.
18. Berezin V, Bock E, Poulsen FM. (2000). The neural cell adhesion molecule. Curr. Opin. Drug Discov. Dev. 2000;3: 605–609.
19. Cremer H, Chazal G, Goridis C, Represa A. NCAM is essential for axonal growth and fasciculation in the hippocampus. Mol Cell Neurosci. 1997; 8(5):323-35.

20. Brusés JL, Rutishauser U. Roles, regulation, and mechanism of polysialic acid function during neural development. Biochimie. 2001; 83(7):635-43.
21. Rougon G, Hobert O.New insights into the diversity and function of neuronal immunoglobulin superfamily molecules. Annu Rev Neurosci. 2003; 26:207-38
22. Cole GJ, Glaser L. A heparin-binding domain from N-CAM is involved in neural cell-substratum adhesion. J Cell Biol. 1986; 102:403–412.
23. Cole GJ, Akeson R. Identification of a heparin binding domain of the neural cell adhesion molecule N-CAM using synthetic peptides. Neuron. 1989; 2:1157–1165.
24. Grumet M, Flaccus A, Margolis RU. Functional characterization of chondroitin sulfate proteoglycans of brain: interactions with neurons and neural cell adhesion molecules. J Cell Biol. 1993; 120:815–824.
25. Storms SD, Anvekar VM, Adams LD, Murray BA. Heterophilic NCAM-mediated cell adhesion to proteoglycans from chick embryonic brain membranes. Exp Cell Res. 1996; 223:385–394.
26. Sariola H, Saarma M. Novel functions and signalling pathways for GDNF. J Cell Sci. 2003; 116:3855–3862.
27. Williams EJ, Furness J, Walsh FS, Doherty P. Activation of the FGF receptor underlies neurite outgrowth stimulated by L1, N-CAM, and N-cadherin. Neuron. 1994; 13:583–594.
28. Paratcha G, Ledda F, Ibanez CF. The neural cell adhesion molecule NCAM is an alternative signaling receptor for GDNF family ligands. Cell. 2003; 113:867–879.
29. Cavallaro U, Niedermeyer J, Fuxa M, Christofori G. N-CAM modulates tumour-cell adhesion to matrix by inducing FGF-receptor signalling. Nat Cell Biol. 2001; 3(7):650-657
30. Mühlenhoff M, Eckhardt M, Gerardy-Schahn R. Polysialic acid: three-Dimensional structure, biosynthesis and function. Curr Opin Struct Biol 1998; 8(5): 558-564.
31. Angata K, Fukuda M. Polysialyltransferases: major players in polysialic acid synthesis on the neural cell adhesion molecule. Biochimie. 2003; 85: 195-206.

32. Theodosis DT, Bonhomme R, Vitiello S, Rougon G, Poulain DA. Cell surface expression of polysialic acid on NCAM is a prerequisite for activity-dependent morphological neuronal and glial plasticity. J Neurosci. 1999; 19:10228-10236.

33. Metsuyanim S, Harari-Steinberg O, Buzhor E, Omer D, Pode-Shakked N, Ben-Hur H, Halperin R, Schneider D, Dekel B. Expression of stem cell markers in the human fetal kidney. *Plos One* 2009; 4: e6709.

34. Zeromski J, Szczepanski M, Mozer L. Prevalence of CD56 /NCAM molecule in nervous system immune system and endocrine glands—accidental coincidence?. Endokrynol Pol. 2005; 56:78–82.

35. Etzell JE, Keet C, McDonald W, Banerjee A. Medulloblastoma simulating acute myeloid leukemia: case report with a review of “myeloid antigen” expression in nonhematopoietic tissues and tumors. J Pediatr Hematol Oncol. 2006; 28:703–710.

36. Wick MR. Immunohistology of neuroendocrine and neuroectodermal tumors. Semin Diagn Pathol. 2000; 17:194–203

37. Liang X, Greffe B, Garrington T, Graham DK. Precursor natural killer cell leukemia. Pediatr Blood Cancer. 2008;50:876–878.

38. Strekalova H, Buhmann C, Kleene R, Eggers C, Saffell J, Hemperly J, Weiller C, Muller-Thomsen T, Schachner M. Elevated levels of neural recognition molecule L1 in the cerebrospinal fluid of patients with Alzheimer disease and other dementia syndromes. Neurobiol Aging. 2006; 27:1–9.

39. Kaiser U, Oldenburg M, Jaques G, Auerbach B, Havemann K. Soluble CD56 (NCAM): a new differential-diagnostic and prognostic marker in multiple myeloma. Ann Hematol. 1996; 73:121–126.

40. Marković-Lipkovski J, Müller CA, Klein G, Flad T, Klatt T, Blaschke S, Wessels JT, Müller GA. Neural cell adhesion molecule expression on renal interstitial cells. Nephrol Dial Transplant. 2007; 22(6):1558-1566.

41. Ronkainen H, Soini Y, Vaarala MH, Kauppila S, Hirvikoski P. Evaluation of neuroendocrine markers in renal cell carcinoma. Diagn Pathol. 2010; 5:28.

42. Garin-Chesa P, Fellinger EJ, Huvos AG, Beresford HR, Melamed MR, Triche TJ, Rettig WJ. Immunohistochemical analysis of neural cell adhesion molecules.

Differential expression in small round cell tumors of childhood and adolescence. Am J Pathol. 1991; 139(2):275-286.

43. Daniel L, Lechevallier E, Bouvier C, Coulange C, Pellissier JF. Adult mesoblastic nephroma. Pathol Res Pract. 2000;196(2):135-139.
44. Daniel L, Bouvier C, Chetaille B, Gouvernet J, Luccioni A, Rossi D, Lechevallier E, Muracciole X, Coulange C, Figarella-Branger D. Neural cell adhesion molecule expression in renal cell carcinomas: relation to metastatic behavior. Hum Pathol. 2003; 34(6):528-532.
45. Dressler GR: The cellular basis of kidney development. Annu Rev Cell Dev Biol. 2006, 22:509-529.
46. Woolf AS. The life of the human kidney before birth: its secrets unfold. Pediatr Res. 2001; 49 (1): 8–10.
47. Cho EA, Dressler GR. In The Kidney: From Normal Development to Congenital Disease. San Diego: Academic Press. 2003; pp 195–210.
48. Rosenblum ND. Developmental biology of the human kidney. Semin Fetal Neonatal Med. 2008; 13 (3): 125–132.
49. Nouwen EJ, Dauwe S, van der Biest I, De Broe ME. Stageand segment-specific expression of cell-adhesion molecules N-CAM, A-CAM, and L-CAM in the kidney. Kidney Int. 1993; 44: 147–158.
50. Klein G, Langegger M, Goridis C, Ekblom P. Neural cell adhesion molecules during embryonic induction and development of the kidney. Development. 1988; 102(4): 749–761.
51. Ferlay J, Autier P, Boniol M, Heanue M, Colombet M, Boyle P. Estimates of the cancer incidence and mortality in Europe in 2006. Ann Oncol 2007; 18: 581-592.
52. Koul H, Huh JS, Rove KO, et al. Molecular aspects of renal cell carcinoma: a review. Am J Cancer Res 2011;1(2):240-254.
53. Cairns P. Renal Cell Carcinoma. Cancer Biomark 2011; 9(1-6): 461-473.13.

54. Finley DS, Pantuck AJ, ARIE S. Belldegrun AS. Tumor Biology and Prognostic Factors in Renal Cell Carcinoma. The Oncologist 2011; 16(suppl 2): 4-13.

55. Morris MR, Maher ER. Epigenetics of renal cell carcinoma: the path towards new diagnostics and therapeutics. Genome Med 2010; 2: 59.

56. Jemal A, Siegel R, Ward E, et al. Cancer statistics, 2009. CA Cancer J Clin. 2009; 59:225-249.

57. Cohen HT, McGovern FJ. Renal-cell carcinoma. N Engl J Med. 2005; 353:2477-2490.

58. Cirović SL, Cegar BS, Vjestica JM, Dundjerović DM, Stojanović MM, Vuksanović AM, Mitrović DB, Lazić MD, Tulić CD, Marković-Lipkovski JZ. Expression of neural cell adhesion molecule in renal cell carcinoma. Acta Chir Iugosl. 2012;59(1):39-44

59. Xian W, Schwertfeger KL, Rosen JM. Distinct roles of fibroblast growth factor receptor 1 and 2 in regulating cell survival and epithelial-mesenchymal transition. Mol Endocrinol 2007; 21: 987-1000.

60. Zecchini S, Bombardelli L, Decio A, Bianchi M, Mazzarol G, Sanguineti F, Aletti G, Maddaluno L, Berezin V, Bock E, Casadio C, Viale G, Colombo N, Giavazzi R, Cavallaro U. The adhesion molecule NCAM promotes ovarian cancer progression via FGFR signalling. EMBO Mol Med 2011; 3: 480-94.

61. Boor P, Ostendorf T, Floege J. Renal fibrosis: novel insights into mechanisms and therapeutic targets. Nat Rev Nephrol. 2010; 6:643–656.

62. Meran S, Steadman R. Fibroblasts and myiofibroblasts in renal fibrosis. Int J Exp Path. 2011; 92: 158-167.

63. Kalluri R, Weinberg RA. The basics of epithelial-mesenchymal transition. J Clin Invest. 2009; 119: 1420-1428.

64. Zeisberg EM, Potenta SE, Sugimoto H, Zeisberg M, Kalluri R. Fibroblasts in kidney fibrosis emerge via endothelial-to-mesenchymal transition. J Am Soc Nephrol. 2008; 19: 2282-2287

65. Schrimpf C, Duffield JS. Mechanisms of fibrosis: the role of the pericyte. Curr Opin Nephrol Hypertens. 2011; 20: 297-305.
66. Strutz F, Muller G.A. Renal fibrosis and the origin of the renal fibroblast. Nephrol Dial Transplant. 2006; 21: 3368–3370.
67. Kochoyan A, Poulsen FM, Berezin V, Bock E, Kiselyov VV. Structural basis for the activation of FGFR by NCAM. Protein Sci. 2008; 17: 1698-1705.
68. Sims-Lucas S, Cusack B, Baust J, Eswarakumar VP, Masatoshi H, Takeuchi A, Bates CM. Fgfr1 and the IIIc isoform of the Fgfr2 play critical roles in the matanephric mesenchyme mediating early inductive events in kidney development. J Cell Sci. 2007; 120: 4388-4394.
69. Xian W, Schwertfeger KL, Rosen JM. Distinct roles of fibroblast growth factor receptor 1 and 2 in regulating cell survival and epithelial-mesenchymal transition. Mol Endocrinol. 2007; 21: 987-1000
70. Takagi J, Strokovich K, Springer TA et al. Structure of integrin α5β1 in complex with fibronectin. EMBO J. 2003; 22: 4607-4615
71. Wagrowska-Danilewicz M, Danilewicz M, Walz T. Expression of alpha5beta1 and alpha6beta1 integrins in IgA nephropathy (IgAN) with mild and severe proteinuria. An immunohistochemical study. Int Urol Nephrol. 2004; 36: 81-87.
72. Lazzeri E, Mazzinghi B, Romagnani P. Regeneration and the kidney. Curr Opin Nephrol Hypertens. 2010 ;19(3):248-53.
73. Sagrinati C, Netti GS, Mazzinghi B, et al. Isolation and characterization of multipotent progenitor cells from the Bowman's capsule of adult human kidneys. J Am Soc Nephrol 2006; 17:2443–2456
74. Bussolati, B., Bruno, S., Grange, C., Buttiglieri, S., Deregibus, M. C., Cantino D, and Camussi G. Isolation of renal progenitor cells from adult human kidney. Am. J. Pathol. 2005; 166, 545–555
75. Müller CA, Markovic-Lipkovski J, Klatt T, Gamper J, Schwarz G, Beck H, Deeg M, Kalbacher H, Widmann S, Wessels JT, Becker V, Müller GA, Flad T. Human-Defensins HNPs-1, -2, and -3 in Renal Cell Carcinoma: Influences on Tumor Cell Proliferation. Am J Pathol 2002; 160: 1311-24.
76. Motamedi FJ, Badro DA, Clarkson M, Lecca MR, Bradford ST, Buske FA, Saar K, Hübner N, Brändli AW, Schedl A. WT1 controls antagonistic FGF and BMP-

pSMAD pathways in early renal progenitors. Nat Commun. 2014;5:4444.

77. Thedieck C, Kalbacher H, Kuczyk M, Müller GA, Müller CA, Klein G. Cadherin-9 is a novel cell surface marker for the heterogeneous pool of renal fibroblasts 2f. PLoS One. 2007; 2(7):e657.
78. Fux CM, Krug M, Dityatev A, Schuster T, Schachner M. NCAM180 and glutamate receptor subtypes in potentiated spine synapses: an immunogold electron microscopic study. Mol Cell Neurosci. 2003; 24: 939–950.

79. Stork O, Welzl H, Wolfer D, Schuster T, Mantei N, Stork S, Hoyer D, Lipp H, Obata K, Schachner M. Recovery of emotional behaviour in neural cell adhesion molecule (NCAM) null mutant mice through transgenic expression of NCAM180. Eur J Neurosci. 2000; 12: 3291–3306.

80. Noble M, Albrechtsen M, Moller C, Lyles J, Bock E, Goridis C, Watanabe M, Rutishauser U. Glial cells express N-CAM/D2-CAM-like polypeptides in vitro. Nature. 1985; 316: 725–728.

81. Dityatev A, Dityateva G, Sytnyk V, Delling M, Toni N, Nikonenko I, Muller D, Schachner M. Polysialylated neural cell adhesion molecule promotes remodeling and formation of hippocampal synapses. *J* Neurosci. 2004; 24: 9372–9382.

82. Harari-Steinberg O, Metsuyanim S, Omer D, Gnatek Y, Gershon R, Pri-Chen S, Ozdemir DD, Lerenthal Y, Noiman T, Ben-Hur H, Vaknin Z, Schneider DF, Aronow BJ, Goldstein RS, Hohenstein P, Dekel B. Identification of human nephron progenitors capable of generation of kidney structures and functional repair of chronic renal disease. EMBO Mol Med. 2013; (10):1556-68.

83. Rutishauser U. Polysialic acid in the plasticity of the developing and adult vertebrate nervous system. Nat Rev Neurosci. 2008; 9(1): 26-35.
84. Hildebrandt H, Becker C, GluÈer SR, Rösner H, Gerardy-Schahn R, Rahmann H. Polysialic acid on the neural cell adhesion molecule correlates with expression of polysialyltransferases and promotes neuroblastoma cell growth. Cancer Res. 1998; 58: 779-784.

85. El Maarouf A, Rutishauser U. Removal of polysialic acid induces aberrant pathways, synaptic vesicle distribution, and terminal arborization of retinotectal axons. J Comp Neurol. 2003; 460: 203-211.

86. Tang J, Rutishauser U, Landmesser L. Polysialic acid regulates growth cone behavior during sorting of motor axons in the plexus region. Neuron. 1994; 8: 40-414.

87. El Maarouf A, Petridis AK, Rutishauser U. Use of polysialic acid in repair of the central nervous system. Proc Natl Acad Sci. 2006; 103: 16989–16994.

88. Mani SA, Guo W, Liao MJ, Eaton EN, Ayyanan A, Zhou AY, Brooks M, Reinhard F, Zhang CC, Shipitsin M, Campbell LL, Polyak K, Brisken C, Yang J, Weinberg RA. The epithelial–mesenchymal transition generates cells with properties of stem cells. Cell 2008; 133: 704–715.

89. Schopperle WM, DeWolf WC The TRA-1-60 and TRA-1-81 human pluripotent stem cell markers are expressed on podocalyxin in embryonal carcinoma. 2007; Stem Cells 25:723–730

90. Andrews PW, Banting G, Damjanov I, Arnaud D, Avner P Three monoclonal antibodies deWning distinct diVerentiation antigens associated with diVerent high molecular weight polypeptides on the surface of human embryonal carcinoma cells. Hybridoma 1984; 3:347–361

91. Badcock G, Pigott C, Goepel J, Andrews PW The human embryonal carcinoma marker antigen TRA-1-60 is a sialylated keratan sulfate proteoglycan. Cancer Res 1999; 59:4715–4719

92. Fesenko I, Franklin D, Garnett P, Bass P, Campbell S, Hardyman M, Wilson D, Hanley N, Collins J. Stem cell marker TRA-1-60 is expressed in fetal and adult kidney and upregulated in tubulo-interstitial disease. Histochem Cell Biol. 2010; 134(4):355-69

93. Bühring HJ, Treml S, Cerabona F, de Zwart P, Kanz L, Sobiesiak M. Phenotypic characterization of distinct human bone marrow-derived MSC subsets. Ann N Y Acad Sci. 2009 ;1176:124-34

94. Sobiesiak M, Sivasubramaniyan K, Hermann C, Tan C, Orgel M, Treml S, Cerabona F, de Zwart P, Ochs U, Müller CA, Gargett CE, Kalbacher H, Bühring

HJ. The mesenchymal stem cell antigen MSCA-1 is identical to tissue non-specific alkaline phosphatase. Stem Cells Dev. 2010 ;19(5):669-77.

95. Motzer RJ, Bander NH, Nanus DM. Renal-cell carcinoma. N Engl J Med 1996;335:865– 73

96. Whang YE, Godley PA. Renal cell carcinoma. Curr Opin Oncol 2003;15:213–6.

97. Hanahan D, Weinberg RA. The hallmarks of cancer. Cell 2000; 100:57– 70.

98. Francavilla C, Cattaneo P, Berezin V, Bock E, Ami D, de Marco A, Christofori G, Cavallaro U. The binding of NCAM to FGFR1 induces a specific cellular response mediated by receptor trafficking. J Cell Biol 2009; 187(7):1101-1116.

99. Lehembre F, Yilmaz M, Wicki A, Schomber T, Strittmatter K, Ziegler D, Kren A, Went P, Derksen PW, Berns A, Jonkers J, Christofori G. NCAM-induced focal adhesion assembly: a functional switch upon loss of E-cadherin. EMBO J. 2008; 27(19):2603-2615.

100. Kiselyov VV, Skladchikova G, Hinsby AM, Jensen PH, Kulahin N, Soroka V, Pedersen N, Tsetlin V, Poulsen FM, Berezin V, Bock E. Structural basis for a direct interaction between FGFR1 and NCAM and evidence for a regulatory role of ATP. Structure 2003;11(6):691-701.

101. Prag S, Lepekhin EA, Kolkova K, Hartmann-Petersen R, Kawa A, Walmod PS, Belman V, Gallagher HC, Berezin V, Bock E, Pedersen N. NCAM regulates cell motility. J Cell Sci. 2002;115(Pt2):283-292.

102. Tsimafeyeu I, Demidov L, Stepanova E, Wynn N, Ta H. Overexpression of fibroblast growth factor receptors FGFR1 and FGFR2 in renal cell carcinoma. Scand J Urol Nephrol. 2011; 45(3):190-195.

103. Tomlinson DC, Baxter EW, Loadman PM, Hull MA, Knowles MA. FGFR1-induced epithelial to mesenchymal transition through MAPK/PLCγ/COX-2-mediated mechanisms. PLoS One. 2012;7(6):e38972.

104. Nielsen S, Agre P. The aquaporin family of water channels in kidney. Kidney Int 1995; 48:1057–1068.

105. Meng F, Rui Y, Xu L, Wan C, Jiang X, Li G. Aqp1 enhances migration of bone marrow mesenchymal stem cells through regulation of FAK and β-catenin. Stem Cells Dev. 2014; 1;23(1):66-75.

106. Mazal PR, Stichenwirth M, Koller A, Blach S, Haitel A, Susani M. Expression of aquaporins and PAX-2 compared to CD10 and cytokeratin 7 in renal neoplasms: a tissue microarray study. Mod Pathol. 2005 Apr;18(4):535-40.

107. Strutz F, Zeisberg M. Renal fibroblasts and myofibroblasts in chronic kidney disease. J Am Soc Nephrol 2006; 17: 2992-2998.

108. Vansterthem D, Gossiaux A, Decleves AE, Caron N, Nonclercq D, Legrand A, Toubeau G. Expression of nestin, vimentin and NCAM by renal interstitial cells after ischemic tubular injury. J Biomed Biotechnol. 2010; 2010: 193259.

109. Kochoyan A, Poulsen FM, Berezin V, Bock E, Kiselyov VV. Structural basis for the activation of FGFR by NCAM. Protein Sci. 2008; 17: 1698-1705.

110. Kiselyov VV, Soroka V, Berezin V, Bock E. Structural biology of NCAM homophilic binding and activation of FGFR. J Neurochem 2005; 94: 1169-1179.

111. Sanchez-Heras E, Howell FV, Williams G, Doherty P. The fibroblast growth factor receptor acid box is essential for interaction with N-cadherin and all of the major isoforms of neural cell adhesion molecule. J Biol Chem. 2006; 281: 35208-35216.

112. Kelynack KJ, Hewitson TD, Nicholls KM, Darby IA, Becker GJ. Human renal fibroblasts contraction of collagen I lattices is an integrin mediated process. Nephrol Dial Transplant. 2000; 15: 1766-1772

113. Norman JT, Fine LG. Progressive renal disease: fibroblasts, extracellular matrix, and integrins. Exp Nephrol. 1999; 7: 167-177

114. Diestel S, Hinkle CL, Schmitz B, Maness PF. NCAM 140 stimulates integrin-dependent cell migration by ectodomain shedding. J Neurochem. 2005; 95: 1777-1784.

115. Schmid RS, Maness PF. L1 and NCAM adhesion molecules as signaling coreceptors in neuronal migration and process outgrowth. Curr Opin Neurobiol. 2008 Jun;18(3):245-50.

116. Wary KK, Vogel SM, Garrean S, Zhao YD, Malik AB. Requirement of α4β1 and α5β1 integrin expression in bone-marrow-derived progenitor cells in preventing endotoxin-induce lung vascular injury edema in mice. Stem Cells.

2009; 27: 3112-3120.

117. Abbate M, Brown D, Bonventre JV. Expression of NCAM recapitulates tubulogenic development in kidneys recovering from acute ischemia. Am J Physiol. 1999; 277: F454-F463.

118. Zeisberg M, Neilson EG. Biomarkers for epithelilal-mesenchymal transitions. J Clin Ivest. 2009; 119: 1429-1437.

119. Shimoyama Y, Tsujimoto G, Kitajima M, Natori M. Identification of three human type-II classic cadherins and frequent heterophilic interactions between different subclasses of type-II classic cadherins. Biochem J. 2000; 349(Pt 1):159-67.

Appendix 1

(CodonCode Aligner data for NCAM-120, NCAM-140 and NCAM-180)

Cell line : Weri-Rb NCAM 120 kDa


```
gi|62088465|d...  AAGAC GCAGC CAGTC CAAGG GGAAC CCAGT GCACC TAAGC TCGAA GGGCA
                  |2025 |2030 |2035 |2040 |2045 |2050 |2055 |2060 |2065 |2070
Contig1           ----- ----- ----- ----- ----- ----- ----- ----- ----- -----

gi|62088465|d...  GATGG GAGAG GATGC AAACT CTATT AAAGT GAACC TGATC AAGCA GGATG
                  |2075 |2080 |2085 |2090 |2095 |2100 |2105 |2110 |2115 |2120
Contig1           ----- ----- ----- ----- ----- ----- ----- ----- ----- -----

WERI_Rb_FORW_...  TNGGC GTGCC CCCNT NCAGN ACACT ATTCT GGTCA GGTAC CGAGA CGCTC
gi|62088465|d...  ACGGC GGCTC CCCCA TCAG- ACACT AT-CT GGTCA GGTAC CGAG- CGCTC
                  |2125 |2130 |2135 |2140 |2145 |2150 |2155 |2160 |2165 |2170
Contig1           TNGGC GTGCC CCCNT NCAGN ACACT ATTCT GGTCA GGTAC CGAGA CGCTC

WERI_Rb_FORW_...  TCCTC CGAAT GGAAA CCAGA GATCA GGAAT CCCGT CTGGC AGTGA CCACG
gi|62088465|d...  TCCTC CGAGT GGAAA CCAGA GATCA GGC-T CCCGT CTGGC AGTGA CCACG
                  |2175 |2180 |2185 |2190 |2195 |2200 |2205 |2210 |2215 |2220
Contig1           TCCTC CGAAT GGAAA CCAGA GATCA GGAAT CCCGT CTGGC AGTGA CCACG

WERI_Rb_FORW_...  TCATG CTGAA GTCCC TGGAC TGGAA TGCTG AGTAT GAGGT CTACG TGGTG
gi|62088465|d...  TCATG CTGAA GTCCC TGGAC TGGAA TGCTG AGTAT GAGGT CTACG TGGTG
                  |2225 |2230 |2235 |2240 |2245 |2250 |2255 |2260 |2265 |2270
Contig1           TCATG CTGAA GTCCC TGGAC TGGAA TGCTG AGTAT GAGGT CTACG TGGTG

WERI_Rb_FORW_...  GCTGA GAACC AGCAA GGAAA ATCCA AGGCG GCTCA TTTTG TGTTC AGGAC
gi|62088465|d...  GCTGA GAACC AGCAA GGAAA ATCCA AGGCG GCTCA TTTTG TGTTC AGGAC
                  |2275 |2280 |2285 |2290 |2295 |2300 |2305 |2310 |2315 |2320
Contig1           GCTGA GAACC AGCAA GGAAA ATCCA AGGCG GCTCA TTTTG TGTTC AGGAC
```

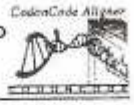

```
WERI_Rb_FORW_...  CTCGG CCCAG CCCAC AGCCA TCCCA GCAAC CTTGG GAGGC AATTC TGCAT
gi|62088465|d...  CTCGG CCCAG CCCAC AGCCA TCCCA GCAAC CTTGG GAGGC AATTC TGCAT
                  |2325  |2330  |2335  |2340  |2345  |2350  |2355  |2360  |2365  |2370
Contig1           CTCGG CCCAG CCCAC AGCCA TCCCA GCAAC CTTGG GAGGC AATTC TGCAT

WERI_Rb_FORW_...  CCTAC ACCTT TGTCT CATTG CTTTT CTCTG CAGTG ACTCT TCTTT TGCTC
gi|62088465|d...  CCTAC ACCTT TGTCT CATTG CTTTT CTCTG CAGTG ACTCT TCTTT TGCTC
                  |2375  |2380  |2385  |2390  |2395  |2400  |2405  |2410  |2415  |2420
Contig1           CCTAC ACCTT TGTCT CATTG CTTTT CTCTG CAGTG ACTCT TCTTT TGCTC

WERI_Rb_FORW_...  TGTTA G-AAN ACGNN NANCN AANNN ANNNG NCNTN TCNNA ANNNN TNNCN
gi|62088465|d...  TGTTA GGAAC TTGAA CACAA AAATT AAATT TGCT- TAAAA GCCCA GTTCC
                  |2425  |2430  |2435  |2440  |2445  |2450  |2455  |2460  |2465  |2470
Contig1           TGTTA G-AAN ACGNN NANCN AANNN ANNNG NCNTN TCNNA ANNNN TNNCN

WERI_Rb_FORW_...  NNANN NANNG CTCAA CANCA TNNNT CNCCN N-CCT C-CNN NACCC NGNTN
gi|62088465|d...  TATGA AAAAG ATCAG TGCCC CCTTT GGAAG AACCT GGCAG GACCA CCATG
                  |2475  |2480  |2485  |2490  |2495  |2500  |2505  |2510  |2515  |2520
Contig1           NNANN NANNG CTCAA CANCA TNNNT CNCCN N-CCT C-CNN NACCC NGNTN

WERI_Rb_FORW_...  ANCAT NANNN NNNNT NGCNC CTTNN CNNNN CTGCT NTNCN CTNAG NNNNT
gi|62088465|d...  GCCAC AGCTG CTGAG CAACC ATTCT GTGTG GAAGA GAAGG TTTTG TGATT
                  |2525  |2530  |2535  |2540  |2545  |2550  |2555  |2560  |2565  |2570
Contig1           ANCAT NANNN NNNNT NGCNC CTTNN CNNNN CTGCT NTNCN CTNAG NNNNT

WERI_Rb_FORW_...  CCGNC CNACN NNCCC CCGAG NCNNC CTNNT NNNTN NGNTN ACNTN TTNAN
gi|62088465|d...  GGAAA AAGCT TTACC TCCAG ACATG -TCAC CACTC ACAGA TACTT TTGTG
                  |2575  |2580  |2585  |2590  |2595  |2600  |2605  |2610  |2615  |2620
Contig1           CCGNC CNACN NNCCC CCGAG NCNNC CTNNT NNNTN NGNTN ACNTN TTNAN
```

```
WERI_Rb_FORW_...  CNNNA TNCNN CANTC GNATC TNCNN NNNNC TNNTG CCANN NNNTN TNCCN
gi|62088465|d...  CCAC- TTCAT AAGGA GTTTG CCCCC TTTT- TAATG GCAGT AAAAA -----
                  |2625  |2630  |2635  |2640  |2645  |2650  |2655  |2660  |2665  |2670
Contig1           CNNNA TNCNN CANTC GNATC TNCNN NNNNC TNNTG CCANN NNNTN TNCCN

WERI_Rb_FORW_...  NNNNT TNCNN NCTCN CCGTC TNNTN ANNTN NNNCT NCNTT CTANC NNNNN
gi|62088465|d...  GAATT TGAGA GCTC- ---TT TCTTT AAATG CTATT T-TTA AAAAC CATCA
                  |2675  |2680  |2685  |2690  |2695  |2700  |2705  |2710  |2715  |2720
Contig1           NNNNT TNCNN NCTCN CCGTC TNNTN ANNTN NNNCT NCNTT CTANC NNNNN

WERI_Rb_FORW_...  TNNAA NGTAN GCNGA NNANN NAANA CACC- CTACN CNCNC TCTCA NAA-G
gi|62088465|d...  TGCTA GATTT ACAGA GAAGT TTCTG CATAT CTGCT ACTTG TTGCA TTTTG
                  |2725  |2730  |2735  |2740  |2745  |2750  |2755  |2760  |2765  |2770
Contig1           TNNAA NGTAN GCNGA NNANN NAANA CACC- CTACN CNCNC TCTCA NAA-G

WERI_Rb_FORW_...  GTCCC CNNNC TNNNG NCANN CACNN CTANN NCGNN NCCAA NGATN CNTCN
gi|62088465|d...  GGTTC AAACC TAAAT ATGAT GTAGC AGAGG AAGAA TTCTA AGTAC CTTCT
                  |2775  |2780  |2785  |2790  |2795  |2800  |2805  |2810  |2815  |2820
Contig1           GTCCC CNNNC TNNNG NCANN CACNN CTANN NCGNN NCCAA NGATN CNTCN

WERI_Rb_FORW_...  NNCCC GCN
gi|62088465|d...  AAAGC TTGTG TCAGA TTGTT AAAAT CACCA CACAT TCCCC TCATT CTAAC
                  |2825  |2830  |2835  |2840  |2845  |2850  |2855  |2860  |2865  |2870
Contig1           NNCCC GCN-- ----- ----- ----- ----- ----- ----- ----- -----

gi|62088465|d...  TCTGT GCTCC TTGTC CTCCC TTCAA TAATA ATTGG CTTTG CTTGC AATTA
                  |2875  |2880  |2885  |2890  |2895  |2900  |2905  |2910  |2915  |2920
Contig1           ----- ----- ----- ----- ----- ----- ----- ----- ----- -----
```

```
gi|62088465|d...  AGCAT TTA
                  |2925 |2930
Contig1           ----- ---
```

140 kDa NCAM

Cell line WeRi-Rb
NK - normal kidney sample

CodonCode Aligner: ncamvariant2, Contig1
14. Februar 2011 12:47:23 CET
Page 1 of 3

```
gi|117320546|ref|NM_1...  TGTTC AGGAC CTCGG CCCAG CCCAC AGCCA TCCCA GCCAA CGGCA GCCCC ACCTC AGGCC TGAGC ACCGG GGCCA
                          |2436 |2441 |2446 |2451 |2456 |2461 |2466 |2471 |2476 |2481 |2486 |2491 |2496 |2501 |2506
Contig1                   ----- ----- ----- ----- ----- ----- ----- ----- ----- ----- ----- ----- ----- ----- -----

                                                                                    TTA TGCAC CTG-C TACTT CCTGA ACANG
WERI_Rb_140F_A02_02                                                                 TTTTT TGNNG CTGCC TACTT CCTGA NCTTT
02048HK_F_B02_04                                                    TGTCC TGCTC CTGGT GGTTG TGGAC ATCAC CTG-C TACTT CCTGA ACAAG
<< 02048NK_R_B03_03                                                 TGTCC TGCTC CTGGT GGTTG TGGAC ATCAC CTG-C TACTT CCTGA ACAAG
<< 02048TK_R_C03_05                                                                 TTA TTTCG CTG-C TNCTT N-TGT ATTTT
A89_F_D02_08                                                        TGTCC TGCTC CTGGT GGTTG TGGAC ATCAC CTG-C TACTT CCTGA ACAAG
<< A89_R_D03_07                                                     TGTCC TGCTC CTGGT GGTTG TGGAC ATCAC CTG-C TACTT CCTGA ACAAG
gi|117320546|ref|NM_1...  TCGTG GCCAT CCTCA TCGTC ATCTT CGTCC TGCTC CTGGT GGTTG TGGAC ATCAC CTG-C TACTT CCTGA ACAAG
                          |2511 |2516 |2521 |2526 |2531 |2536 |2541 |2546 |2551 |2556 |2561 |2566 |2571 |2576 |2581
Contig1                   ----- ----- ----- ----- ----- TGTCC TGCTC CTGGT GGTTG TGKAC ATCAC CTG-C TACTT CCTGA ACAAG
```

A89-PE
fetal kidney sample

TL-tumor kidney sample

NCAM 140kDa

CodonCode Aligner: ncamvariant2, Contig1
14. Februar 2011 12:47:24 CET
Page 2 of 3

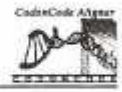

```
                                    lang
                                    5p 8
WERI_Rb_140F_A02_02                 TGTGG C-CTG TTCAT GTGCA TTGCG GTCAA CCTGT GTGGA AAAGC CGGGC CCGGG GCCAA GGGCA AGG-A CATGG
NK [02048NK_F_B02_04          154   TGTGG C-CTG TTCAT GTGCA TTGCG GTCAA CCTGT GTGGA AAAGC CGGGC CCGGG GCCAA GGGCA AGGTA CATGG
NK [<< 02048NK_R_B03_03       151   TGTGG C-CTG TTCAT GTGCA TTGCG GTCAA CCTGT GTGGA AAAGC CGGGC CCGGG GCCAA GGGCA AGG-A CATGG
TU [02048TK_F_C02_06          190                                       GT GTGGA AAAGC CGGGC CCGGG GCCAA GGGCA AGG-A CATGG
TU [<< 02048TK_R_C03_05       194   TGTGG C-CTG TTCAT GTGCA TTGCG GTCAA CCTGT GTGGA AAAGC CGGGC CCGGG GCCAA GGGCA AGG-A CATGG
FK [A89_F_D02_08              251   TGTGG CTCTG TTCAT GTGCA TTGCG GTCAA CCTGT GTGGA AAAGC CGGGC CCGGG GCCAA GGGCA AGG-A CATGG
FK [<< A89_R_D03_07           247   TGTGG C-CTG TTCAT GTGCA TTGCG GTCAA CCTGT GTGGA AAAGC CGGGC CCGGG GCCAA GGGCA AGG-A CATGG
gi|117320546|ref|NM_1...            TGTGG C-CTG TTCAT GTGCA TTGCG GTCAA CCTGT GTGGA AAAGC CGGGC CCGGG GCCAA GGGCA AGG-A CATGG
                                    |2586 |2591 |2596 |2601 |2606 |2611 |2616 |2621 |2626 |2631 |2636 |2641 |2646 |2651 |2656
Contig1                             TGTGG CTCTG TTCAT GTGCA TTGCG GTCAA CCTGT GTGGA AAAGC CGGGC CCGGG GCCAA GGGCA AGG-A CATGG


WERI_Rb_140F_A02_02                 NAGGA GGGCA AGGCC GCCTT CTCGA AAGAT GAGTC CAAGG AGCCC AT-CG TGGAG GTTCG AACGG AGGAG GAGAG
NK [02048NK_F_B02_04                NAGGA GGGCA AGGCC GCCTT CTCGA AAGAT GAGTC CAAGG AGCCC AT-CG TGGAG GTTCG AACGG AGGAG GAGAG
NK [<< 02048NK_R_B03_03             -AGGA GGGCA AGGCC GCCTT CTCGA AAGAT GAGTC CAAGG AGCCC AT-CG TGGAG GTTCG AACGG AGGAG GAGAG
TK [02048TK_F_C02_06                -AGGA GGGCA AGGCC GCCTT CTCGA AAGAT GAGTC CAAGG AGCCC ATGCG TGGAG GTTCG AACGG AGGAG GAGAG
TK [<< 02048TK_R_C03_05             -AGGA GGGCA AGGCC GCCTT CTCGA AAGAT GAGTC CAAGG AGCCC AT-CG TGGAG GTTCG AACGG AGGA
FK [A89_F_D02_08                    TAGGA GGGCA AGGCC GCCTT CTCGA AAGAT GAGTC CAAGG AGCCC AT-CG TGGAG GTTCG AACGG AGGAG GAGAG
FK [<< A89_R_D03_07                 -AGGA GGGCA AGGCC GCCTT CTCGA AAGAT GAGTC CAAGG AGCCC AT-CG TGGAG GTTCG AACGG AGGAG GAGAG
gi|117320546|ref|NM_1...            -AGGA GGGCA AGGCC GCCTT CTCGA AAGAT GAGTC CAAGG AGCCC AT-CG TGGAG GTTCG AACGG AGGAG GAGAG
                                    |2661 |2666 |2671 |2676 |2681 |2686 |2691 |2696 |2701 |2706 |2711 |2716 |2721 |2726 |2731
Contig1                             TAGGA GGGCA AGGCC GCCTT CTCGA AAGAT GAGTC CAAGG AGCCC AT-CG TGGAG GTTCG AACGG AGGAG GAGAG
```

NCAM-140 kDa

CodonCode Aligner: ncamvariant2, Contig1
14. Februar 2011 12:47:25 CET

```
WERT_Rb_140F_A02_02          GACCC CAAAC CATGA TGGAG GGAAA CACAC AGAGC CCAAC GAGAC CACGC CACTG ACGGA GCCCG AGAAG GACT
02048HK_F_B02_04             GACCC CAAAC CATGA TGGAG GGAAA CACAC AGAGC CCAAC GAGAC CACGC CACTG ACGGA GCCCG AGAAG GACT
<< 02048NK_R_B03_03          GACCC CAAAC CGTTA TGGAG GGAAA AACAC AGAGC CCGGG GCCCC CAAAA A
02048TK_F_C02_06             GACCC CAAAC CATGA TGGAG GGAAA CACAC AGAGC CCAAC GAGAC CACGC CACTG ACGGA GCCCG AGAAG GAC
A89_F_D02_08                 GACCC CAAAC CATGA TGGAG GGAAA CACAC AGAGC CCAAC GAGAC CACGC CACTG ACGGA GCCCG AGAAG GAC
<< A89_R_D03_07              GACCC CAAAC C
gi|117320546|ref|NM_1...     GACCC CAAAC CATGA TGGAG GGAAA CACAC AGAGC CCAAC GAGAC CACGC CACTG ACGGA GCCCG AGAAG GGCCC
                             |2736 |2741 |2746 |2751 |2756 |2761 |2766 |2771 |2776 |2781 |2786 |2791 |2796 |2801 |2806
Contig1                      GACCC CAAAC CATGA TGGAG GGAAA CACAC AGAGC CCAAC GAGAC CACGC CACTG ACGGA GCCCG AGAAG GACT-


gi|117320546|ref|NM_1...     CGTAG AAGCA AAGCC AGAGT GCCAG GAGAC AGAAA CGAAG CCAGC GCCAG CCGAA GTCAA GACGG TCCCC AATGA
                             |2811 |2816 |2821 |2826 |2831 |2836 |2841 |2846 |2851 |2856 |2861 |2866 |2871 |2876 |2881
Contig1                      ----- ----- ----- ----- ----- ----- ----- ----- ----- ----- ----- ----- ----- ----- -----


gi|117320546|ref|NM_1...     CGCCA CACAG ACAAA GGAGA ACGA
                             |2886 |2891 |2896 |2901 |2906
Contig1                      ----- ----- ----- ----- ----
```

Wert-Ps1

180

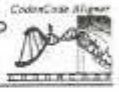

```
gi|16551608|d...  CCCGG ACCCG GAGCC CACCC AGCCC GGAGC CGCGA AGAGC CCGGC CGAGG
                  |439  |444  |449  |454  |459  |464  |469  |474  |479  |484
Contig1           ----- ----- ----- ----- ----- ----- ----- ----- ----- -----

gi|16551608|d...  CAGCC ACAGC CCTTG CTAGC CCGAA GAGCG AGGCT GCCTC CGTCA GCACC
                  |489  |494  |499  |504  |509  |514  |519  |524  |529  |534
Contig1           ----- ----- ----- ----- ----- ----- ----- ----- ----- -----

Probe2_1-2F_A1... NTTTA CCCTT GCCCG GGGCG AGGCA CTTTA AAATG GCACG AAGGG GAACT
gi|16551608|d...  ACAAA CCCTT -CCCA GGGCG AGG-A CTTTA AAATG G-ACG AAGGG -AACT
                  |539  |544  |549  |554  |559  |564  |569  |574  |579  |584
Contig1           NTTTA CCCTT GCCCG GGGCG AGGCA CTTTA AAATG GCACG AAGGG GAACT

Probe2_1-2F_A1... TCAAG NACCC CAGNA TATTG ACCTT GCAAA GGATG TTTTT GCAGC CCTGG
<< Probe2_1-2...      G -ACCC CAG-A TATTG ACCTT GCNAA GGATG TTTTT GCAGC CCTGG
gi|16551608|d...  TCAAG -ACCC CAG-A TATTG ACCTT GCAAA GGATG TTTTT GCAGC CCTGG
                  |589  |594  |599  |604  |609  |614  |619  |624  |629  |634
Contig1           TCAAG NACCC CAGNA TATTG ACCTT GCNAA GGATG TTTTT GCAGC CCTGG

Probe2_1-2F_A1... GCTCT CCTGC TNCCG CCGCT GGGGC CANTG GACAA GCCCN TGAGC TTGCT
<< Probe2_1-2...  GCTCT CCTGC TCCCG CCGCT GGGGC CAGTG GACAA GCCCC TGAGC TTGCT
gi|16551608|d...  GCTCT CCTGC TCCCG CCGCT GGGGC CAGTG GACAA GCCCC TGAGC TTGCT
                  |639  |644  |649  |654  |659  |664  |669  |674  |679  |684
Contig1           GCTCT CCTGC TCCCG CCGCT GGGGC CAGTG GACAA GCCCC TGAGC TTGCT

Probe2_1-2F_A1... CCTTC CACTG CAGAC AGCTC TGTTT CGCCT GCGCC AGCAA AGACC GAGAA
<< Probe2_1-2...  CCTTC CACTG CAGAC AGCTC TGTTT NGCCT GCGCC AGCAA AGACC GAGAA
gi|16551608|d...  CCTTC CACTG CAGAC AGCTC TGTTT CGCCT GCGCC AGCAA AGACC GAGAA
                  |689  |694  |699  |704  |709  |714  |719  |724  |729  |734
Contig1           CCTTC CACTG CAGAC AGCTC TGTTT NGCCT GCGCC AGCAA AGACC GAGAA
```

P1

```
Probe2_1-2F_A1... GGGCC CTNTA AAACC AAAAA NNGAG TGCCA GGNGA CANAT NCTAN CCCNN
<< Probe2_1-2...  GGGCC CCGTA GAAGC AAAGC CAGAG TGCCA GGAGA CAGAA ACGAA GCCAG
gi|16551608|d...  GGGCC CCGTA GAAGC AAAGC CAGAG TGCCA GGAGA CAGAA ACGAA GCCAG
                  |739  |744  |749  |754  |759  |764  |769  |774  |779  |784
Contig1           GGGCC CTGTA AAAGC AAAAC NAGAG TGCCA GGNGA CAGAA NCTAN GCCNG


Probe2_1-2F_A1... NTCC
<< Probe2_1-2...  CGCCA GCCGA AGTCA AGACG GTCCC CAATG ACGCC ACACA GACAA AGGAG
gi|16551608|d...  CGCCA GCCGA AGTCA AGACG GTCCC CAATG ACGCC ACACA GACAA AGGAG
                  |789  |794  |799  |804  |809  |814  |819  |824  |829  |834
Contig1           NGCCA GCCGA AGTCA AGACG GTCCC CAATG ACGCC ACACA GACAA AGGAG


<< Probe2_1-2...  AA
gi|16551608|d...  AACGA GAGCA AAGCA TGATG GGTGA AGAGA ACCGA GCAAA GATCA AAATA
                  |839  |844  |849  |854  |859  |864  |869  |874  |879  |884
Contig1           AA--- ----- ----- ----- ----- ----- ----- ----- ----- -----


gi|16551608|d...  AAAAG TGACA CAGCA GCTTC ACCAG AGCAT TTCCA ACACC ACAGA CACAC
                  |889  |894  |899  |904  |909  |914  |919  |924  |929  |934
Contig1           ----- ----- ----- ----- ----- ----- ----- ----- ----- -----


gi|16551608|d...  AC
                  |939
Contig1           --
```

P2

Biography

Sanja (Ljubiša) Ćirović was born on 19 February 1980 in Belgrade, Republic of Serbia. She graduated molecular biology and physiology at the Faculty of Biology, University of Belgrade, on 27 December 2005 with an average score of 8.49 and grade 10 at graduate exam. She enrolled doctoral studies at Medical Faculty, University of Belgrade, at department of Molecular Medicine on 2006/2007. Scientific Council for medical science at University of Belgrade on meeting held on July 5, 2011 approved the doctoral dissertation entitled "Expression of the neural cell adhesion molecule (NCAM) in healthy and diseased renal tissue." Prof. Dr. Jasmina Markovic-Lipkovski was named as mentor of doctoral dissertation. She is currently employed as an associate at the Institute of Pathology, Medical Faculty University of Belgrade. Sanja Ćirović was employed at the Medical Faculty in Belgrade since May 2006; as research assistant at the Ministry of Education Science and Technology Development (MESTD) projects. She had made an experimental part of doctoral thesis at the Institute of Pathology, Medical Faculty University of Belgrade and at Institute for Medical Research, Karl Eberhardt University of Tübingen, in the laboratory of Prof. Dr. Claudia Müller, within international cooperation between Medical Faculty, University of Belgrade and the "Karl Eberhardt" University Tübingen, supported by the Alexander von Humboldt and DAAD Foundation.

Sanja Ćirović received the DAAD scholarship for training in doctoral studies in 2011. In October 2011, at the First Macedonian Congress of Pathologists she won the first prize from ERA-EDTA Association for the best poster presentation dedicated to the expression of NCAM on renal progenitors. Also she had obtained two scholarships from the European Society of Pathology for poster presentations at 24^{th} and 25^{th} European Congress of Pathology in 2012 and 2013. As an author and co-author she has published 8 papers *in extenso* in foreign and domestic scientific journals (SCI list), and she has presented several papers at national and international conferences. She is a member of the European Society of Pathologists (ESP), the European Renal Association (ERA-EDTA) and Serbian Association of Pathology and Cytology (UPCS). She is married and has son Bogdan and daughter Mila.

Biografija

Sanja (Ljubiša) Ćirović je rođena 19.02.1980. godine u Beogradu, Republika Srbija. Diplomirala je na Biološkom fakultetu Univerziteta u Beogradu, na studijskoj grupi molekularna biologija i fiziologija 27.12.2005. godine sa prosečnom ocenom 8,49 i ocenom 10 na diplomskom ispitu. Doktorske studije upisala je na Medicinskom fakultetu, Univerziteta u Beogradu, na smeru Molekularna medicina, školske 2006/2007 godine. Veće naučnih oblasti medicinskih nauka na VII sednici održanoj 5. jula 2011.godine odobrilo je izradu doktorske disertacije Sanji Ćirović pod nazivom „Ekspresija neuralnih ćelijskih adhezionih molekula (*NCAM*) u zdravom i obolelom bubrežnom tkivu“. Za mentora doktorske disertacije određena je prof. dr Jasmina Marković-Lipkovski. Od maja 2006. zaposlena je na Medicinskom fakultetu u Beogradu kao istraživač pripravnik, a potom i kao istraživač saradnik na projektima MNTR. Trenutno je zaposlena kao stručni saradnik na Institutu za patologiju, Medicinskog fakulteta, Univerziteta u Beogradu. U okviru projekata MNTR, i tokom međunarodne saradnje između Univerziteta u Beogradu i Univerziteta *„Karl Eberhardt“* u Tübingenu (podržane od strane *Alexander von Humboldt i DAAD* fondacija), urađen je eksperimentalni deo doktorske disertacije delom na Institutu za patologiju Medicinskog fakulteta u Beogradu i delom na Institutu za medicinska istraživanja *Karl Eberhardt,* Univerziteta u Tibingenu, u laboratoriji prof. dr Claudie Müller.

Sanja Ćirović dobitnik je DAAD stipendije za stručno usavršavanje u okviru doktorskih studija za 2011 godinu. U oktobru 2011. godine na Prvom Makedonskom kongresu patologa dobila je prvu nagradu ERA-EDTA asocijacije za najbolju poster prezentaciju posvećenu ekspresiji NCAM-a na renalnim progenitorima. Takođe dobitnik je dve stipendije Evropskog udruženja patologa za radove predstavljene na Evropskom kongresu patologa 2012. i 2013. godine. Kao autor i koautor publikovala je 8 radova *in extenso* u stranim i domaćim naučnim časopisima (SCI lista), i prezentovala je više stručnih radova na domaćim i stranim kongresima. Član je Evropskog udruženja patologa (ESP), Evropske renalne asocijacije (ERA-EDTA) i Urduženja patologa i citologa Srbije (UPCS). Udata je i majka je sedmogodišnjeg Bogdana i šestomesečne Mile.

Prilog 1.

Izjava o autorstvu

Potpisana Sanja Ćirović

broj upisa _____

Izjavljujem

da je doktorska disertacija pod naslovom

Ekspresija neuralnih adhezionih molekula (NCAM) u zdravom i obolelom bubrežnom tkivu (Expression of neural cell adhesion molecules (NCAM) in healthy and diseased renal tissue)

_____

_____

- rezultat sopstvenog istraživačkog rada,
- da predložena disertacija u celini ni u delovima nije bila predložena za dobijanje bilo koje diplome prema studijskim programima drugih visokoškolskih ustanova,
- da su rezultati korektno navedeni i
- da nisam kršio/la autorska prava i koristio intelektualnu svojinu drugih lica.

Potpis doktoranda

U Beogradu, 4.12.2014.god.

_____

Prilog 2.

Izjava o istovetnosti štampane i elektronske verzije doktorskog rada

Ime i prezime autora ____Sanja Ćirović_____

Broj upisa _____

Studijski program _____Molekularna medicina_____

Naslov rada Ekspresija neuralnih adhezionih molekula (NCAM) u zdravom i obolelom bubrežnom tkivu (Expression of neural cell adhesion molecules (NCAM) in healthy and diseased renal tissue)

Mentor __Prof. dr Jasmina Marković-Lipkovski_____

Potpisani __Sanja Ćirović_____

izjavljujem da je štampana verzija mog doktorskog rada istovetna elektronskoj verziji koju sam predao/la za objavljivanje na portalu **Digitalnog repozitorijuma Univerziteta u Beogradu.**

Dozvoljavam da se objave moji lični podaci vezani za dobijanje akademskog zvanja doktora nauka, kao što su ime i prezime, godina i mesto rođenja i datum odbrane rada.

Ovi lični podaci mogu se objaviti na mrežnim stranicama digitalne biblioteke, u elektronskom katalogu i u publikacijama Univerziteta u Beogradu.

Potpis doktoranda

U Beogradu, 4.12.2014.god.

Prilog 3.

Izjava o korišćenju

Ovlašćujem Univerzitetsku biblioteku „Svetozar Marković" da u Digitalni repozitorijum Univerziteta u Beogradu unese moju doktorsku disertaciju pod naslovom:

Ekspresija neuralnih adhezionih molekula (NCAM) u zdravom i obolelom bubrežnom tkivu (Expression of neural cell adhesion molecules (NCAM) in healthy and diseased renal tissue)

koja je moje autorsko delo.

Disertaciju sa svim prilozima predao/la sam u elektronskom formatu pogodnom za trajno arhiviranje.

Moju doktorsku disertaciju pohranjenu u Digitalni repozitorijum Univerziteta u Beogradu mogu da koriste svi koji poštuju odredbe sadržane u odabranom tipu licence Kreativne zajednice (Creative Commons) za koju sam se odlučio/la.

1. Autorstvo

2. Autorstvo - nekomercijalno

3. Autorstvo – nekomercijalno – bez prerade

4. Autorstvo – nekomercijalno – deliti pod istim uslovima

5. Autorstvo – bez prerade

6. Autorstvo – deliti pod istim uslovima

(Molimo da zaokružite samo jednu od šest ponuđenih licenci. kratak opis licenci dat je na poleđini lista).

Potpis doktoranda

U Beogradu, 4.12.2014.god.